Dissertation

The role of micro-RNAs in the development of chronic myelomonocytic leukemia

submitted by

Johannes Lorenz Berg

for the Academic Degree of

Doctor of Philosophy

(PhD)

at the

Medical University of Graz, Department of Internal Medicine, Division of Hematology

under the Supervision of

Assoc.-Prof. PD Dr. med. univ. Armin ZEBISCH

2021

Statutory Declaration

I hereby declare that this thesis is my own original work and that I have fully acknowledged by name all of those individuals and organizations that have contributed to the research for this thesis. Due acknowledgement has been made in the text to all other material used. Throughout this thesis and in all related publications I followed the “Standards of Good Scientific Practice and Ombuds Committee at the Medical University of Graz“.

Johannes Lorenz Berg

Disclosures

This thesis has been published in the following original papers:

Micro-RNA-125a mediates the effects of hypomethylating agents in chronic myelomonocytic leukemia

Johannes Lorenz Berg[1], Bianca Perfler[1], Stefan Hatzl[1], Marie-Christina Mayer[1], Sonja Wurm[1], Barbara Uhl[1], Andreas Reinisch[1], Ingeborg Klymiuk[2], Sascha Tierling[3], Gudrun Pregartner[4], Gerhard Bachmaier[4], Andrea Berghold[4], Klaus Geissler[5,6], Martin Pichler[7,8], Gerald Hoefler[9], Herbert Strobl[10], Albert Wölfler[1], Heinz Sill[1] and Armin Zebisch[1,11]

[1]Division of Hematology, Medical University of Graz, Austria; [2]Core Facility Molecular Biology, Medical University of Graz, Austria; [3]Department of Genetics, University of Saarland, Germany; [4]Institute for Medical Informatics, Statistics and Documentation, Medical University of Graz, Austria; [5]5th Medical Department with Hematology, Oncology and Palliative Medicine, Hospital Hietzing, Vienna, Austria; [6]Sigmund Freud University, Vienna, Austria; [7]Division of Oncology, Medical University of Graz, Graz, Austria; [8]Department of experimental therapeutics, The University of Texas MD Anderson Cancer Centre, Houston, TX, USA; [9]Diagnostic and Research Institute of Pathology, Medical University of Graz, Graz, Austria; [10]Otto Loewi Research Centre, Immunology and Pathophysiology, Medical University of Graz, Austria; [11]Otto-Loewi Research Centre for Vascular Biology, Immunology and Inflammation, Division of Pharmacology, Medical University of Graz, Austria.

Clinical Epigenetics 13, 1 (2021); DOI: 10.1186/s13148-020-00979-2

EZH2 inactivation in RAS-driven myeloid neoplasms hyperactivates RAS-signaling and increases MEK inhibitor sensitivity

Johannes Lorenz Berg[1], Bianca Perfler1, Stefan Hatzl[1], Barbara Uhl[1], Andreas Reinisch[1], Gudrun Pregartner2, Andrea Berghold2, Thomas Penz[3], Michael Schuster[3], Klaus Geissler[4,5], Andreas Prokesch[6,7,8], Carsten Müller-Tidow[9], Gerald Hoefler[10], Karl Kashofer[10], Albert Wölfler[1], Heinz Sill[1], Veronica Caraffini*[1,11], and Armin Zebisch*[1,12]

[1]Division of Hematology, Medical University of Graz, Graz, Austria; [2]Institute for Medical Informatics, Statistics and Documentation, Medical University of Graz, Graz, Austria; [3]CeMM Research Center for Molecular Medicine of the Austrian Academy of Sciences, Vienna, Austria; [4]5th Medical Department with Hematology, Oncology and Palliative Medicine, Hospital Hietzing, Vienna, Austria; [5]Sigmund Freud University, Vienna, Austria; [6]Gottfried Schatz Research Center for Cell Signaling, Metabolism & Aging, Medical University of Graz, Graz, Austria; [7]Division of Cell Biology, Histology and Embryology, Medical University of Graz, Graz, Austria; [8]BioTechMed-Graz, Graz, Austria; [9]University Hospital Heidelberg, Heidelberg, Germany; [10]Diagnostic and Research Institute of Pathology, Medical University of Graz, Graz, Austria; [11]MRC Cancer Unit, University of Cambridge, Cambridge, United Kingdom; [12]Otto-Loewi Research Center for Vascular Biology, Immunology and Inflammation, Division of Pharmacology, Medical University of Graz, Graz, Austria; *these authors contributed equally to this work

Leukemia 2021; in Press; DOI: 10.1038/s41375-021-01161-0

All co-authors declare that they have no conflicts of interest with the content of this thesis and have explicitly agreed to use their data in the thesis.

Doctoral candidate Johannes Lorenz Berg received funding from Joseph-Skoda Awards to A. Zebisch and A. Reinisch, the Leukämiehilfe Steiermark and was trained within the frame of the PhD Program Molecular Medicine of the Medical University of Graz. This research was also supported by the Biobank Graz.

Acknowledgment

As I move closer to the finishing line of this adventure into science, I want to pay tribute and my deepest regards to the people, who made their essential contributions to this thesis.

Firstly, I want to thank my supervisor, Dr. Armin Zebisch, for taking me into his team, trusting me with this task and guiding me through the ups and downs, dead ends and new finds. Thank you for being a great mentor who always openly speaks his mind and has always an ear for new ideas.

I also want to thank the members of my thesis committee, Prof. Heinz Sill, Prof. Gerald Hoefler and my co-supervisor Dr. Andreas Reinisch who continuously gave valuable feedback and took their time to ask critical questions. Additionally, I want to express my gratitude to all our collaborators who contributed their time and work leading up to the publication of two papers. I really enjoyed studying at the Medical University of Graz. Therefore, I also want to thank my Alma Mater and the great people from the doctoral school Molecular Medicine for fostering my scientific development.

Major thanks goes to my colleagues and friends in the lab for this great time. Science is much more fun if you can do it together and share the great moments - finally solving a problem - but also the moments of calamity when the experiment fails for the third time. Especially, I want to thank Bianca, who was there almost from the beginning to the end and who always gave her unconfined support, shared meals and redheaded laughs. Also to Ani, Vero, Karin, Sayan, Simin, Angelika and all the others for the great discussions, the useful help and the occasional happenings who made me feel part of a scientific community.

One of the big motivational drivers and source of endless support is my family. Without you, this thesis would not have been possible. Thank you Babsi, for your loving encouragement and uplifting spirit, giving me the strength to carry through. Also to my parents who showed me the wonders of the natural science all throughout my life. And finally, I want to dedicate this thesis to both of my sons, Marlon and Theophil, who I adore for their never ending curiosity. May you always search and find all the answers to your questions.

Index

List of Abbreviations

7AAD	7-aminoactinomycin
ABCMML	Austrian biodatabase for CMML
AKT	protein kinase B
ALL	acute lymphoblastic leukemia
AML	acute myeloid leukemia
APC	Allophycocyanin
AraC	cytarabine
ASXL-1	additional sex combs like-1
Aza	Azacitidine
BAD	Bcl-2-Antagonist-of-Cell-Death
BCL-2	B-cell lymphoma 2
BCR/ABL-1	breakpoint cluster region/Abelson murine leukemia viral oncogene homolog-1
BM	bone marrow
BrdU	Bromodeoxyuridine
BSC	best supportive care
c-FOS	FBJ murine osteosarcoma viral oncogene homolog
CMML	Chronic myelomonocytic leukemia
c-MYC	myelocytomatosis viral oncogene homolog C
CB	clinical benefit
CBL	Casitas B-lineage Lymphoma
CCLE	The Cancer Cell Line Encyclopedia
CEBPA	CCAAT/enhancer-binding protein alpha
ChIP	Chromatin Immuno Precipitation
CHIP	clonal hematopoiesis with indeterminate potential
CML	chronic myeloid leukemia
COSMIC	Catalogue of Somatic Mutations in Cancer
CP	CMML patient
CPSS	CMML-specific prognostic scoring system
CR	complete remission
CREB	cAMP Responsive Element Binding Protein
CRISPR	clustered regularly interspaced short palindromic repeats
DBS	double strand breaks
Dec	Decitabine
DGCR-8	DiGeorge syndrome critical region gene-8
DMEM	Dulbecco's Modified Eagles Medium
DMSO	dimethyl sulfoxide
DZNep	3-Deazaneplanocin A

EED	embryonic ectoderm development
ELK1	ETS Like-1 protein
ELN	The European Leukemia Net
EMA	European Medicines Agency
ERK	extracellular signal-regulated kinase
EZH2^{inact}	*EZH2* inactivation
FAB	French-American-British system
FACS	fluorescent activated cell sorting
FBS	fetal bovine serum
FDA	Food and Drug Administration
FGFR-1	fibroblast growth factor receptor-1
FLT3	fms like tyrosine kinase 3
FLT3-ITD	*FLT3* internal tandem duplication
RAS^{mut}	Ras pathway mutations
FSC	forward scatter
G-CSFR	granulocyte colony-stimulating factor receptor
GAPs	GTPase-activating proteins
GDP	guanosine diphosphate
GEFs	guanine nucleotide exchange factors
GEO	Gene Expression Omnibus
GM-CSF	granulocyte-macrophage colony-stimulating factor
GRB2	growth factor receptor-bound protein- 2
GSEA	gene set enrichment analysis
GTP	guanosine triphosphate
H3K27me3	Histone3-K27 trimethylation
HBSS	Hanks's buffered saline solution
HMAs	hypomethylating agents
HMAs	hypomethylating agents
HMS	hypomethylierende Substanzen
HRP	horseradish peroxidase
HSCs	hematopoietic stem cells
HSCT	hematopoietic stem cell transplantation
HSPCs	hematopoietic stem and progenitor cells
IDH-1	Isocitrate dehydrogenase 1
KRAS	Kirsten Rat Sarcoma
LSC	leukemic stem cell
LSK	Lin-/Sca1+/c-Kit+
MAPK	mitogen-activated protein kinase
MCL-1	myeloid cell leukemia 1
MDS	myelodysplastic syndromes

miRNAs, miRs	micro RNAs
MN	myeloid neoplasms
MPD	myeloproliferative disorder
MPN	myeloproliferative neoplasm
MR	marrow response
MRD	minimal residual disease
MSCs	mononuclear cells
MUG	Medical University of Graz
NF1	Neurofibromin 1
NGS	Next generation sequencing
NPM1	Nucleophosmin
NR	no response
NRAS	Neuroblastoma RAS viral oncogene homolog
OS	overall survival
PAM	protospacer-adjacent motif
PB	peripheral blood
PBS	phosphate buffered saline
PCA	principal component analysis
PCM-1/JAK-2	Pericentriolar material 1/janus kinase-2
PD	progressive disease;
PDGFR	platelet derived growth factor receptor
PE-Cy7	Phycoerythrin/Cyanine 7
pERK	ERK phosphorylation
PI3K	phosphoinositide 3-kinases
pIpC	polyinosinic-polycytidylic acid
PR	partial response
PRC2	polycomb repressor complex 2
PTPN11	protein-tyrosine phosphatase11
PVDF	to polyvinylidene difluoride membranes
Ran-GTP	RAS-related nuclear protein-GTP
RISC	RNA induced silencing complex
RNA-seq	RNA sequencing
RPKM	RNA-seq Reads Per Kilobase Million
RTKs	receptor tyrosine kinases
RUNX1	Runt-related transcription factor 1
sAML	secondary AML
Sca-1	Stem cells antigen-1
shi-RNA	small hairpin inhibitor
shRNA	small hairpin RNA
SNPs	single nuclear polymorphisms

SOS	son of sevenless homolog
SRSF-2	arginine rich splicing factor-2
SRSF2	Serine And Arginine Rich Splicing Factor 2
SSC	side scatter
STAT	signal transducer and activator of transcription
SUZ12	suppressor of zeste 12 homolog
TBS	tris base saline
TCGA	The Cancer Genome Atlas AML cohort
TET-2	tet methylcytosine dioxygenase-2
UTR	untranslated region
V2 RSEM	V2-RNA-seq by Expectation-Maximization
VAF	variant allele frequency
VNTR	variable number of tandem repeat profiling
WBM	whole bone marrow
WHO	World Health Organization

List of Figures

List of Tables

Abstract

Chronic myelomonocytic leukemia (CMML) is an aggressive neoplastic disease originating from malignant hematopoietic stem cells (HSCs). CMML leukemogenesis is often driven by genetic mutations occurring in HSCs, frequently affecting genes of the epigenetic machinery or signaling mutations, that hyperactive the RAS-MAPK/ERK pathway. Therapeutic options for CMML are limited, especially in unfit patients, where the use of hypomethylating agents (HMAs) shows only temporary efficacy. Deregulated micro RNAs (miRNAs, miRs) are potential players in CMML pathogenesis making them promising targets for future therapeutic intervention.

In the first part of this thesis, we focused on miRNAs involved in CMML leukemogenesis. Initially, we confirmed results from a microarray miRNA expression screen performed in my master thesis. We additionally analyzed $Lin^-/Sca1^+/c\text{-}Kit^+$ (LSK) hematopoietic stem and progenitor cells (HSPCs) from a $Kras^{G12D}$-induced CMML mouse model and demonstrated the consistent downregulation of miR-125a. We additionally corroborated these findings in 36 primary CMML specimen employing qPCR analysis. Functional *in-vitro* assays in myeloid cell lines with stable overexpression of miR-125a showed anti-leukemic effects. Next, we explored the molecular mechanisms leading to the decrease of miR-125a levels using bisulfite sequencing. This revealed the hypermethylation of the upstream/promoter region of miR-125a. Interestingly, the HMA azacitidine (Aza) could reverse hypermethylation and significantly increase miR-125a levels in myeloid cell lines. Further, qPCR analysis of serially obtained primary CMML specimen demonstrated higher miR-125a levels after HMA treatment, an effect specifically seen in patients with clinical response. To investigate the potential role of miR-125a in mediating Aza efficacy, we used miRNA inhibitors and CRISPR/Cas9-mediated knockout to prevent HMA-induced miR-125a upregulation in myeloid cell lines. Most importantly, the silencing of miR-125a reduced the cytotoxic efficacy of Aza in these cells, indicating that miR-125a mediates some of the anti-leukemic effects of HMAs.

The second part of this thesis is based on the next generation sequencing (NGS) analysis of our CMML patient cohort. We observed a potential co-occurrence of *RAS* (*NRAS* and *KRAS*) and *EZH2* mutations, which we aimed to investigate further. Previous clinical studies that tested

targeted therapy against RAS-driven myeloid neoplasms (MNs) using MEK inhibitors have so far delivered disappointing results. We hypothesized, that ineffectiveness of this treatment approach is caused by other co-occurring genetic aberrations. Based on our preliminary results we investigated the co-existence of mutations in RAS modulators (*RAS^{mut}* defined as *KRAS, NRAS, CBL, NF1, PTPN11* mutations) and inactivation of the histone methyltransferase EZH2 (*EZH2^{inact}* defined as mutations and/or chromosomal aberrations). In a data mining approach, we found *EZH2^{inact}* significantly enriched in 450 primary CMML and acute myeloid leukemia (AML) patients with *RAS^{mut}*, which also correlated with shorter overall survival. Additional *in-vitro* assays could demonstrate that pharmacologic and shRNA-mediated inhibition of *EZH2* in *RAS^{mut}* myeloid cell lines amplified oncogenic MAPK/ERK signaling. Interestingly, the co-occurrence of *RAS^{mut}*/*EZH2^{inact}* also increased the sensitivity to MEK inhibitors in these cells. Finally, we explored the underlying mechanisms of *RAS^{mut}*/*EZH2^{inact}*-mediated MAPK/ERK hyperactivation. RNA-sequencing analysis could show the upregulation of genes that activate the RAS-MAPK/ERK pathway. Taken together, *RAS^{mut}* and *EZH2^{inact}* often co-exist in MN and synergistically amplify RAS-MAPK/ERK signaling. In turn, the increased dependency on the hyperactivation of RAS-signaling sensitize *RAS^{mut}*/*EZH2^{inact}* cells to MEK inhibition, thus giving a first rational for novel therapy approaches in selected MN cases.

Zusammenfassung

Die chronische myelomonozytäre Leukämie (CMML) ist eine aggressive neoplastische Erkrankung der hämatopoetischen Stammzelle. Die CMML wird meist von Mutationen im epigenetischen Systems, sowie in Aktivatorgenen der RAS-MAPK/ERK Signalkaskade ausgelöst. Die Therapiemöglichkeiten für die CMML sind begrenzt und eine Behandlung mit hypomethylierenden Substanzen (HMS) zeigt nur kurzweilige Effekte. Eine wichtige Rolle in der Krankheitsentwicklung der CMML spielen miRNAs, welche auch als potentielle Angriffspunkte für zukünftige Behandlungen gelten.

Im ersten Teil dieser Dissertation, befassten wir uns mit miRNAs, die in der Leukämogenese der CMML involviert sind. Dafür haben wir die präliminären Ergebnisse einer miRNA Microarray Expressionsanalyse bestätigt, welche im Rahmen meiner Masterarbeit durchgeführt wurde. Diese Daten konnten nun durch Analysen von $Lin^-/Sca1^+/c\text{-}Kit^+$ (LSK) hämatopoetischen Stamm und Vorläuferzellen aus einem $Kras^{G12D}$-induzierten CMML Mausmodell ergänzt werden. Dies identifizierte die miR-125a als eine der am stärksten herunterregulierten miRNAs, was auch in qPCR Analysen von 36 CMML Patient*innenproben bestätigen werden konnte. Die lentivirale miR-125a Überexpression in myeloischen Zelllinien hatte anti-leukämischen Effekte zur Folge. Eine Bisulfit Sequenzierung der miR-125a Promoterregion zeigte einen Hypermethylierung, welche zur einer verminderten miR-125a Expression führt. Interessanterweise konnte durch die Behandlung mit der HMS Azacitidin (Aza) die Hypermethylierung aufgehoben und die Expression von miR-125a wiederhergestellt werden. Darüber hinaus konnten in seriellen CMML Patientenproben erhöhte miR-125a Werte nach einer HMS Therapie festgestellt werden. Dies war besonders in Patient*innen mit einem guten klinischen Ansprechen auf HMS evident. Um eine mögliche Funktion von miR-125a für die Wirkungsweise von Aza zu untersuchen, wurden sowohl miR-125a Inhibitoren, als auch ein CRISPR/Cas9 basierter Knockout angewendet, um den durch Aza induzierten Anstieg von miR-125a zu verhindern. Dies zeigte, dass die Inaktivierung von miR-125a die zytotoxischen Effekte einer Aza Behandlung erheblich reduzierte und legt eine Rolle von miR-125a als Mediator der antileukämischen Wirkung von HMS nahe.

Der zweite Teil dieser Dissertation basiert auf der Sequenzierungsanalyse unserer CMML Kohorte, die einen möglichen Zusammenhang zwischen *RAS* (*NRAS* und *KRAS*) und *EZH2* Mutationen aufzeigte, den wir im Detail untersuchen wollten. Klinischen Studien zur gezielten Inhibierung von RAS in myeloischen Neoplasien hatten bis jetzt enttäuschende Ergebnisse. Ein möglicher Grund dafür könnten zusätzlich Mutationen sein, die eine effektive Behandlung mit RAS Signalwegsinhibitoren verhindern. Hier fokussieren wir uns auf die Koexistenz von Mutationen in *RAS* Modulatoren (RAS^{mut}: *KRAS, NRAS, CBL, NF1, PTPN11* Mutationen) und die genetische Inaktivierung der Histonmethyltransferase *EZH2* ($EZH2^{inact}$ definiert als Mutation oder chromosomale Veränderung). Eine Datenbankenanalyse von insgesamt 450 CMML und akuter myeloischer Leukämie Patient*innen ergab eine signifikante Häufung von $EZH2^{inact}$ in Fällen mit RAS^{mut}, die auch mit einem kürzeren Gesamtüberleben korreliert war. *In-vitro* Assays mit RAS^{mut} myeloischen Zelllinien konnten außerdem zeigen, dass die pharmakologische oder durch shRNA mediierte Inhibition von EZH2 zu einer Amplifikation der RAS-MAPK/ERK Signalkaskade führt. Das gleichzeitige Auftreten von RAS^{mut} und $EZH2^{inact}$ verstärkte außerdem die Empfindlichkeit gegenüber MEK Inhibitoren in diesen Zellen. Eine RNA Sequenzierung konnte zudem eine erhöhte Expression von RAS-MAPK/ERK Aktivatoren aufzeigen. Zusammenfassend wirken RAS^{mut} und $EZH2^{inact}$ synergistisch um den RAS-MAPK/ERK Signalweg zu hyperaktivieren, was zu einer erhöhten Sensitivität gegenüber MEK Inhibitoren führt und liefert so erste Anhaltspunkte für eine gezielte Therapie dieser myeloischen Neoplasien.

1. Introduction

1.1. Classification of myeloid malignancies

Myeloid malignancies are clonal hematopoietic disorders. They are divided into chronic diseases, such as myelodysplastic syndromes (MDS), myeloproliferative neoplasms (MPN) and chronic myelomonocytic leukemia (CMML) on the one hand, and acute malignancies such as acute myeloid leukemia (AML) on the other. Of relevance for this thesis are the entities CMML and AML, which will be discussed in more detail.

1.1.1. CMML

1.1.1.1. Clinical characteristics, diagnostic criteria and epidemiology

CMML is an aggressive malignancy arising from hematopoietic stem cells (HSCs). It is defined by myelodysplastic as well as myeloproliferative features and is classified by the World Health Organization (WHO) as an MDS and MPN overlapping entity (1).

Affected hematopoietic stem and progenitor cells (HPSCs) show increased proliferation and clonally expand into the myelomonocytic lineage (2). In CMML patients, this leads to a persistent increase of myelomonocytic cells, predominantly monocytes and granulocytes, in the bone marrow (BM), peripheral blood (PB) and the spleen. Although most of these cells differentiate into mature cells they often show myelodysplastic characteristics and impaired functionality (3,4). Additionally, excessive myelomonocytic cells can suppress normal blood cell formation and lead to BM insufficiency. Therefore, CMML patients are at an increased risk for infections and often present with severe signs of anemia such as fatigue, effort intolerance, dyspnea and, if untreated, ischemic organ damage (2). Total leukocyte counts are often increased but leukopenia also occurs as a result of myelodysplastic BM changes. Further, blood coagulation can be impaired in cases were thrombopoiesis is affected. A frequently observed complication is the formation of splenomegaly caused by the infiltration of myelomonocytic cells into the spleen. In rare cases, leukemic cells can also invade non-hematopoietic tissue such as the skin (5).

The diagnosis for CMML can be made after the analysis of PB and BM and includes the following WHO criteria (6,7):

I. Persistent PB monocytosis greater than 1×10^9/L with at least 10% of the total leukocytes being monocytes
II. Missing of the Philadelphia chromosome or the breakpoint cluster region/Abelson murine leukemia viral oncogene homolog-1 (*BCR/ABL-1*) fusion gene
III. Less than 20% blasts in the PB or BM (including myeloblasts, monoblasts and promonocytes)
IV. Absence of the platelet derived growth factor receptor (*PDGFR*) A, *PDGFRB* or fibroblast growth factor receptor-1 (*FGFR-1*) gene rearrangements as well as the pericentriolar material-1/janus kinase-2 (*PCM-1/JAK-2*) fusion gene.
V. Signs of dysplasia in at least one myeloid lineages. In case of absent or minimal myelodysplasia the diagnose can still be established if:

- A cytogenetic or molecular genetic abnormality can be detected in the BM cells
- or the monocytosis persists for at least 3 months (and other etiologies can be dismissed)
- and all other requirements are met

For the differential diagnosis of CMML, characteristic chromosomal translocations have to be considered, because they are specifically associated with other myeloid malignancies. The *BCR/ABL-1* fusion gene is only found in chronic myeloid leukemia (CML), while *PDGFRA*, *PDGFRB and* the *PCM-1/JAK-2* fusion gene often lead to severe eosinophilia and responsiveness to targeted therapy (8–10).

CMML can further be subdivided into three prognostically distinct classes using blast counts:

- CMML-0: less than 2% blasts in the PB and/or less than 5% in the BM
- CMML-1: blast count of 2- 4% in the PB and/or 5-9% in the BM
- CMML-2: 5-19% blasts in the PB and/or 10-19% blasts in the BM or occurring Auer rods

If the amount of blast cells exceeds 20% in the PB or BM the CMML has progressed to AML. The transformation from CMML to AML takes place in about 25% of patients (11). It is more common in patients with CMML-2 than in CMML-1 and occurs with a 5-year risk of 63% and 18%, respectively (12). This secondary type of AML is often hard to treat and associated with a negative prognosis and inferior overall survival (OS) (13).

CMML is diagnosed mainly in the elderly population with a median age ranging between 65 to 75 years (11). Because of several re-classification of CMML by the WHO the exact incidence was unclear but is now estimated at 4 cases per million people per year. Interestingly, men are more likely to be diagnosed with CMML with a ratio of 2:1 for yet unknown reasons.

1.1.1.2. Molecular pathogenesis / clonal evolution

Standardized molecular characterization of CMML patients using karyotyping and next-generation sequencing have identified numerous recurrent mutations and cytogenetic aberrations. Around 30% of CMML patients show chromosomal changes while 90% are carrying genetic mutations (14,15).

The most common karyotypes are trisomy 8, monosomy 7, aberrations in chromosome 12p and 7q deletions (15,16). Trisomy 10, 19 and 21, deletions of 5q, 11q and 12p as well as additions in 17p and complex karyotypes (3 or more aberrations) can also be present. Cytogenetic changes are often associated with poor prognosis and higher blast counts (17)

Another driver for the pathogenesis of CMML are somatic mutations that accumulate in HSCs over a person's lifetime. It is estimated that exonic mutations are acquired at of 1,3 (± 0,2) mutations every 10 years (18). Specific mutations in tumor-suppressor or oncogenes can then convey a fitness advantage and lead to the clonal expansion of the HSC. However, early mutational events are not sufficient to initiate malignant leukemia. Instead, patients that carry these genetic lesions develop a clonal hematopoiesis with indeterminate potential (CHIP) that shows no changes in cellular morphology (19). If the affected HSC clone acquires additional mutations, CHIP can evolve into MDS, CMML and eventually AML.

Early mutations in CMML include inactivating mutations in the methylcytosine dioxygenase *TET-2* (ten-eleven translocation 2) or the *ASXL-1* (additional sex combs like-1) genes (20). Both of these tumor-suppressors are governing the epigenetic regulation of genes and are mutated in 40-60% of all CMML cases (21,22). Secondary mutations often occur in genes that control splicing, such as serine and arginine rich splicing factor-2 (*SRSF-2*), or signaling molecules, most importantly *RAS* (*NRAS* (Neuroblastoma RAS viral oncogene homolog) and *KRAS* (Kirsten Rat Sarcoma)) and *JAK-2* (20,23). These additional driver mutations can lead to the malignant transformation of the HSC clone and are associated with increased proliferation and survival as well as granulocyte-macrophage colony-stimulating factor (GM-CSF) hypersensitivity (24). Other mutations that activate the RAS /MAPK (mitogen-activated protein kinase) / ERK (extracellular signal-regulated kinase) pathway are *NRAS*, *KRAS*, *CBL*, *NF1* and *PTPN11* (Casitas B-lineage Lymphoma; Neurofibromin 1; (25,26). *RAS* mutations are associated with a myeloproliferative CMML phenotype and have a negative impact on the prognosis of the patient (23). Implications of the RAS/ MAPK pathway in CMML and AML will be discussed in more detail later.

Recurrent mutations are found in the categories (2,27):

- Epigenetic regulators (*EZH2, ASXL1, TET2, DNMT3A, IDH1* and *IDH2*)
- Spliceosome components (*SF3B1, SRSF2, U2AF1* (*U2AF35*), *ZRSR2*, *SF3A1*, *PRPF40B, U2AF2* (*U2AF65*) and *SF1*);
- DNA damage response genes (*TP53*);
- and intracellular signaling and transcription factors (*JAK2*, *SH2B3, KRAS, NRAS, CBL, FLT3, RUNX1* and *NPM1*).

Although, no mutations are exclusively specific to CMML the most frequently detected are *TET2* (~60%), *ASXL1* (~40%), *SRSF2* (Serine and Arginine Rich Splicing Factor 2; ~50%), *RUNX1* (Runt-related transcription factor 1; ~15%), *RAS* (~30%) and *CBL* (~15%).

The pathogenesis of CMML has also been recapitulated in several transgenic mouse models. Activating mutations in *NRAS* and *KRAS* as well as *TET-2* and *ASXL-1* deletions lead to the

development of a CMML-like myeloproliferative neoplasm or myelodysplastic disorder and have been useful tools to investigate the pathogenic mechanisms of these diseases (28–31).

1.1.1.3. Risk stratification

CMML patients have a very variable risk profile and prognosis. While high-risk patients often exhibit an aggressive clinical phenotype and a high inherent potential for AML transformation, low risk patients show a more indolent form of disease (14). In consequence the median OS can range between 5 to 97 months (17,32).

Due to this alternating course of the disease, various risk stratification systems have been established that incorporate different parameters determining the patient's prognosis. One of the most widely used models for risk stratification is the CMML-specific prognostic scoring system (CPSS) (33,34). This stratification scheme integrates FAB (French-American-British) group and WHO CMML-subtypes, CMML-specific cytogenetic risk stratification and the patient's dependency on erythrocyte transfusions to predict OS and leukemia-free survival. Special emphasis is put on cytogenetics including patients with high-risk (trisomy 8 or aberrations of chromosome 7, or complex karyotype), low risk (normal karyotype or isolated loss of Y chromosome) and intermediate risk aberrations (all other chromosomal changes; (14)). To determine the prognostic score the CPSS grants one point for each applicable variable and two points for high-risk cytogenetic abnormalities. Based on these parameters the CPSS defines four risk groups: low risk group (0 points with 72 month median OS), intermediate-1 risk group (1 points with 31 month median OS), intermediate-2 risk group (2-3 points with 13 month median OS), and high risk patients (4-5 points with 5 month median OS).

Other scoring system have been developed by the Groupe Francophone des Myelodysplasies, MD Anderson Prognostic Scoring System and the Mayo scoring system (32,35,36). Some somatic mutations present an independent risk factor for CMML patients. Mutations in the transcriptional regulator *ASXL1* (excluding missense mutations) or the histone methyltransferase *EZH2* impose a negative impact on the prognosis for CMML patients (37).

1.1.1.4. Therapeutic approaches for CMML

The therapeutic options for CMML can be divided into three categories with different tolerability and curative or life-prolonging potentials. Firstly, hematopoietic stem cell transplantation (HSCT) is considered the only potentially curative therapy for CMML (38). However, old age and co-morbidities often make patients ineligible for this therapeutic approach. Additionally, HSCT can cause a number of severe adverse effects, such as graft-versus-host disease, and 30% of patients ultimately relapse.

The second treatment strategy is the use of hypomethylating agents (HMAs). Because of its relatively low toxicity and high tolerability, it can be an option for patients that are unfit for HSCT (39). Decitabine (Dec) and Aza have been approved for the treatment of CMML and show efficacy in 40-70% of patients (11). These HMAs are cytidine analogs that inhibit DNA methyltransferases when administered in low doses and thereby cause a demethylation of DNA. In CMML, frequent epigenetic mutations, such as *TET2* or *DNMT3A* (DNA (cytosine-5)-methyltransferase 3A), are associated with aberrant genomic methylation patterns, that can cause the silencing of tumor-suppressor genes and favor leukemic growth (40–42). HMAs can partly reverse this process, although the exact mechanism remains incompletely understood and only few targets genes have been identified so far (41). However, the response to HMAs is limited as drug-resistant clones eventually evolve and relapsed patients show a detrimental prognosis (43).

The third treatment approach for CMML is named best supportive care (BSC) and is mainly applied in older and/or unfit patients (2,7). It includes symptomatic treatment for cytopenias like erythrocyte or thrombocyte transfusions or erythropoiesis stimulating agents, such as erythropoietin. In patients with myeloproliferative features, treatment with the myelo-ablative agent hydroxyurea can be employed to treat monocytosis and organomegaly. Furthermore, BSC includes prophylactic treatment with antibiotics to lower the risk of infections.

Overall, the treatment options for CMML are limited and the need for new targeted therapies is evident. However, several clinical trials currently investigate new agents or combination

therapy that target key signaling pathways such as the RAS/MAPK pathway, JAK/STAT (signal transducer and activator of transcription) signaling or immune-modulatory drugs (44).

1.1.2. Acute myeloid leukemia

Like CMML, AML is a malignant and aggressive disorder that originates in the stem and progenitor cells of the hematopoietic system. It is characterized by the uncontrolled proliferation of myeloid blasts. Excessive amounts of blast can be found in the BM, the PB or in some cases as organ infiltrates. A hallmark of AML is a blast count of more than 20% in the BM or PB, which also indicates a differential diagnose to CMML.

1.1.2.1. Clinical characteristics, diagnostic criteria and epidemiology

AML patients are often present with unspecific symptoms linked to cytopenias that are caused by the expansion of leukemic blast in the BM that successively disturb normal hematopoiesis. These symptoms include anemia-associated fatigue, bleeding caused by thrombocytopenia and impaired wound healing as well as infections caused by neutropenia (45). Extramedullary infiltration of blast can occur in 9-19% of cases where the cells for solid tumors termed myeloid sarcoma (MS) or leukemia cutis if present in the skin (46,47). Hepato-splenomegaly can occur and often correlates with transformed preceding myeloproliferative disorders (48). The diagnosis for AML is established upon examination and analysis of the BM and PB.

AML can arise *de novo* if patients had no related hematologic illness before the diagnosis, secondary (sAML) if CMML, MDS or MPN transforms to AML or as therapy-related when AML develops after chemo- or radiotherapy that was used to treat another primary malignancy (49).

The 2016 WHO classification for AML takes recurrent genetic abnormalities, immunologic phenotype, clinical manifestations and morphology into account (49). The major categories for AML are defined as: AML with recurrent genetic abnormalities, AML with myelodysplasia-

related changes, therapy-related myeloid neoplasms, acute MS, myeloid proliferations related to Down syndrome as well as myeloid leukemia that is not otherwise specified.

Another classification system was established by the FAB group (50). The FAB classification sub-divides AML according to the maturation and type of myeloid cell that are involved.

- M0: undifferentiated
- M1: myeloblastic without maturation
- M2: myeloblastic with maturation
- M3: promyelocytic
- M4: myelomonocytic
- M4Eo: myelomonocytic with bone marrow eosinophilia
- M5: monocytic
- M6: erythroleukemia
- M7: megakaryoblastic

AML can be diagnosed in patients of all ages but is especially prevalent in adults over 65 (51). While the incidence in the younger populations is around 1,8 per 100000 people per year, it increases to an annual 15 to 20 cases per 100000 in the population over 70 years old (52,53). AML is the most frequently occurring form of acute leukemia in adults (51,54).

1.1.2.2. Molecular pathogenesis / clonal evolution

The leukemogenesis of AML is based on the step-wise culmination of specific genetic lesions in HSPCs. This process is driven by ageing or can be triggered by treatment-related radiation and chemotherapy (55). Similar to CMML, at least two genetic aberrations are usually necessary to induce acute leukemia, often with a history of CHIP (19). However, AML patients usually carry at least 13 mutations on average (56). These mutations can occur in molecules of cell signaling pathways that control proliferation and survival or disturb normal differentiation or epigenetic signaling in HSCs. Frequently detected mutations are *FLT3* (fms like tyrosine kinase 3; 28% frequency), *CEBPA* (CCAAT/enhancer-binding protein alpha; 27%), *NRAS* and

KRAS (12%), *TP53* (8%) and *c-KIT* (4%) (56). Other recurrent mutations include *NPM1* (Nucleophosmin) and aberrations in regulatory epigenetic genes like *DNMT3A*, *TET2*, and *IDH-1* (Isocitrate dehydrogenase 1) and *IDH-2*, which are overall detected in up to 40% of cases. If these mutations are acquired, they disturb key cellular processes that can lead to uncontrolled proliferation, self-renewal and differentiation block of a clonal population of HSCs. At the core of a clonal cell population stands the leukemic stem cell (LSC). This type of cell can instigate leukemia and is defined by the ability to cause a transplantable AML in murine xenograft models (57). However, AML is not a static disease. It is subjected to constant clonal evolution as more mutations can be accumulated with each cell division. This leads to the generation of new subclonal cell populations with a distinct mutational landscape (58).

Chromosomal aberrations are also a common finding during standard diagnostic karyotyping and are often associated with specific subtypes of AML. Well characterized cytogenetic translocations include t(8:21)(q22;q22) ore inversion of chromosome 16 (inv(16)(p13q22)) in core-binding factor AML and t(15:17)(q22;q21) in acute promyelocytic leukemia (59).

1.1.2.3. Prognosis and therapeutic approaches

Although, novel therapeutic approaches have been established for the treatment of AML, the outcome for most patients is still poor. Up to 80% of patients will not survive more than one year after they have been diagnosed with AML (60). In order to find the right therapeutic approach the individual risk stratification is elemental. One of the biggest risk factors is still advanced age, low performance status and comorbidities (45). Additionally, cytogenetic aberrations and gene mutations are important parameters for risk assessment. The European Leukemia Net (ELN) stratifies AML patients in the favorable, intermediate and adverse risk groups according to criteria specified in Table 1 (61).

Favorable risk group
· t(8;21)(q22;q22.1); *RUNX1 -RUNX1T1*
· inv(16)(p13.1q22) or t(16;16)(p13.1;q22); *CBFB-MYH11*
· mutated *NPM1* without *FLT3-ITD* or with *FLT3-ITD* low
· biallelic mutated *CEBPA*
Intermediate risk group
· mutated *NPM1* and *FLT3-ITD* high
· wildtype *NPM1* without *FLT3-ITD* or with *FLT3-ITD* low (without adverse-risk genetic les
· t(9;11)(p21.3;q23.3); *MLLT3-KMT2A*
· cytogenetic abnormalities not classified as favorable or adverse
Adverse risk group
· t(6;9)(p23;q34.1); *DEK-NUP214*
· t(v;11q23.3); *KMT2A* rearranged
· t(9;22)(q34.1;q11.2); *BCR-ABL1*
· inv(3)(q21.3q26.2) or t(3;3)(q21.3;q26.2); *GATA2 ,MECOM (EVI1)*
· del chr5 or del(5q); -7; -17/abn(17p)
· complex karyotype, monosomal karyotype
· wildtype *NPM1* and *FLT3-ITD* high
· mutated *RUNX1*
· mutated *ASXL1*
· mutated *TP53*

Table 1: The 2017 risk-stratification for AML according to the ELN. Complex karyotype: ≥3 unfavorable chromosome aberrations; *FLT3-ITD* (*FLT3* internal tandem duplication) status was assessed in DNA fragment analysis to determine the allelic ratio between the *FLT3-ITD* and wildtype *FLT3* (low allelic ratio: <0.5; high allelic ratio: ≥0.5)

The therapy of AML is based on different approaches. Younger and/or fit patients with a good health status and the absence of significant comorbidities can be treated with high-dose chemotherapy, eventually followed by HSCT. These approaches have a curative intention. On the other side, older and often unfit patients that are incapable of tolerating treatment-related toxicities of the high-dose approaches are treated with less aggressive therapeutics and BSC

(45). The treatment for patients eligible for high-dose chemotherapy can be divided in two stages. The first phase is termed induction therapy, which uses a 7+3 day regime of cytarabine and anthracyclines (e.g. daunorubicin or idarubicin), respectively, to achieve complete remission (CR) (51). CR is achieved if the amount of blast cells decreases below 5% in the BM and normal hematopoiesis is restored. A majority of 70-80% of patients below the age of 60 reaches CR but would relapse within a short period of time because of remaining and hard to detect LSCs. To prevent the re-expansion of leukemic cells, subsequent consolidation therapy is initiated as the second phase of this treatment scheme. Depending on the risk stratification of the patient, post-remission therapy can consist of two to four cycles chemotherapy or HSCT (62). Patients with favorable risk profile can receive intermediate-dose cytarabine or a combination of cytotoxic and cytostatic agents, while intermediate and high-risk patients undergo allogenic HSCT (63). Those patients who fail to respond to induction therapy can also be treated with additional high-dose chemotherapy and subsequent HSCT (64). Recent studies have shown that even in the case of CR, patients often show a minimal residual disease (MRD) (65). This is a situation, where the criteria of CR are fulfilled, but where leukemic blasts can be detected with more sensitive methods (such as qPCR, flow cytometry and NGS). While this situation is associated with adverse outcome in affected patients, the exact consequences for the clinical routine are still a matter of debate (45). Less aggressive forms of therapy for older and unfit patients include the use of HMAs, low-dose cytarabine and BSC as described for CMML above (45,66). Unfortunately, however, these therapies are not considered curative.

Recent advances in AML therapy are trying to overcome treatment-related toxicity by targeting specific gene mutations or cells. The last few years have shown tremendous progress in this field of molecularly targeted therapy with several drugs being newly licensed for the treatment of AML by the U.S. Food and Drug Administration (FDA) and/or the European Medicines Agency (EMA). These include midostaurin (FLT3 inhibitor, (67)), gilteritinib (FLT3 inhibitor, (68)) venetoclax (BCL2 (B-Cell CLL/Lymphoma 2) inhibitor,(69)), enasidenib (IDH2 inhibitor,(70)), ivosidenib (IDH1 inhibitor, (71,72)) and glasdegib (Hedgehog signaling inhibitor, (73)). Consequently, AML therapy nowadays is more than just deciding whether a patient is fit or unfit for high-dose chemotherapy, but also includes a targeted approach that is based on the occurrence of specific molecular aberrations. While some of these new agents are

administered in combination with the standard chemotherapy, some are designed as alternatives for these approaches (61,67,68).

Two of the greatest challenges in AML therapy are relapse and the occurrence of chemoresistance. The majority of successfully treated patients will eventually relapse due to MRD or therapies will lose their efficacy as resistant clones emerge. Relapsed AML is notoriously hard to treat and possesses a dismal prognosis (74).

1.2. The RAS proto-oncogene

The RAS small GTPases belong to a superfamily of highly conserved signaling proteins that transduce extracellular stimuli to the inside of the cell (75). All of its members contain a guanine nucleotide binding domain and are important players in regulating cell growth, apoptosis and other pivotal functions. These features turn some of these proteins into potent proto-oncogenes. Here we focus on the clinically most important representatives NRAS, KRAS and HRAS.

1.2.1. Signal transduction and functions of RAS

RAS proteins cycle between an active and an inactive state (76). This depends on the binding of RAS to guanosine triphosphate (GTP), a process regulated by guanine nucleotide exchange factors (GEFs), which induce a conformational change and activates the protein. To discontinue the signaling process GTPase-activating proteins (GAPs) trigger the hydrolytic cleavage of GTP to guanosine diphosphate (GDP), resulting in an inactivated RAS-GDP complex.

RAS stands at the top of a signaling cascade, called the RAS/RAF/MEK/ERK pathway, which is activated by membrane bound receptors that convey growth factor, mitogen or cytokine signaling (77). Most of these receptors belong to the group of receptor tyrosine kinases (RTKs), which become active after ligand binding and trigger autophosphorylation of the internal receptor domain. These phosphorylated residues recruit Src homology-2 domain containing adaptor proteins like GRB2 (growth factor receptor-bound protein- 2) and further bind to GEFs

like SOS (son of sevenless homolog) to facilitate RAS activation. This process is localized on the intracellular site of the membrane, where RAS is anchored via a C-terminal farnesyl group. It has been shown that the association of RAS on the plasma membrane is essential for normal signaling and its ability for cell transformation (78). Once RAS is activated it can phosphorylate and thereby transactivate multiple downstream effectors, the most important being the RAF/MEK/ERK and the PI3K (phosphoinositide 3-kinases) /AKT (protein kinase B) pathway (79). Phosphorylated ERK1/2 is a key effector kinase that has more than 150 target proteins (80–82). It is able to translocate into the nucleus where it can activate transcription factors, such as CREB (cAMP Responsive Element Binding Protein) and c-MYC (myelocytomatosis viral oncogene homolog C), which in turn regulate gene expression. Additionally, it has been shown that RAS signaling is involved in the transcriptional regulation of micro RNAs (miRNAs, miRs) as well as the epigenome, which both play important roles in leukemogenesis (83).

It has to be noted that these signaling cascades are not exclusively linear processes, as in fact, extensive crosstalk between members of the RAS pathway and other pathways exists (79,84,85). Moreover, many isoforms of signaling proteins with different substrate specificities have been identified, adding even more complexity to this intracellular signaling network (79). One important way to regulate this network is through scaffolding proteins, which control protein-protein interaction as well as the localization and precisely timed assembly of signaling complexes (86,87).

1.2.2. *RAS* mutations in myeloid malignancies

Mutations in *RAS* genes are frequent events in tumorigenesis and can be detected in 20-30% of all human cancers (88). *KRAS* mutations are more common in solid cancers, especially in the lung, the pancreas and the colon. The predominant isoform in myeloid malignancies is *NRAS*, although *KRAS* mutations are also detected in a significant amount of cases (15,89). Especially in CMML with ~30%, and AML with 15-40% mutations in the RAS pathway are common and function as important drivers for leukemogenesis (90).

RAS mutations are able to transform normal cells to become cancerous. This has also been shown in a variety of animal models targeting different cell types and organs (26,91). Although, the expression of mutant RAS in HSPCs causes a CMML-like myeloproliferative disorder (MPD) in mice, *RAS* mutations are usually not isolated events but occur with cooperative mutations to initiate leukemogenesis (23). In CMML mutant *RAS* is associated with myeloproliferative features and AML-transformation (26). Interestingly, *RAS* mutations are also significantly enriched in myelomonocytic subtypes of AML (M4/M5) and transformed CMML exhibits the same phenotype (75).

Most mutations in *RAS* genes are found within the hotspot regions of codon 12,13 and 61 (78). These mutations impair the hydrolytic activity of RAS and lower the binding affinity to GEFs, which result in the stabilization of the now constitutively active RAS-GTP complex. Consequently, activated RAS accumulates in the cell and excessively activates downstream effector proteins within the MAPK and AKT pathway. This greatly effects pivotal cell processes like proliferation and cell cycle, differentiation and apoptosis. Important mediators for this are transcription factors. For instance c-MYC, ELK1 (ETS Like-1 protein) and c-FOS (FBJ murine osteosarcoma viral oncogene homolog) are activated by phosphorylated ERK and activate gene expression signatures associated with proliferation (92). Furthermore, myeloid differentiation and skewed lineage commitment of HSCs are caused by the hijacking of the CM-CSF and interleukin-3 pathway through mutant RAS and are considered hallmarks for CMML (78,93). This results in the excessive phosphorylation of STAT5 and the activation of the myeloid transcription factor PU.1 (84,94). Activation of the MAPK and AKT pathway also prevents the initiation of apoptosis, either via direct protein interaction between apoptotic regulators such as BCL-2, BAD (Bcl-2-Antagonist-of-Cell-Death), MCL-1 (myeloid cell leukemia 1) and Caspase 9, or through the regulation of their expression and intracellular abundance (95–97).

Excessive RAS signaling in leukemia does not only depend on mutations in *RAS* genes alone, but can also be caused by additional mutations disrupting important modulators of the pathway. Apart from *NRAS* and *KRAS*, these include *NF1, CBL, PTPN11*, which are known as RASopathy genes and are recurrently mutated in myeloid malignancies (98,99). NF1, CBL and

PTPN11 are all important regulators of RAS signaling, which fine tune the response to extracellular RTKs or directly regulate RAS. Mutations in these genes lead to the excessive activation of downstream targets. Furthermore, mutated receptors like c-KIT, G-CSFR (granulocyte colony-stimulating factor receptor) or FLT-3 upstream of RAS can also contribute to the hyperactivity of the pathway. The multitude of mutations affecting RAS signaling becomes evident in 55-74% of AML patients, in which the pathway is constitutively active (26,100).

1.2.3. Therapeutic options targeting RAS

On account of the prominent role that is taken by aberrant RAS signaling in CMML, AML and other hematologic malignancies, intense research has been undertaken to develop targeted drugs (101). One of the biggest obstacles during that endeavor was the protein structure of RAS, as it is relatively small and lacks binding pockets for inhibitory drugs. One alternative approach was to target the farnesyl anchor that localizes the RAS proteins close to the plasma membrane, which is an essential step for its function. Farnesyl transferase inhibitors, targeting the enzyme responsible for this post-transcriptional modification, unfortunately showed little efficacy in clinical trials as compensatory mechanisms, mediated by geranyl-transferase and other enzymes, substituted this process (102,103).

Other approaches focused on blocking the signal further downstream of the pathway. MEK inhibitors are able to attenuate leukemia development in *RAS*-driven mouse models but did show unfavorable results in clinical trials of AML and CMML (104). Although, some response was shown in *RAS*-mutated patients, other factors, such as cooperative mutations, seem to influence the oncogene-dependency of leukemic cells on activated RAS signaling. Such a scenario has been investigated in a TET2 deficient and NRAS mutated mouse model, where the co-occurrence of both mutations increased the sensitivity to MEK inhibition (105).

Latest advances try to disrupt the signal transduction between RAS and RAF as well as AKT. The novel agent Rigosertib binds to the interaction site of these proteins and thereby inhibits the phosphorylation of RAF and AKT (103,106). Although, results from animal studies hold

some promise, clinical trials of Rigosertib in CMML and AML are still ongoing and needs to be thoughtfully evaluated (107).

1.3. Micro RNAs

MiRNAs are short non-coding single-stranded RNAs that are important epigenetic regulators of gene expression. They are highly conserved amongst eukaryotes and range from 16-29 nucleotides in length (108–110). Genomically, they are located in intergenic regions equipped with independent promoters but are also found in introns of protein coding genes. Additionally, they are often organized and co-transcribed in miRNA clusters, including several miRNAs often sharing functional targets (111).

The transcription of miRNAs is processed by polymerase II and III as 100-1000nt long transcripts called primary miRNA (pri-miRNA)(112). Subsequently, The RNase II Drosha in conjunction with DGCR-8 (DiGeorge syndrome critical region gene-8) forms a micro-processor complex to further cleave the primary transcripts into 70-80nt long pre-miRNAs (107). These pre-miRNAs form self-complementary hairpin structures and can be transported from the nucleus to the cytosol by exportin-5 and Ran-GTP (RAS-related nuclear protein-GTP). Finally, the RNase Dicer further shortens the double-stranded transcript to yield the mature miRNA. Upon recruitment of Argonaut-2, one of the miRNA strands (either the 5p or 3p strand) is degraded, while the leading strand remains bound to forms the RNA induced silencing complex (RISC). This RNA-directed complex can now bind to complementary or near-complementary mRNA sequences to prevent protein translation through mRNA deadenylation, endonucleic cleavage or the inhibition of ribosomal binding (113).

Interestingly, the mRNA targets are not determined by the full sequence of the mature miRNA but is mainly guided by its ~8nt long seed sequence, which shows some tolerance to mismatches (114). This does not only drastically increase the number of possible target genes but has also implications for gene silencing. While perfectly complementary mRNAs are cleaved and degraded, binding that includes mismatches usually leads to transcriptional silencing. The majority of miRNAs target sequences in the 3’ untranslated region (UTR) of mRNAs. However,

other, so-called non-canonical binding sites, in the 5'UTRs, introns or exons of genes have been described and validated to mediate translational repression (115). Unfortunately, non-canonical miRNA interactions often remain unstudied as most reporter assays used to identify mRNA targets focus on 3' UTRs.

Through miRNA-mediated post-transcriptional regulation, it is estimated that up to 30% of all proteins coding genes are under the regulation of miRNAs, thereby making them a key player in the fine-tuning of intracellular processes (116).

1.3.1. The role of miRNAs in cancer and myeloid malignancies

Since the discovery of miRNA signaling over 25 years ago, it has been well established that the expression of miRNAs is highly deregulated in various malignancies, often mediating a fitness advantage for cancerous cells. A landmark study by Johnson et al. was able to draw the line from nematode cells to human cancer by demonstrating that the let-7 miRNA was directly targeting *RAS* expression (117). Thereafter, miRNAs in cancer and leukemia have been categorized into two distinct classes: oncomiRs and tumor-suppressor miRNAs. While oncomiRs are usually upregulated in malignant cells targeting tumor-suppressive proteins, tumor-suppressor miRNAs have the opposite effect.

From a mechanistic point of view, aberrant miRNA expression can be linked to cytogenetic changes, like chromosomal amplifications or deletions that include miRNA loci. This has been shown in AML patients with trisomy 8, where the oncomiRs miR-124a and miR-30d, are upregulated in a gene-dose related effect (107). Smaller genomic changes, like single nuclear polymorphisms (SNPs) and point mutations can also alter target sites, seed sequences or the biogenesis of miRNAs, thereby changing their targetome (118). This has been demonstrated for a rare SNP of the miR-125a sequence, which reduced the translational repression of target genes (119). Furthermore, many miRNAs are governed by transcription factors that are mutated or over-activated in cancer. One prominent example is c-MYC, which functions as a transcriptional repressor for a vast signaling network of tumor-suppressor miRNAs, such as miR-34a, miR-29c or the let-7 miRNA family (120). Other mechanisms of miRNA silencing

have been attributed to epigenetic changes, such as histone modifications and promoter hypermethylation. Reduced miR-193a expression in primary AML samples and cell lines could be linked to excessive promoter methylation, which in turn, influenced the expression of the targeted proto-oncogene c-KIT (121). Additionally, it has been demonstrated that mutations in DNA methyltransferase and other epigenetic regulators are associated with decreased miRNA expression and thereby support tumorigenesis (122,123).

To determine the true oncogenic potential of miRNAs in leukemogenesis, transgenic mouse models, recapitulated the loss or overexpression of a specific miRNAs, are indispensable tools. For example, the ectopic overexpression of miR-155 in murine BM cells, a miRNA also overexpressed in some subtypes of AML, caused the onset of a myeloproliferative disease (124). In another study by Zhao et al., the deletion of miR-146a in mice lead to the development of myeloproliferation, splenomegaly and transplantable myeloid sarcomas after 18-22 months (125). This mirrors some of the aspects of MDS, where miR-146a downregulation has also been found (126). From a greater perspective however, most miRNAs fail to produce malignant phenotypes and play only a minor role in tumor initiation as their aberrant expression rarely exist as isolated events in cancer and leukemia (127,128).

Apart from their functional importance, miRNAs signatures are valuable factors in predicting the prognosis and survival of leukemia patients (129). In cytogenetically normal high-risk AML patients the expression of miR-181a and miR-181b has a positive prognostic impact on the clinical course of the disease. Low expression of miR-181 family members is associated with an increased risk of therapy failure and relapses, and decreased survival (130). MiRNAs can also be used as biomarkers for chemoresistance (131). As demonstrated by work from our own group, miR-23a mediates resistance to cytarabine and is associated with dismal outcome for AML patients, who were assigned to this treatment regime (132). Moreover, miRNAs can be employed to accurately differentiate tumor and leukemia samples, even in cases where gene expression pattern failed to classify the tested samples (133). A specific miRNA expression profile, consisting of miR-128a, miR-128b, let-7b and miR-223 can be employed to differentiate AML from acute lymphoblastic leukemia (ALL) with an accuracy of more than 97% (134). Other miRNAs, are specific to cytogenetic abnormal subgroups of AML, as shown for miR-

382 and t(15;17)/PML–RARα-positive AML and can aid accurate diagnostic decisions (135,136).

1.3.2. miRNA expression patterns in *RAS*-mutated CMML

The role of miRNAs in the pathogenesis and therapy of CMML is only incompletely understood. Deregulated expression of miRNAs in CMML has been demonstrated within small cohorts of patients, where specific miRNAs where associated with distinct CMML sub-categories (137).

Within my master thesis, I aimed to identify relevant deregulated miRNAs in *RAS*-mutated CMML (30). Therefore, we investigated the expression of nearly 2000 miRNAs in a $Kras^{G12D}$-driven *in-vivo* model of CMML (138,139). Transgenic mouse models have the advantage of avoiding the genetic heterogeneity of patient samples that can obscure experimental analysis. A microarray-based expression profiling of isolated murine HSPCs (CD-11b^{-}/Ly-6G^{-}/CD-117^{+}) showed a distinct miRNA signature, with 30 differentially expressed miRNAs. The majority of 26 miRNAs exhibited reduced expression, while 4 miRNAs were significantly upregulated in this cell population. The most significantly deregulated miRNAs included miR-26a, miR-150, the miR-99b / miR-125a / let-7e cluster as well as the miR-296 / miR-298 cluster. Although, no experiments were conducted to delineate the function of these miRNAs in CMML pathogenesis, this preliminary data presents evidence that *RAS* mutations regulate a specific set of miRNAs in CMML.

1.3.3. Therapeutic approaches targeting miRNAs

Therapeutic interventions targeting miRNAs are an appealing approach in leukemia therapy. Manipulating or restoring their expression could potentially target a multitude of proteins involved in mediating tumor-promoting properties. However, this seemingly advantageous trait can also prove to be a pitfall of miRNA therapy, as unwanted protein regulation might convey

adverse effects and toxicity. Two different approaches have been suggested. On the one hand, to directly target miRNA signaling using synthetic oligonucleotides to either inhibit or mimic their expression. Or, on the other hand, indirect and often pharmacological measures to control or reconstitute the processing and expression of endogenous miRNAs.

One way to silence overexpressed oncomiRs is to use specific anti-sense oligonucleotides, known as antagomiRs or modified locked nucleic acids. Application of a miR-196b-directed antagomiR to human leukemic progenitor cells decreased their colony-formation capacity and proliferation and delayed leukemogenesis in a AML xenograft model (140). Another way to reduce pathologically overexpressed miRNAs are miRNA sponges. These are long synthetic oligonucleotides that possess a large number of miRNA binding sites, thereby competitively decreasing the abundance of free oncomiRs. In addition to miRNA silencing, the introduction of tumor-suppressor miRNAs as primary hairpin constructs has also been investigated. The first ever clinical trial testing miRNA mimics investigated miR-34a replacement therapy in advanced solid cancers and initially also included multiple myeloma patients. Although proving successful delivery, target gene regulation and some clinical activity of the miRNA constructs, the study had to be canceled after immunologic adverse effects that resulted in the death of four patients (141).

The biggest obstacles in miRNA therapy remain the stability and delivery of the constructs. While degradation can be prevented with methoxyethyl or methylene bridge modification on the 2'-position of the ribose molecule, targeted delivery of miRNA therapeutics proves to be difficult and largely depends on virus-based applications (142,143). However, liposomal or nanoparticle delivery systems for leukemia therapy are currently investigated (144).

A more established method for the indirect targeting of miRNA expression is the use of epigenetic drugs (145). This allows to reverse transcriptional silencing through hypermethylation or pathological histone modifications and restore normal miRNA levels. The HMAs Aza and Dec show clinical efficacy in CMML and AML and have been shown to cause the re-expression of tumor-suppressor miRNAs (134). The same was true for histone deacetylase inhibitors, like trichostatin A, which were associated with the decrease of histone 3 Lysin 27 trimethylation (H3K27me3) and upregulated miR-124a levels (146). Noteworthy,

some miRNAs are markers for the clinical activity of HMAs. Abnormal expression of miR-17, miR-100 and miR-133b was able to predict the response to Aza in high-risk MDS and AML patients and could be used in future treatment decisions (147).

Despite some drawbacks, miRNAs-directed therapy for leukemia or other malignant diseases carries a great potential for the development of future therapeutics.

1.4. Enhancer of zeste homolog 2

EZH2 is the catalytically active subunit of the polycomb repressor complex 2 (PRC2), which is a epigenetic master regulator of histone methylation. Apart from EZH2, the PCR2 consists of the subunits SUZ12 (suppressor of zeste 12 homolog) and EED (embryonic ectoderm development), forming a lysine 27 specific histone methyltransferase (148,149). PCR2 functions as a transcriptional repressor and its target genes are linked to HSC activity, the regulation of cell differentiation and self-renewal (150,151). Like many epigenetic regulators, EZH2 can play dual roles, as either tumor-suppressor or oncogene, in the context of different malignancies. While overexpression and gain-of function mutations have been detected in solid cancers, missense mutations, deletions or reduced expression of EZH2 are characteristic for myeloid neoplasms (37,148). In CMML and MDS, the loss of EZH2 expression has a negative impact on the patient's outcome, including event-free survival (152). Interestingly, analysis of EZH2 in de novo AML showed no correlation between mutations and overall survival but revealed a significant association with low BM blast count instead (153).

EZH2 knockout models of MNs have shed more light on the role of EZH2 in leukemic development. A recent *in-vivo* study of *EZH2* knockout in a *NRAS*-mutated mouse model demonstrated that loss of EZH2 promotes leukemogenesis and leads to an aggressive malignant phenotype (154). This suggests a cooperative relationship of EZH2 loss and *RAS* mutations in the development of MNs. Similar effects have also been demonstrated in solid tumors, where EZH2 loss potentiates the activation of the RAS/MAPK signaling pathway in a *Kras*-driven mouse model of lung adenocarcinoma (151).

Although pharmacologic targeting of EZH2 has been pursued, these efforts have mainly focused on the inhibition of its catalytic activity and protein abundance (151). These approaches are unsuitable for the treatment of myeloid neoplasms, where EZH2 activity is mainly inactivated. However, it is possible that the increased activation of the RAS/MAPK signaling by co-occurring EZH2 loss and mutations in *RAS* genes increases the oncogene dependency on this pathway. This might open a therapeutic window for the intervention with MEK inhibitors in patients carrying these aberrations.

2. Hypothesis and Aims

MicroRNAs are important regulators of malignant disorders, such as CMML. However, our understanding about the role of miRNAs in the leukemogenesis and treatment of CMML is still incomplete. In this thesis, we hypothesize that specific miRNAs, deregulated in RAS-driven CMML, are functionally involved in mediating oncogenic properties in leukemic cells. To test this hypothesis, we select highly deregulated miRNAs from a *Kras*^{G12D}-induced *in-vivo* model of CMML and investigate their expression in human CMML specimen. Further, the selected miRNAs candidates will be used for different *in-vitro* based experiments, in which the effects of ectopic miRNA overexpression, knockdown or the pharmacological treatment on myeloid cells will be investigated.

Additionally, RAS pathway mutations are frequently detected in CMML and other difficult to treat MNs, where they facilitate leukemogenesis. Even though targeted pharmacological inhibition of the RAS pathway was effective in murine CMML models, only limited efficacy could be observed in clinical trials. Here we hypothesize, that the co-occurrence of other genetic aberrations is responsible for the ineffectiveness of this treatment approach. Furthermore, specific additional mutations could create new vulnerabilities that increase the sensitivity to pharmacologic targeting. Preliminary observations within the NGS analysis of our CMML cohort showed a pattern of frequent mutations in RASopathy genes and the histone modifier EZH2. Therefore, we will investigate the co-occurrence of these genes in MNs and elucidate their effects on targeted therapy.

3. Materials and Methods

3.1. Primary human samples

All primary human samples were obtained and collected at the Division of Hematology, Medical University of Graz (MUG). These studies were reviewed and approved by the institutional review board (28-481 ex 15/16 and EK 30-464 ex 17/18) and were conducted in accordance with the declaration of Helsinki. Primary CMML patient specimens were obtained from PB and/or BM of CMML patients. Healthy controls were obtained from BM specimens from healthy donors, and from patients with lymphatic diseases without BM infiltration. Additionally, $CD34^+$ cells from umbilical cord blood samples were used as healthy controls.

3.1.1. Sample preparation and storage

- Dulbecco's Phosphate Buffered Saline (PBS), Gibco, Cat. No. 14190-094
- Lymphoprep Solution, Axis-Shield, Stemcell Technologies, Cat. No. 07801
- Giemsas Azur-Eosin-Methylenblaulösung, Merck Millipore, Cat. No. 1.09204.0500
- May-Grünwalds Eosin-Methylenblaulösung, Merck Millipore, Cat. No. 1.01424.0500
- EasySep™ Human Cord Blood CD34 Positive Selection Kit II (Stemcell Technologies, Cat. No. 17896)

Samples were processed on the day of collection and cryopreserved for subsequent analysis. In brief, the samples were mixed with an equal volume of PBS and topped with Lymphoprep solution (Axis-Shield) followed by centrifugation at 2500 rpm for 20 min at room temperature. The Lymphoprep solution contains high-mass polysaccharides that create a density gradient to separate whole blood samples into layers of plasma, erythrocytes, granulocytes and mononuclear cells (MNCs). The MSC layer was collected using a sterile Pasteur pipette, washed two times with PBS and up to $1x10^7$ cells/tube were viably frozen and stored in liquid nitrogen. Cytospin preparations of all samples were stained with Giemsa–May Grünwald and examined under the microscope to exclude samples with less than 80% myelomonocytic cell

content. Samples from healthy donors were collected from umbilical cord blood specimens originating from normal full-term deliveries. To isolate the $CD34^+$ HSPCs the magnetic bead-based EasyStep Human Cord Blood $CD34^+$ Selection Kit (Stemcell Technologies) was used according to the manufacturer's instructions and viably frozen and stored in liquid nitrogen. BM aspirates from healthy donors were dried on glass slides and stored without additional staining.

3.1.2. Next generation sequencing

NGS of primary CMML specimens was conducted at the Diagnostic and Research Institute of Pathology at the MUG or as part of the Austrian biodatabase for CMML (ABCMML,(155)). For samples sequenced at the MUG, an Ion Torrent Sequencing platform was employed for the detection of recurrent MN mutations (Table 2). The exact workflow of NGS has been described by our group in more detail previously (156). Sequencing within the ABCMML has been described in detail previously (155). To ensure the quality of the sequencing only mutations with sufficient coverage of x1000 were included. Further, we defined a threshold for the variant allele frequency (VAF) of > 5%. The VAF describes the occurrence of mutated genomic loci in a cell population and can be used to identify subclonal mutations. To further differentiate true mutations from single polymorphisms occurring in the healthy population we only included variant frequencies of less than 0,01% in accordance with the 1000-genome-project (157).

Table 2. List of Genes and sequenced regions included in the MUG-NGS analysis.

Gene	Locus
ANKRD26	full coding
ASXL1	exon 12
BCOR	full coding
BRAF	hotspot Exon 15
CALR	exon 9
CBL	exon 8,9
CEBPA	full coding
CSF3R	exon 14-17
CXCR4	exon 2
DDX41	full coding
DNMT3A	full coding
ELANE	full coding
ETNK1	exon 3
ETV6	full coding
EZH2	exon 16-19
FLT3	exon 14-16.20,21
GATA2	full coding
HAX1	full coding
IDH1	exon 4
IDH2	exon 4
JAK2	exon 13
KIT	exons 8,10,11,17
KRAS	exon 2,3
MPL	exon 10
NF1	full coding
NPM1	exon 11
NRAS	exon 2,3
PHF6	full coding
PTPN11	exon 3,13
RUNX1	exon 3-8
SETBP1	hotspot exon 4
SF3B1	exon 14-16
SF3B2	full coding
SFRP1	full coding
SRP72	full coding
SRSF2	hotspot exon 1
STAG2	full coding
STAT3	exon 20,21
STAT5B	hotspot
TET2	exon 3-11
TP53	full coding
U2AF1	exon 2,7,9
WT1	exon 7,9
ZRSR2	full coding

3.2. CMML mouse model

3.2.1. Ethical considerations

All animal experiments where conducted according to the ethical standards of the Medical University of Graz and were approved by the Federal Ministry for Science, Research and Economy (GZ: BMBWF-66.010/0041-V/3b/2019).

3.2.2. The *Kras^{G12D} Mx1-Cre* mouse model

- polyinosinic-polycytidylic acid (pIpC), Sigma # P0913
- CD11b FACS Abs (CD11b eFlour), eBioscience # 48-0112-82

For the investigation of aberrant miRNAs in CMML, we initially chose a *Kras*-driven murine *in-vivo* model on a C57/BL6 strain background. With this approach, it is possible to overcome the great mutational heterogeneity in CMML patients, which can complicate array-based expression screening. Mice carrying the *Kras^{G12D} Mx1-Cre* transgene develop a MPD that closely resembles human CMML (CMML-like MPD (30). The driver for the oncogenic transformation is the somatic substitution of glycine to aspartate in codon 12 of one *Kras* allele. Hyperactivating hotspot-mutations in exon 12,13 and 61 of the *Ras* proto-oncogene are amongst the most prevalent genetic aberrations in CMML (26). However, unhindered expression of mutated *Kras^{G12D}* is embryonically lethal (158). To generate mice, which develop CMML-like MPD the expression of the *Kras^{G12D}* transgene must be inducible and restricted to hematopoietic cells in the BM. Therefore, the oncogenic *Kras* allele is silenced by an upstream stop-codon, flanked with loxP sites. For the activation of the mutant *Kras^{G12D}* allele, the loxP sites are recognized and excised by the sequence-specific Cre recombinase (159). The expression of Cre in turn is governed by the *Mx1* promoter, which is primarily expressed in the hematopoietic system (160). This promoter can be activated by interferon α/β or by the injection of the interferon-inducing pIpC. This system is useful to control the expression of *Kras^{G12D}* and to regulate the onset of disease development through the application of pIpC resembling a somatic

mutation of *Kras*. It has to be noted that spontaneous Mx1 promoter activation and recombination of loxP sites caused by endogenous interferon have been reported in this transgenic expression system (161). To reduce the chance of such a scenario the animals were housed in a special-pathogen-free environment and checked regularly for infections.

For these experiments 30 day old mice carrying the *Mx1-Cre*$^{+}$*/Kras*^{G12D} genotype and *Mx1-Cre*$^{+/-}$*/Kras*^{wt} controls received three intraperitoneal injections of 250µg pIpC (Sigma) every alternate day. To confirm the presence of CMML-like MPD and associated monocytosis in theses mice the cell count of CD-11b^{+} peripheral blood (PB), BM and Spleen cells were tested using flow cytometry. Further, spleen size and weight were recorded for signs of splenomegaly. This model has already been used for miR expression arrays in my master thesis previously. More details about this model, about the breeding strategy and genotyping have been extensively described within the master thesis (137).

3.2.3. Bone marrow isolation

- Isoflurane, AbbVie, Cat. No.17651
- Hanks' Balanced Salt Solution (HBSS), Gibco, Thermo Fischer, Cat. No. 14025050
- Fetal bovine serum (FBS) HyClone, GE Healthcare Life Sciences, Cat. No.SV3018003
- Antibiotic-antimycotic Mix (anti-anti) Gibco, Thermo Fischer, Cat. No.15240062
- BD Pharm Lyse Buffer, BD Biosciences, Cat. No. 555899

The isolation of murine bone marrow has been extensively described within my Master thesis as well and the reader is referred to this publication (137). Briefly, murine bone marrow was isolated after sacrificing of the animals by cervical dislocation after anesthesia with a mixture of 4% isoflurane (AbbVie) and O_2 (1,5 l/min). Pelvic bones, hind limps, sternum and spine were collected and excessive muscle tissue was removed using surgical scissors and sterile wipes. The bones were suspended in HBSS (Thermo Fischer) supplemented with 5% heat-inactivated FBS and 1% anti-anti (Thermo Fischer Scientific, including 100U/mL penicillin, 100 mg/mL streptomycin and 0.25 mg/mL amphotericin B) and subsequently crushed using a sterile mortar while working under constant lamina flow. The BM cells were then passed

through a 70µm nylon cell strainer and washed with 1xHBSS. BD Pharm lysing buffer (BD Bioscience) was then used to lyse remaining erythrocytes. Afterwards, the cells were washed again, resuspended in 1ml of HBSS and the cell number was determined using a Casy cell counter (Innovatis).

3.2.4. Flow cytometer analysis and sorting of hematopoietic myeloid stem and progenitor cells

To investigate deregulated miRNAs in *Kras*^{G12D}-driven CMML, we used fluorescent activated cell sorting (FACS) with two different sorting approaches to obtain specimen that are enriched with HSCs. In my Master thesis, we previously described the sorting of CD-11b^{-}/Ly-6G^{-}/CD-117^{+} BM cells isolated from *Kras*^{G12D} mice and *Kras*^{wt} controls (137). The more frequent CD-11b^{-}/Ly-6G^{-}/CD-117^{+} cells were used for subsequent array-based miRNA expression screening, as this method requires more RNA. To verify the expression of deregulated miRNAs in a more confined HSPC population enriched for HSCs, we now additionally sorted Lin^{-}/Sca-1^{+}/c-Kit^{+} (lineage negative/ stem cells antigen-1 negative/c-Kit negative) myeloid stem and progenitor cells using a BD FACS Aria III (BD Bioscience).

3.2.5. Sorting of Lin^{-}/Sca-1^{+}/c-Kit^{+} myeloid stem and progenitor cells

- Mouse Hematopoietic Progenitor Stem Cell Enrichment Set, BD Biosciences, Cat. No. 558451.
- 7-aminoactinomycin (7AAD) BD Bioscience, Cat. No. 559925
- CD117 (c-Kit)7/APC (Allophycocyanin), Anti-mouse, BD Pharmingen, Cat. No. 553356
- Sca-1 /PE-Cy7 (Phycoerythrin/Cyanine 7), Anti-mouse, eBiosience, Cat. No. 25-5981-82
- Streptavidin/APC-Cy7, BD Pharmingen, Cat. No. 554063

To obtain specimen of the rare Lin^{-}/Sca-1^{+}/c-Kit^{+} HSPC population, we performed a lineage depletion followed by FACS. For the first step, we used antibody coated magnetic beads from

the Mouse Hematopoietic Progenitor Stem Cell Enrichment Set (BD Biosciences). This removes the majority of mature hematopoietic cells of the lymphoid and myeloid lineage to reduce the number of cells for subsequent FACS. The magnetic nanoparticles are conjugated with streptavidin that can bind to biotinylated antibodies to pull out cells carrying the corresponding antigen. In more detail, CD-3e and CD-45R antibodies were used to distinguish T- and B-lymphocytes, respectively. Mature cells from the myeloid lineage, like erythrocytes, granulocytes and monocytes, were detected with TER-119, CD-11b and Ly-6G/C antibodies. For the labeling of the isolated BM, the cells were resuspended in cell staining buffer at a density of $1x10^7$ cells/ml and mixed with 5µl/$1x10^6$ of lineage depletion antibody cocktail. The cells were left on ice for a 15min incubation, diluted with washing buffer and centrifuged at 300g for 7min. Then, the supernatant was completely removed and 5µl/$1x10^6$ of magnetic nanoparticle solution was used to resuspend the cells. Then, the cell solution was further diluted to a density of $2x10^7$ cells/ml and transferred to a round bottom tube in close proximity to a magnet for 8min. The positively labeled cells were pulled to the wall of the tube, while unlabeled cells, including stem and progenitor cells, remained in solution. This negative fraction was retained using a sterile Pasteur pipette. The procedure was repeated with the resuspended positive fraction before the lineage negative cells were further proceeded for FACS.

For the flow cytometric sorting of $Lin^-/Sca\text{-}1^+/c\text{-}Kit^+$ cells, we selected viable cell populations using FSC (forward scatter), SSC (side scatter) and 7ADD (Fig. 1A,B). 7AAD intercalates into double stranded DNA but can only penetrate through damaged cell membranes. Thus, viable cells with an intact cell membrane are not stained with 7AAD and can be selected for further sorting. To exclude residual mature cells that were not removed during lineage depletion, the cells were stained again with lineage specific primary antibodies (Fig. 1C). To minimize the number of fluorophores used in the sorting, we used secondary antibodies conjugated to APC-Cy7 to detect all lineage specific markers. In a final step, the stem cell factor receptor c-Kit (CD-117) and HSC marker Sca-1 were used to detect a population of stem cell enriched progenitors (Fig. 1D). The combination of Sca-1 and c-Kit markers can yield a progenitor cell population that contain up to 10% HSCs (162).

The lineage depleted cells were prepared for FACS as followed: 5µl of each biotinylated lineage antibodies (CD-3e, CD-45R, TER-119, CD-11b and Ly-6G/C from the Mouse Hematopoietic Progenitor Stem Cell Enrichment Set), 8µl of anti-mouse Sca-1/PE-Cy7 (eBiosience) and 15µl of anti-mouse CD-117/APC (BD Pharmingen) in 1ml of PBS (phosphate buffered saline). The cells were incubated for 15min at room temperature and protected from light. Then, the cells were washed with PBS, centrifuged at 1500rpm for 5min and labeled with 10µl of secondary streptavidin/APC-Cy7 antibody (BD Pharmingen). The cells were again incubated and washed as described above and resuspended in 500µl PBS for sorting.

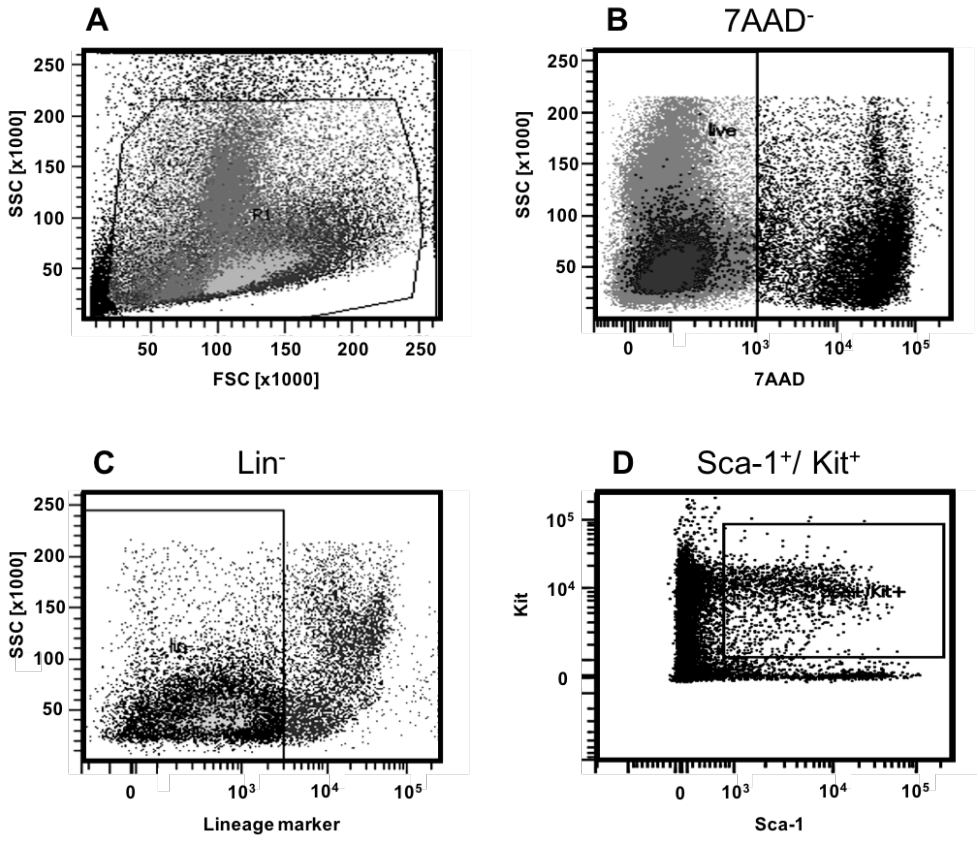

Figure 1. Sorting of Lin$^-$/Sca-1$^+$/c-Kit$^+$ stem and progenitor cells from isolated BM cells. A. In the first sorting step, cells are selected for their size (FSC) and granularity (SSC) to exclude cellular debris. The gated cells include all lineage negative hematopoietic cells including stem and progenitor cells; **B.** Cells gated from A are plotted for their granularity (SSC) and the fluorescent intensity of 7AAD, which stains non-viable cells. Live cells are gated

for further sorting; **C.** In the next step, lineage negative (Lin^-) cells are selected to exclude residual mature lymphoid and myeloid cells. Lineage marker include CD-3e, CD-45R, TER-119, CD-11b and Ly-6G/C coupled with the APC-Cy7 fluorophore; **D.** In the last sorting step, the fluorescent intensities of c-Kit and Sca-1 stem cell markers are plotted to detect a further enriched double positive HSPC population.

3.3. miRNA analysis

3.3.1. RNA isolation

- miRNeasy Micro Kit, Qiagen, Cat. No. 217084
- QIAzol Lysis Reagent, Qiagen, Cat. No. 79306
- Chloroform 99,5%, Sigma-Aldirch, Cat. No. C2432
- Ethanol absolute for analysis, Merck, Cat. No. 1009831011

Total RNA from sorted murine BM cells, primary human samples or cell culture experiments was isolated using the miRNeasy Micro Kit (Qiagen) following the manufacturer's instructions. This column-based extraction method is specialized in capturing small RNA fragments, including miRNAs. In more detail, the cells were washed with PBS and lysed using 700µl QIAzol (Qiagen). To ensure complete lysis, cell homogenates were repeatedly passed through a 21G needle using a 1ml syringe. The samples were then mixed with 140µl chloroform (Sigma-Aldrich) and the liquid-phases were separated after 15min of centrifugation at 13000rpm and 4°C. Thereafter, the aqueous phase was precipitated with 1,5x the sample volume of pure ethanol (Merck) and transferred to the spin column. This was followed by several washing steps using high-salt buffers and a DNase I digestion for 30min at 37°C to remove any genomic DNA. Finally, the columns were washed with 80% ethanol, dried and eluted in 14µl nuclease-free water. RNA concentration and quality was assessed using a nanodrop spectral photometer (ThermoFischer) for qPCR analysis. Until further analysis the RNA Samples were stored at -80°C.

3.3.2. quantitative real-time PCR

- miScript II RT Kit, Qiagen, Cat. No. 218161
- miScript SYBR Green PCR Kit, Quantitect, Qiagen, Cat. No. 218075

3.3.2.1. Complementary DNA synthesis

The measurement of miRNA gene expression in a qPCR reaction requires the conversion of RNA to complementary DNA (cDNA) using the enzyme reverse transcriptase (RT). Therefore, we used the miScript II RT kit (Qiagen) to synthesize cDNA from isolated RNA samples following the manufacturer's instructions. This kit combines a polyadenylation with a simultaneous RT reaction. The polyadenylation uses the PAP enzyme to add several adenosine residues to the 3'end of the miRNA. This poly-A tail serves as a binding site for poly-T primers that mark the starting point for the RT. These primers include a universal tag sequence, which can be recognized by qPCR primers in the later analysis. A total amount of 500ng RNA was diluted to 12µl using PCR-grade water. Additionally, a mastermix was set up containing 4µl of HiSpect Buffer, 2µl of Nucleics mix and 2µl of RT Mix per reaction. Subsequently, the RNA was merged with the mastermix to yield a 20µl reaction, which was incubated at 37°C for 60min followed by 5min at 95°C and immediately cooling to 4°C. For further use, the cDNA samples where diluted with PCR-grade water to a final concentration of 2ng/µl and stored at -20°C.

3.3.2.2. Quantitative real-time PCR analysis

Quantitative real-time PCR (qPCR) was used to measure miRNA expression in murine HSPCs, primary human specimen and *in-vitro* experiments. This qPCR approach uses SYBR Green I (Qiagen) as an intercalating fluorescent dye for the quantification of miRNAs in a primer specific PCR. SYBR Green forms fluorescent complexes with double stranded DNA, which are directly proportional to the amount of amplified cDNA present in each sample. The fluorescent intensity was measured at the end of each elongation cycle. The primer design for this PCR uses universal reverse primers that recognize the previously added 3' tag of the cDNA and miRNA specific forward primers to amplify the target sequence. To ensure the specificity

of the PCR, the melting curve of the reaction product was checked for deviations. All primers were established using standard curves to ensure optimal PCR conditions and efficiency (see Table 3 for Primer information).

Table 3: Primer sequences or ordering information

qPCR Primer	Ordering information	
Hs-miR-125a-5p	Qiagen, Cat# MS00003423	
SNORD72	Qiagen, Cat# MS00033719	
SNORD61	Qiagen, Cat# MS00033705	
RNU6b	Qiagen, Cat# MS00033740	
Bisulfite Sequencing	**Forward**	**Reverse**
Reaction 1	5'-AAGGGAAGAATAAATGGGAGATAT-3'	5'-ACCTAACTTCCCCCCTACCCC-3'
Reaction 2	5'-GGAGGGGAGTTAGGGAAAGT-3'	5'-ACCTAACTTCCCCCCTACCCC-3'
sgRNA	**Guide Sequence**	
sgRNA 1	5'-GGACCTAGAGACTGGCAACA-3'	
sgRNA 2	5'-TTAACCTGTGAGGACATCCA-3'	
PCR Primer	**Forward**	**Reverse**
miR-125a locus	5'-TGCTGTGTCTCTGTGGCTTC-3'	5'-GGCCAGGGGAGAAGCTAGTA-3'

The reactions were set up in triplicates using 5µl SYBR Green PCR Mastermix (Quantitect), 1µl universal Primer (0,5µM, Qiagen), 1µl miRNA specific miScript Primer (0,5µM, Qiagen) and 2µl PCR-grade water and were pipetted into a 96-well plate. Then, 1µl of diluted cDNA (2ng/reaction) were added to the reaction mix and the plate was sealed with a transparent foil. After 2min of centrifugation at 800G the plates were transferred to a Light Cycler 480 (Roche) and run according to Table 4. The table is reproduced from (163) with permission from Clinical Epigenetics.

Table 4: Thermocycler steps for qPCR expression analysis

Temperature	Time	Step	
95°Cs	15min	Taq DNA Polymerase Activation	
95°C	15 sec	Denaturation	**30 Cycles**
62°C	30 sec	Primer Annealing	
72°C	30 sec	DNA Elongation	
4°C	Hold	Storage	

3.3.2.3. Calculation of relative gene expression

The relative gene expression of miRNAs from qPCR experiments was calculated using the $\Delta\Delta C_T$ method (164). Therefore, a threshold for fluorescent intensity is defined within the log phase of the qPCR reaction. The fluorescence measurements at the end of each elongation step are then used to determine the crossing point of the intensity curve of each sample and the threshold. This PCR cycle is defined as the C_T value. A higher expression of a given gene causes earlier crossing of the threshold and therefore a lower C_T cycle. However, it cannot be discriminated if a lower C_T cycle is indeed caused by higher gene expression or due to pipetting errors.

Therefore, we used internal controls to normalize the expression of target genes. The small nucleolar and nuclear RNAs SNORD-61, SNORD-72 and RNU-6b were selected as reference genes for their stable expression in target cells. To normalize target gene expression the geometrical mean of the reference gene C_T values was subtracted from the averaged C_T of the target gene to calculate the ΔC_T value (ΔC_T= C_T (target) - C_T (reference)). For the comparison of target gene expression in different groups of mice, patients and cell lines one ΔC_T value was used as a calibrator. The calibrator serves as a reference point and is used to calculate the $\Delta\Delta C_T$ value ($\Delta\Delta C_T$= ΔC_T (target) - ΔC_T (calibrator)). For the relative quantification of target genes in mice, we used the ΔC_T of an arbitrarily selected *Kras*^{wt} control mouse as calibrator. Patient specimen and cell line experiments were calibrated to the expression value of U937 or

respective overexpression or knockdown control cell lines. Because of the exponential amplification, that takes place during the qPCR, the $\Delta\Delta C_T$ can be used to determine the relative gene expression by calculating 2 to the power of the $\Delta\Delta C_T$ value. The resulting fold change defines the calibrator target gene expression as 1. An overexpression of the target gene will result in a fold change >1 wile a downregulation is described by values between 0 and 1. Therefore, a fold change of 0,5 represents half of the calibrator's target gene expression while a fold change of 2 is defined as a doubled expression.

3.4. Cell culture procedures and *in vitro* assays

3.4.1. Cell culture

- RPMI-1640 Medium (with L-glutamine), Sigma, Cat. No. R8758
- Dulbecco's Modified Eagles Medium, (DMEM), Sigma, Cat. No. D5796
- GlutaMAX (L-glutamine for DMEM), Gibco, Cat. No. 35050038

The cell lines 293T, U937, THP1, NB4, GDM-1 and HL60 were obtained from the German National Resource Center for Biological Material (DSMZ, Braunschweig, Germany) and the Core Facility Alternative Biomodels and Preclinical Imaging (MUG). Low passage stocks were frozen and cells were passaged for less than 6 months after resuscitation. Additionally, the cells were screened by variable number of tandem repeat profiling (VNTR) for authentification. The cells were maintained at 37°C and 5% CO_2 in RPMI-1640, for U937, HL60, THP1 and NB4 cells, or DMEM, for 293T packaging cells. The medium was supplemented with 10% FBS and 1x anti-anti. DMEM medium was further supplemented with 1x GlutaMAX (Gibco).

3.4.2. Lentiviral transduction

- CalPhos Mammalian Transfection Kit, Clontech/Takara, Cat. No. 631312
- pMSCV-miR-125a, Vector: pEZX-MR03, Genecopoeia, Cat. No. HmiR0309-MR03)
- pMSCV scrambled control, Genecopoeia, Cat. No. CmiR0001-MR03-10

- pMSCV-shEZH2, Vector: psi-LVRU6GP, Genecopoeia, Cat. No. CS-HSH095626-LVRU6GP-01-a
- Puromycin, Gibco, Cat. No. 1113803

To investigate the effects of miR-125a and EZH2 signaling we created a number of transgenic cell lines using lentiviral transduction. Constructs that are delivered into the cell by lentiviral particles are integrated into the genome and are therefore stably expressed. For better selection of transduced cell populations, the used constructs carry a puromycin resistance cassette as well as an EGFP expression cassette. To produce virus particles the CalPhos Mammalian Transfection Kit (Clontech) was used to transfect 293T packaging cells with the overexpression and knockdown constructs, respectively. The calcium phosphate used in this kit forms complexes with plasmid DNA and can be taken up by the cells, which in turn secrete lentiviral particles into the medium. Subsequently, the virus supernatant was removed and transferred to the target cell line for transduction. The cells recovered for three days and were then selected for EGFP using FACS. Thereafter, the sorted cells were cultured in complete RPMI containing 1.5 µg/ml puromycin (Gibco) and target gene expression was determined using qPCR and/or Western-blot.
THP1 cells were transduced with pMSCV-miR-125a (THP1 miR-125a overexpressing cells, THP1 miR-125a OE) or vector control (THP1 miRcontrol). Further, we transduced THP1 and HL60 cells for the knockdown of EZH2 with the pMSCV-shEZH2 construct (THP1 and HL60 EZH2 KD) or vector control (THP1 EZH2 control, HL60 EZH2 control).

3.4.3. In-vitro assays

- Trypan Blue 0,4%, BioRad, Cat. No. 1450013
- BrdU (Bromodeoxyuridine) Flow Kit, BD Pharmigen, Cat. No. 552598
- AnnexinV-APC, BioLegend, Cat. No. 640920
- AnnexinV binding buffer, BD Pharmigen, Cat. No. 5166121E
- Staurosporine, Abcam, Cat. No. ab120056

- 5-azacitidine (Vidaza), PeproTech, Cat. No. 3206727
- MEK Inhibitor (U0126), Promega, Cat. No. U0126
- CryoSure-DMSO (dimethyl sulfoxide), Wak Chemie, Cat. No. WAK-DMSO-10
- GSK126, BioVision, Cat. No. 2282-1
- DZNep (3-Deazaneplanocin A), Cayman Chemicals, Cat. No. 13828

2.1.1. Growth curve assay

To assess cellular proliferation we conducted growth curve assays for THP1 miR-125a overexpression cells and THP1 miR control cells, respectively. Cells were counted and triplicates of $0{,}8x10^6$ cells were seeded in 2ml media containing 5% FBS using a 24-well cell culture plate. 10µl aliquots were stained with trypan blue (BioRad) and cell density was assessed using the TC-20 (BioRad) for 5 consecutive days.

3.4.3.1. BrdU proliferation assay

Cell cycle progression of THP1 miR-125a overexpressing cells and THP1 miR control cells was assessed in BrdU/ 7AAD flowcytometric assays. BrdU is a thymine analog, which is taken up by proliferating cells and incorporated into newly synthesized DNA. The cells were labeled with fluorescent APC-conjugated anti-BrdU antibodies and the DNA dye 7AAD to determine the cell cycle with FACS. While cells in the resting G_0 state are BrdU negative because they have not incorporated BrdU, proliferating cells are becoming increasingly more BrdU/7AAD positive while they progress through the DNA synthesizing phase (S-phase), forming a typical horseshoe-shaped cell population. The amount of cells, which progress through the S-phase can be used to determine the cell proliferation.
For the BrdU/7AAD assays we used the BrdU Flow Kit (BD Pharmigen) according to the manufacturer's instructions. Therefore, the cells were cultivated in RPMI containing 5% FBS for 72h and diluted to a final cell density of $1x10^6$ cells/ml. Cells were treated with 50µM of BrdU solution for 1h, washed, fixed and permeabilized using the recommended buffers contained in the kit. This was followed by DNase I treatment for 1h at 37°C and subsequent

labeling with anti-BrdU antibodies and 7AAD. Cell cycle progression was measured at a low flow rate (<300 events/sec) using the LSR II flow cytometer (BD Biosciences).

3.4.3.2. Annexin-V apoptosis assay

Cellular apoptosis/survival was assessed by AnnexinV/7AAD staining (BD Biosciences) and detected by flow cytometry. AnnexinV is a polypeptide that can bind to phosphatidylserines under the presence of high Ca^{2+} concentrations. Change in membrane composition and flip of phosphatidylserines from the inside to the outside of the cell membrane are early signs of cell death but are rarely detected in viable cells (165). Additionally, calls that already underwent apoptosis exhibit a perforated cell membrane and can be stained with the exclusion dye 7AAD. For the measurement of apoptosis sensitivity, the cells were cultured in media containing 5% FBS for 72h at a density of $0{,}4x10^6$ cells/ml and treated with 0,5µM staurosporine (Abcam) for 4h. For the treatment with Aza cells were seeded at equal density and cultured in media containing 5% FBS for 48h and then treated with 2,5µM Aza (PeproTech) solubilized in RPMI or RPMI alone for additional 24h. For the treatment of THP1 EZH2 KO cells with the highly selective MEK inhibitor U0126 (Promega) the cells were seeded at an equal density in 0,05% FBS containing media and treated with 5µM or 10µM of MEK inhibitor or equal amounts of DMSO (Wak Chemie) for 24h. Thereafter, cells were collected and washed with PBS solution without Ca^{2+} ions. Finally, the cells where resuspended in AnnexinV binding buffer (BD biosciences), stained with 2,5µl AnnexinV (BioLegend) and 7AAD (BD biosciences) and apoptosis was measured using the CytoFLEX LX flow cytometer (Beckman Coulter).

3.4.4. Determination of RAS-MAPK/ERK activation status in cell lines with and without aberrations in *RAS* and *EZH2*

The increase of ERK phosphorylation through cooperative RAS^{mut} and $EZH2^{inact}$ was tested by the means of pharmacologic EZH2 inhibition and shRNA-mediated *EZH2* knockdown in THP1 and HL60 cells, respectively. These cell lines both carry an activating *NRAS* mutation ($NRAS^{G12D}$ and $NRAS^{Q61L}$, respectively). For the inhibitor treatment, the cells were seeded at $6x10^5$ cells/well in 2ml medium containing 0,05% FBS. For the GSK126 inhibitor the cells

were treated with 3µM inhibitor or equal amounts of DMSO vehicle for 7 days. DZNep or equal amounts of DMSO vehicle were used at 1µM final concentration for 24h. THP1 and HL60 cells that were stably transduced with *EZH2*-specific shRNA or control constructs were seeded at equal density in RPMI containing 0,05% FBS for 24h. Subsequently, the cells were harvested and prepared for Western-blot analysis to determine ERK phosphorylation.

3.4.5. Small hairpin inhibitor transfection

- DharmaFECT 2 Transfection Reagent, Dharmacon, Cat. No. T-2002-02
- miRIDIAN miR-125a hairpin inhibitor, Dharmacon, Cat. No. IH-300624-06-0002
- miRIDIAN negative control, Dharmacon, Cat. No. IN002005-01-05

Small hairpin inhibitors were used for the transient knockdown of miR-125a in THP1 cells. $1x10^6$ cells were seeded 24h before transfection in growth media without antibiotics or antimycotics. To prepare the transfection mix two tubes were prepared with 47,5µl serum-free media and 2,5µl Dharmafect reagent (Dharmacon) or 5µM inhibitor (Dharmacon). After 5min of incubation, the two tubes were combined, mixed carefully and incubated for 20min to facilitate complex formation. Then, the reaction mix was pipetted onto the cells and incubated for 24h before transfection media was replaced again with complete growth media. The cells were then treated with 2,5µM Aza (PeproTech) or vehicle for 24h and apoptosis was measured by AnnexinV/7AAD assay as described above.

3.4.6. CRISPR/Cas9 mediated knockout of miR-125a

- pX458, vector: pSpCas9(BB)-2A-GFP, Addgene # 48138
- QuickExtract™ DNA Extraction Solution, Lucigen, Cat. No. QE0905T
- QIAquick Gel Extraction Kit, Qiagen, Cat. No. # 28704

For the complete knockout of miR-125a we employed a CRISPR (clustered regularly interspaced short palindromic repeats) /Cas9 mediated approach. The Cas9 endonuclease, originally isolated from *Streptococcus pyogenes,* can be directed to a specific locus in in the

genome using a sequence specific single guide RNA (sgRNA). When the Cas9/sgRNA complex binds to the target locus, the endonuclease activity induces a double strand break 3-4 nucleotides upstream of the next available protospacer-adjacent motif (PAM, Fig 2). This strategy can be used for the stable knockout of miRNAs (166). Two sgRNAs were designed to target sites up- and downstream of miR-125a to excise the mature miRNA from its genomic location leading to a homozygous knockout of the gene (see Table 2 for sequences). Therefore, sgRNA oligos were ligated into pX458 plasmids (Addgene), originally generated from the Feng Zhang lab, co-expressing Cas9 and EGFP. The resulting plasmids were then transfected into U937 cells using a Neon Nucleofector (Thermo Fischer) according to the manufacturer's instructions. In brief, the cells were split and cultivated at low density 24h before the experiment. On the day of transfection $1x10^6$ cells were centrifuged at 300G for 5min, washed with PBS and resuspended in transfection buffer. Subsequently, 2µg of each plasmid were added and the cells were aspirated with the transfection tip followed by electroporation with 3 pulses for 30ms at 1300 V. Afterwards, the cells were transferred into a 6-well plate containing complete growth medium without anti-anti. After 48h of recovery single cells expressing EGFP were sorted into a 96-well plate using a FACS Aria III (BD biosciences).

To confirm the successful knockout of miR-125a, genomic DNA was extracted from single cell-derived clones using Quick Extract (Lucigen) with the suggested protocol of a 15min incubation at 65°C followed by an inactivation step at 98°C for 2min. For an initial screen of multiple clones, 1µl of extracted DNA was used to amplify the miR-125a locus in a PCR reaction and amplicons were run on a 4% agarose gel to detect the size shifts caused by the gene knockout (see Table 2 for primer). Bands that exhibited a reduced fragment size were cut out and DNA was extracted using the QIAquick Gel Extraction Kit (Qiagen) in accordance with the manufacturer's protocol. Purified DNA was then sent for Sanger sequencing and loss of miR-125a expression was validated with qPCR.

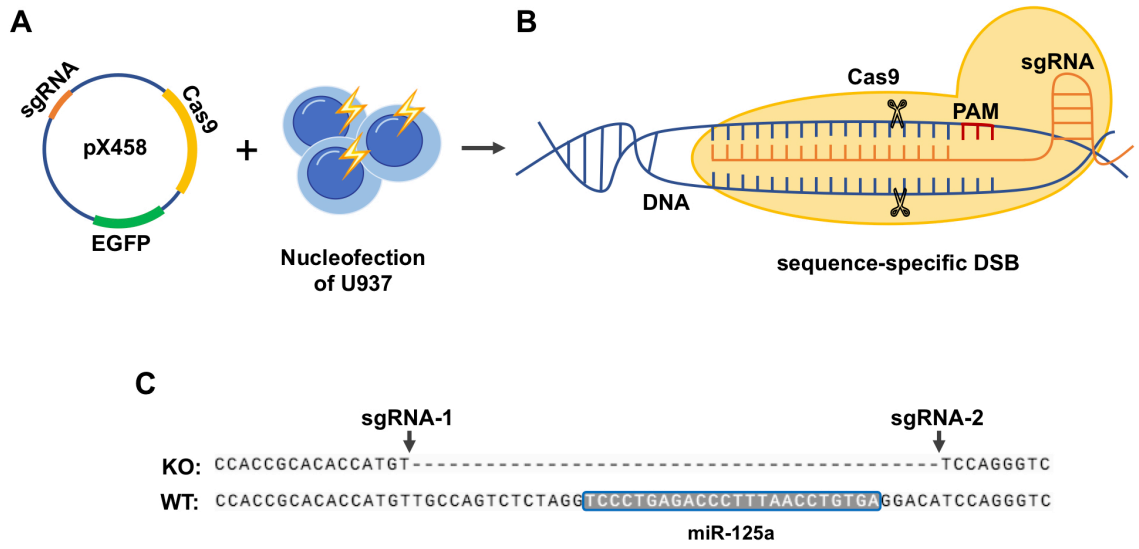

Figure 2.CRISPR/Cas9 mediated knockout of miR-125a. A. Plasmids containing miR-125a-specific sgRNAs and expression cassettes for Cas9 and EGFP were delivered to U937 cells using nucleofection. **B.** The Cas9 forms complexes with the sgRNAs and is directed to the complementary genomic locus. After the complex binds the endonuclease activity of the Cas9 induces sequence specific double strand breaks next to the protospacer-adjacent motif. **C.** The DSB induced up- and downstream of the miR-125a locus cause the excision of the mature miR sequence and induce a complete knockout. EGFP, enhanced green fluorescent protein; sgRNA, single guide RNA; DBS, double strand breaks; PAM, protospacer-adjacent motif; KO, knockout, WT, wildtype. The figure is adapted from (163) with permission from Clinical Epigenetics.

3.5. Western-blot analysis

- RIPA Buffer, Sigma, Cat. No. R0278
- Halt Phosphatase Inhibitor Cocktail, Thermo Scientific, Cat. No. 78420
- Halt Protease Inhibitor Cocktail, Thermo Scientific, Cat. No. 87786
- Mini-Protean TGX Gels 4-15%, BioRad, Cat. No. 456-1083

- Trans-Blot Turbo Transfer Pack (0,2µm PVDF), BioRad, Cat. No. 170-4157
- Tris buffered saline (TBS), Bio-Rad, Cat. No. 1706435
- Tween 20, Sigma, Cat. No. MKCF6671
- Anti-ERK (ERK1 & ERK2) antibody, Sigma, Cat. No. M5670
- Anti-pERK antibody, Cell Signaling Technology, Cat. No. 9102S
- Anti-Vinculin antibody, Abcam, Cat. No. ab129002
- Tri-Methyl-Histone H3 antibody, Cell Signaling Technology, Cat. No. 9733
- Clarity Western ECL substrate, Bio-Rad, Cat. No. 1705060

Cell pellets were washed with PBS and lysed in chilled RIPA-Buffer (Sigma-Aldrich), supplemented with Protease and Phosphatase inhibitor cocktails (Sigma-Aldrich and Thermo Fisher Scientific), by three freeze thawing cycles and repeated vortexing. The lysates were then centrifuged and the protein concentration in the supernatant was measured with DC Protein Assay kit (Bio-Rad) according to the manufacturer's protocol. To prepare the samples for electrophoresis the lysates were mixed with Laemmli sample buffer (Bio-Rad), supplemented with β-mercapto-ethanol (Sigma) and incubated at 95°C for 5min. Immuno-blots were then performed using Mini-PROTEAN TGX gels (Bio-Rad) for electrophoresis and the Trans-Blot Turbo Blotting System (Bio-Rad) for transfer to polyvinylidene difluoride membranes (PVDF, Bio-Rad) membranes. Subsequently, the membranes were blocked in 5% solution of non-fat dry milk and TBST buffer (tris base saline (Bio-Rad) + 0,1% Tween 20 (Sigma)) and incubated with primary pERK, ERK, Vinculin or tri-methylated histone 3 antibody (Cell Signaling Technology). For the detection of the protein we used secondary antibodies linked to horseradish peroxidase (HRP), which can bind to the fc region of the primary antibody. The HRP can then be used to catalyze a luminescent reaction after 5min incubation with the Clarity Western ECL substrate (Bio-Rad). The immune-blots were then imaged using a ChemiDoc MP (Bio-Rad) and further analyzed using ImageJ software (166). To correct for loading errors, the quantification of the detected protein was normalized to the stably expressed loading control Vinculin.

3.6. Bisulfite sequencing

- EpiTect Bisulfite Kit, Qiagen, Cat. No. 59824
- KAPA HiFi HotStart Uracil ReadyMix, Roche, Cat. No. KK2801
- PhiX control DNA, Illumina, Cat. No. FC-110-3001

Bisulfite sequencing was used to assess the methylation status of CpG islands in the promoter region of miR-125a and the demethylating effects of Aza in U937 cells. DNA extraction from U937 cells with and without Aza and subsequent bisulfite conversion was performed using the EpiTect Bisulfite Kit (Qiagen) according to the manufacturer's instructions. In more detail, $0{,}8x10^6$ cells were seeded in complete growth medium and treated with 2,5µM Aza (PeproTech) for 24h. Then $1x10^5$ were resuspended in 10µl PBS and lysed for 30min at 56°C using 10µl of distilled water, 15µl lysis buffer and 5µl proteinase K provided in the EpiTect Lyse All kit (Qiagen). Bisulfite conversion was set up in a 140µl reaction containing DNA Protect buffer, bisulfite solution and 20µl cell lysate. The reaction was placed in a thermal cycler and underwent three rounds of denaturation and incubation steps at 95°C and 60°C, respectively. To clean up converted DNA, the reaction mix was transferred to a spin column and washed with wash buffer, incubated 15min in desulfonation buffer and washed again with wash buffer and 100% ethanol (Merk). Samples were dried by centrifugation for 15min at 5800G and then eluted in 70µl elution buffer.

Bisulfite sequencing analysis was conducted at the Core Facility Molecular Biology of the Medical University of Graz, Austria. To analyze the CpG-rich promoter region of miR-125a, the bisulfite converted DNA was sequenced using an ilumina platform (see Table 3 for primer). In brief, 2µl of bisulfite treated DNA was used in a nested PCR approach. For the first PCR 12,5µl of the KAPA HiFi HotStart Uracil ReadyMix (Roche) were used with 1,25µl DMSO (Wak Chemie) and 0,75µl of each 10 pmol/µl primer in a 25µl reaction. Cycling conditions were of initial denaturation at 95°C for 3 minute followed by 35 cycles of denaturation at 98°C for 20 seconds, annealing at 50°C-60°C for 15 seconds, 72°C elongation for 100 seconds and a final elongation at 72°C for one minute. Two µl of the first PCR reaction were used as template for the second PCR with the same conditions as described above. The PCR products were

checked on a 1,5% agarose gel. Then, the PCR products were indexed and prepared for NGS according Illumina's sequencing library preparation guide. Libraries were sequenced at 8pM on an Illumina MiSeq Desktop sequencer with v3 600 chemistry and 20% PhiX control DNA (Illumina) according to manufacturer's instructions. Data were analyzed with the BiQ Analyzer HT software tool (167).

3.7. RNA sequencing

- TruSeq Stranded mRNA LT sample preparation kit, Illumina, 20020594

To identify genes that are regulated by mutant *RAS* signaling and *EZH2*^{inact} we performed RNA sequencing (RNA-seq) in cooperation with the search Center for Molecular Medicine of the Austrian Academy of Sciences in Vienna. HL60 cells carrying activating *RAS*^{mut} and a stably expressed *EZH2* shRNA (HL60 *EZH2* KD) or control (HL60 *EZH2* control) were cultured for 24h in 0,05% FBS, harvested and total RNA was isolated as described above. The RNA concentrations was measured using a Qubit 2.0 Fluorometric Quantitation system (Thermo Fisher Scientific) and the RNA integrity number (RIN) was assessed using the Experion Automated Electrophoresis System (Bio-Rad). First, RNA-seq libraries were prepared using the TruSeq Stranded mRNA LT sample preparation kit (Illumina). Pre-PCR and post-PCR steps were processed on the Sciclone and Zephyr liquid handling workstations (PerkinElmer), respectively. Next, the concentration and size distribution of the RNA-seq library preps were determined using the Experion Automated Electrophoresis System (Bio-Rad). The samples were then pooled in equimolar concentrations and sequenced on HiSeq 3000/4000 instruments (Illumina) set to 50-base-pair, single-end mode. The real-time analysis software (Illumina) was employed for base calling and further creation of unaligned BAM files. The raw-data was then exported using a custom program based on the Picard tools (https://broadinstitute.github.io/picard/). BAM files were than aligned to the Genome Reference Consortium GRCh38 assembly using the "Spliced Transcripts Alignment to a Reference" (STAR) algorithm (13) and the Ensembl transcript annotation form (version e96, April 2019) as reference transcriptome. STAR was configured according to the ENCODE

project suggestions. Finally, the Bioconductor GenomicAlignments and Bioconductor DESeq2 package were employed to summarize overlaps and identify differentially expressed genes, respectively (https://bioconductor.org/packages/release/bioc/html/GenomicAlignments.html, (168)).

Analysis and quality control of the generated RNA-seq data included principal component analysis (PCA), multi-dimensional scaling and gene expression heatmaps (ggplot2 [https://ggplot2.tidyverse.org (169), Bioconductor ComplexHeatmap - https://bioconductor.org/packages/release/bioc/html/ComplexHeatmap.html - and EnhancedVolcano). Further, we used gene set enrichment analysis (GSEA) to identify signalling pathways that are targeted by cooperative RAS^{mut} and $EZH2^{inact}$ (Enrichr; https://amp.pharm.mssm.edu/Enrichr/ and https://www.gsea-msigdb.org/gsea/index.jsp; (170)) .

3.8. Database retrieval

To investigate the correlation of RAS^{mut} and $EZH2^{\text{inact}}$ in AML we obtained freely accessible data about *EZH2* mRNA expression from The Cancer Genome Atlas AML cohort (TCGA, as V2-RNA-seq by Expectation-Maximization (V2 RSEM) as well as mutation in the RAS-pathway genes *NRAS*, *KRAS*, *CBL*, *NF1* and/or *PTPN11* (171). If available we also retrieved data about mutations and/or copy number losses of *EZH2* from this cohort. Additionally, we also downloaded the same information from The Cancer Cell Line Encyclopedia (CCLE, (172)). *EZH2* mRNA expression was stated as RNA-seq Reads Per Kilobase Million (RPKM). The cBioPortal was used to facilitate the database retrieval (https://www.cbioportal.org/, (173)).

3.9. Statistical analysis

For the comparison of different groups within our experiments, we employed a number of statistical tests. The statistical differences in miR-125a and EZH2 expression in CMML and AML patients, respectively, were assessed using the Mann-Whitney U-test. The U-test is a non-

parametric test that compares two unpaired populations that do not fulfill normal distribution criteria. Therefore, each variable is assigned a rank and the number of ranks in each group is compared to calculate statistical differences. The statistical distribution of each group was compared using the Kolmogorow-Smirnow-test. Further, we employed Spearman's rank correlation coefficient to test for significant correlations between miR-125a expression and patient characteristics, which are represented as continuous variables. To investigate the prevalence of $EZH2^{inact}$ in RAS^{mut} CMML and AML we employed Fisher's exact test, which is used for the comparison of dichotomous variables. The overall-survival of patients was first plotted using Kaplan-Meier curves and then statistically compared using the log rank test. The log rank test is a nonparametric test suitable to compare Kaplan-Meier plots, as it is robust against censored data points.

For the comparison of miR-125a expression before and after HMA treatment in paired patient specimens we used the Wilcoxon signed-rank test. This test is similar to the U-test but considerers the dependency of two paired variables.

The miR-125a expression of $Kras^{G12D}$ *and* $Kras^{wt}$ mice was compared using a Student's t-test for unpaired samples. This parametric test requires continuous variables that follow a normal distribution. $Kras^{G12D}$ *and* $Kras^{wt}$ mice share an identical genetic background, which suggest a normally distributed gene expression pattern.

To compare the miR-125a expression in cell lines following HMA treatment we employed a one-sample t-test. In this test, variables are compared to a fixed mean of a population. As the expression of the control condition was used as the calibrator in qPCR calculations we could compare HMA-treated cells with the specific control mean set to 1.

All other *in-vitro* experiments including growth curve, proliferation and apoptosis assays, CpG methylation and ERK phosphorylation were analyzed employing the paired t-test.

All statistical tests were calculated two-sided and p-values below 0,05 were considered significant. The tests and visualization were processed in SPSS (SPSS Inc., Version 25), Prism 8 (GraphPad) and R version 3.6.1 (https://www.r-project.org/).

4. Results

The following results have been largely published in two original papers in Clinical Epigenetics and Leukemia (163,174)

4.1. **Part 1**: The role of micro RNAs in the development of chronic myelomonocytic leukemia

4.1.1. The expression of miR-125a is reduced in CMML cells

In preliminary experiments, we aimed to characterize miRNA expression profiles in a murine *in-vivo* model of CMML (137). This analysis identified 30 highly deregulated miRNAs in leukemic HSPCs (CD-11b$^-$/Ly-6G$^-$/c-Kit$^+$) of *Mx1-Cre*$^+$/*Kras*^{G12D} mice, that mostly showed diminished expression. To narrow down the number of potential miRNAs, we selected candidates that where amongst the 10 most significantly downregulated miRNAs and showed previously known evidence for a tumor-suppressor function in myeloid neoplasms. Based on this selection, we included miR-26a, miR-150 and miR-125a into the further analysis (Fig. 3A).

CMML is a disease arising from leukemic stem cells. To ensure that the downregulation of selected miRNAs is taking place on a stem cell level and is not biased by myeloid progenitor cells present in the HSPC population, Lin$^-$/Sca-1$^+$/c-Kit$^+$ (LSK) cells were isolated from *Mx1-Cre*$^+$/*Kras*^{G12D} mice and matched wildtype controls. This rare cell population harbors an increased number of HSCs compared to the CD-11b$^-$/Ly-6G$^-$/c-Kit$^+$ cells. Indeed, qPCR expression measurements confirmed the significant decrease of selected miRNA candidates in *Kras* mutated LSK cells, suggesting their downregulation takes place in CMML stem cells (Fig. 3B).

In a next step, we investigated if our findings from a murine model of CMML are also valid in human CMML patients. Therefore, we assessed the expression of selected miRNAs in MNCs from 36 primary CMML patients and compared them to CD-34$^+$ cells from six healthy donors (Fig. 3C). Only miR-125a showed significantly decreased expression in our patient cohort, corresponding to our results from the microarray expression analysis. It has been previously

shown that miR-125a plays a role in myeloid differentiation and is downregulated during hematopoietic maturation (175). As we are comparing a mixed population of CMML MNCs isolated from BM or PB and compare it to sorted CD-34$^+$ control cells, we also included six whole BM (WBM) samples from healthy donors or patients with lymphatic disease without BM infiltration. Comparing the miR-125a expression of these WBM controls with CMML specimen also revealed significantly lower levels of miR-125a in our patient cohort (Fig. 3D). It has to be noted that we could not identify a correlation between mutations in *RAS* genes or *RAS* modulators (*NRAS, KRAS, CBL, PTPN11* or *NF1*) and miR-125a levels within our patient collective, suggesting that miR-125a downregulation is a more general event in CMML rather than attributed to patients with specific RAS mutations (Fig. 3E, for patients mutations see Fig. 4).

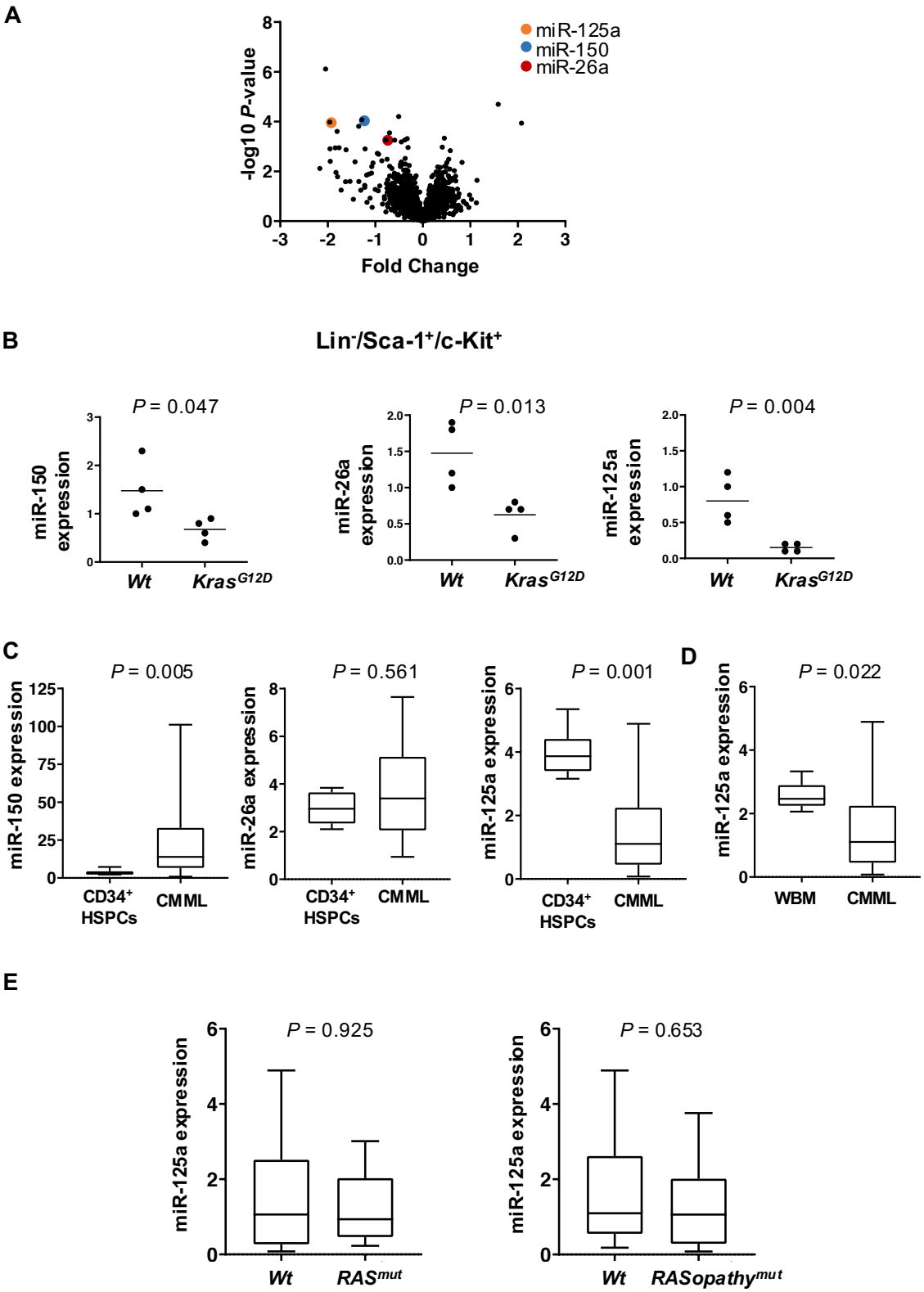

Figure 3. miR-125a is decreased in murine and human CMML. (A) Volcano plot showing the results of the preliminary study investigating differentially expressed miRNAs in HSPCs

from *Mx1-Cre*$^{+}$/*Kras*^{G12D} mice exhibiting a CMML-like MPD (137). On the y-axis negative log10 converted *P*-values are plotted against log2 transformed fold changes on the x-axis with downregulated miRNAs on the left and upregulated miRNA genes on the right site, respectively. **(B)** qPCR expression analysis of selected miRNAs in Lin^{-}/Sca-1^{+}/c-Kit^{+} HSPCs isolated from *Mx1-Cre*$^{+}$/*Kras*^{G12D} and wildtype controls (n=4) confirming the downregulation of miR-150, miR-26a and miR-125a. The dot plots representing the relative expression value of each animal normalized to one selected control mouse set to a value of 1. The horizontal line represents the median expression level and statistical differences were calculated using a paired t-test. **(C)** miRNA expression analysis of primary CMML patient specimen for miR-150, miR-26a and miR-125a depicted as box plots. The relative miRNA expression of 36 CMML patients was compared to six CD34^{+} HSPCs. **(D)** miR-125a expression of 36 CMML specimen compared to WBM from six healthy donors and patients with lymphatic diseases without BM affection. The relative expression was assessed using qPCR analysis and normalized to a calibrator cell line, which was set to a value of 1 (U937 for miR-125a and miR-26a; GDM-1 for miR-150). **(E)** Association of *RAS* mutations and miR-125a expression in primary CMML specimen. Box plots showing miR-125a expression in 33 CMML specimen where NGS data was available. Patients with (n=12) and without (n=21) *RAS* mutations (*NRAS* and *KRAS)* are depicted in the left graph. Patients with (n=21) and without (n=12) *RAS*opathy mutations (*NRAS*, *KRAS*, *NF1*, *CBL*, *PTPN11*) are shown on the right graph. Relative miR-125a expression was calibrated to U937, which was set to a value of 1. For all box plots, statistical differences between groups were assessed using the Mann-Whitney U-test. Wt, wildtype; CMML, chronic myelomonocytic leukemia; WBM, whole bone marrow; HSPCs, hematopoietic stem and progenitor cells. This figure has been adapted from (163) with permission from Clinical Epigenetics.

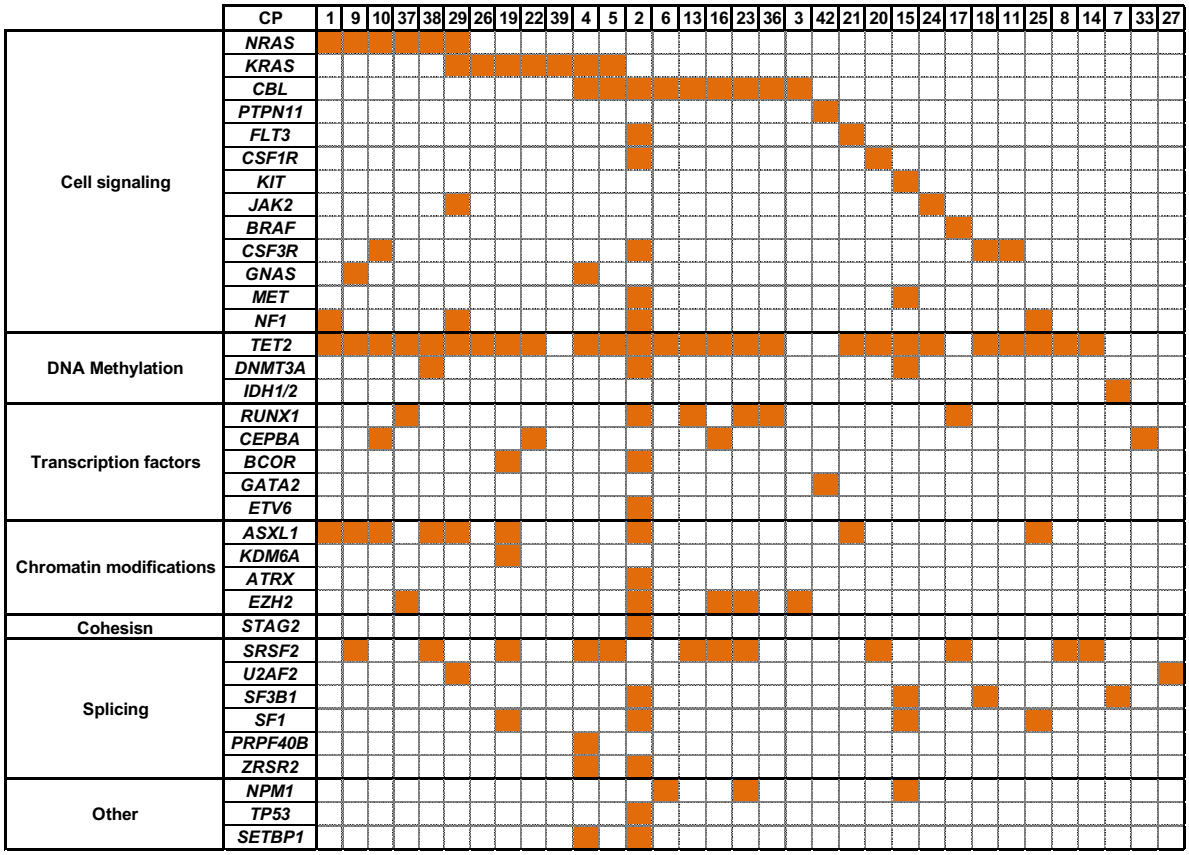

Figure 4. Recurrent mutations in CMML patients. NGS was performed for a panel of 44 genes (for complete gene list see methods section). Sequencing data was obtainable in 33/36 CMML patients. Mutation were called with a coverage of at least 1000x, a frequency in the 1000-genome project of <0.01% and a variant allele frequency (VAF) >5%. Only genes with mutations in ≥1 patient(s) are shown. CP, CMML patient. This figure has been adapted from (163) with permission from Clinical Epigenetics.

4.1.2. Decreased miR-125a expression is of functional relevance for monocytic leukemia cells

In a next step, we aimed to characterize the functional relevance of miR-125a downregulation. Initially, we measured the miR-125a expression of various myeloid leukemia cell lines to identify a suitable cell line model (Fig. 5A). Based on this analysis we selected THP1, a cell line with a distinct downregulation of miR-125a and a myelomonocytic phenotype, for stable overexpression of miR-125a using lentiviral transduction (THP1 miR-125a OE). Overexpression caused a diminished growth rate in these cells in comparison to the control cell line, transduced with an empty vector construct (Fig 5B). This observation could be corroborated in BrdU proliferation assays where miR-125a overexpression reduced the number of cells in the S-phase of the cell cycle (Fig. 5C). Moreover, we assessed the sensitivity of these cells to the apoptosis-inducing agent staurosporine using the FACS-based AnnexinV/ 7-AAD assay. Notably, THP1 miR-125a OE cells showed a substantially higher apoptotic rate in comparison to empty vector control cells (Fig. 5D). These findings suggest that miR-125a is of functional relevance in myelomonocytic leukemia cells and that an increase of miR-125a expression in cells with a decreased miR-125a expression induces anti-leukemic effects.

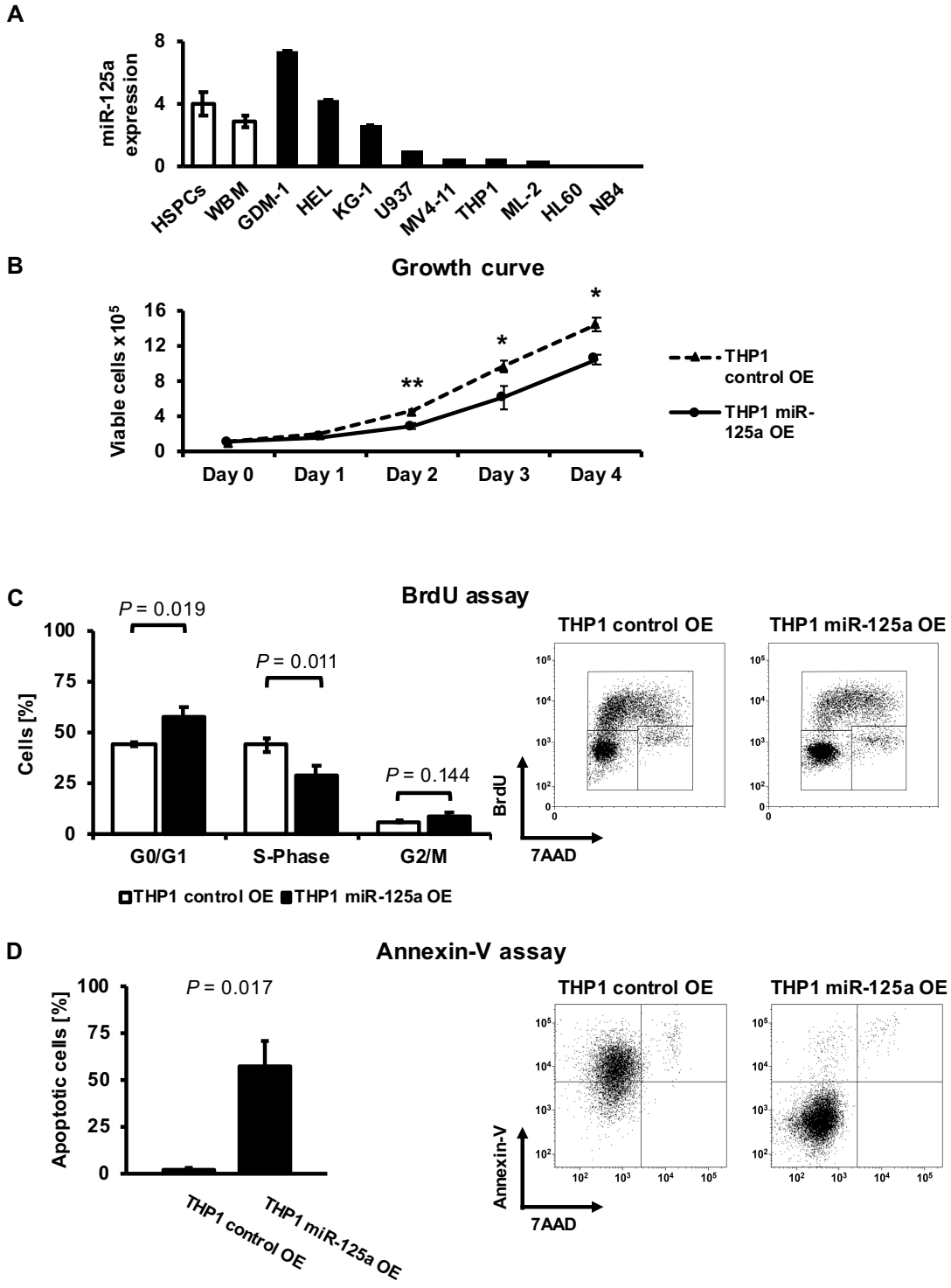

Figure 5. miR-125a expression is of functional relevance for monocytic leukemia cells. (A) For the selection of a suitable cell line model, miR-125a expression of nine myeloid leukemia cell lines was analyzed and compared to CD34+ HSPCs (n = 6) and healthy BM aspirates (n =

6). THP1 cells exhibiting a myelomonocytic phenotype and a decrease of miR-125a expression. Graphs show the relative miR-125a expression calibrated to U937, which was set to a value of 1. **(B)** The growth rate of lentivirally transduced THP1 miR-125a overexpressing cells (THP1 miR-125a OE) and empty vector controls (THP1 control OE) was assessed by seeding $1x10^5$ cells in starvation medium containing 5% FBS and subsequent counting on four consecutive days. **(C)** BrdU/7AAD cell cycle/proliferation assays of THP1 miR-125a OE and controls under 5% serum starvation. FACS plots on the left side show cells in S-phase (top gate), G0/G1-phase (left bottom gate), and G2/M-Phase (right bottom gate) after 30min of BrdU incubation. The graph on the right side shows the percentage of cells in each cell cycle phase. **(D)** miR-125a OE leads to higher sensitivity for apoptosis in Annexin-V/7AAD apoptosis assays. THP1 miR-125a OE and control cells were treatment with 0.5µM staurosporine for 4h. Cells were considered apoptotic when they stained positive for Annexin-V (upper left gate) or Annexin-V/7AAD (upper right gate). Error bars denote the mean +/- standard deviation (SD) of at least three independent experiments. Statistical differences between groups were assessed using a paired t-test. * represent $P < 0.050$, ** denotes $P < 0.010$. HSPCs, hematopoietic stem and progenitor cells; WBM, whole bone marrow; BrdU, Bromodeoxyuridine; 7AAD, 7-Aminoactinomycin. This figure has been adapted from (163) with permission from Clinical Epigenetics.

4.1.3. Decreased expression of miR-125a is caused by promoter hypermethylation and can be reversed by HMA treatment

To investigate the mechanism that causes miR-125a decrease in CMML, we hypothesized that DNA hypomethylation of the upstream/promoter region of miR-125a leads to its epigenetic repression. Mutations in epigenetic regulators are frequent in CMML and excessive methylation has been shown to influence miR-125a expression in myeloid malignancies and other cancers (176). To test this hypothesis, we performed bisulfite sequencing in U937 myeloid leukemia cells that also exhibit a decreased miR-125a expression. We focused on a 324bp locus containing 8 CpG sites in the upstream/promoter region previously characterized by Potenza et al. (177). The bisulfite sequencing analysis confirmed that CpGs in the analyzed region were

methylated (Fig. 6A). Interestingly, when we treated the cells with the HMA Aza, the methylation of CpGs could be significantly reduced.

In a next step, we asked if the treatment with HMAs would also lead to a demethylation-related increase of miR-125a expression. Therefore, we treated the myeloid leukemia cell lines THP1, U937 and NB4, all showing low expression levels of miR-125a, with the HMAs Dec and Aza. In qPCR expression analysis, we could show that the application of HMAs significantly increase miR-125a levels 24h after the treatment (Fig. 6B).

Unfortunately, we could not evaluate the methylation of the miR-125a locus in CMML patients due to low sample quality or other technical reasons. To overcome this drawback, we re-analyzed publicly available methylation array data of primary myeloid leukemia cells retrieved from the Gene Expression Omnibus (GEO; https://www.ncbi.nlm.nih.gov/geo/; GSE40870, (178)). In their experiments, Klco and colleges treated eight AML specimen in *ex-vivo* cultures with either Dec, the chemotherapeutic cytarabine or vehicle control and assessed genome wide methylation using an Illumina HumanMethylation450 BeadChip. Interestingly, their analysis also included a CpG position (cg25417766) located in the miR-125a upstream/promoter region, which showed significantly reduced methylation after Dec application compared to control or cytarabine treated samples (Fig. 6C). Although, absolute changes in methylation are small, the investigators found this to have an impact on global gene expression, suggesting a biologically relevant effect. These findings deliver additional mechanistic evidence for miR-125a repression in AML, a hematologic malignancy closely related to CMML.

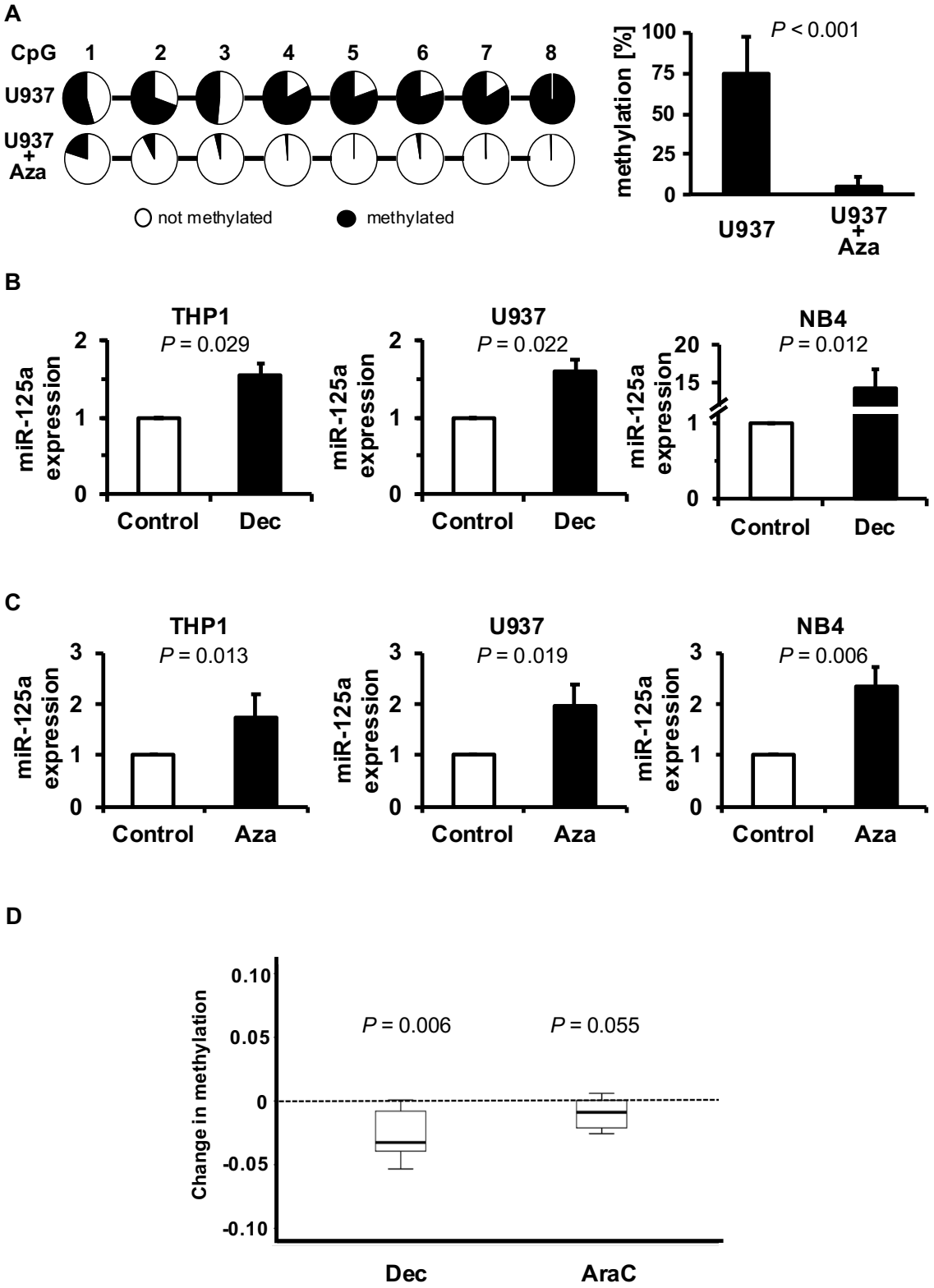

Figure 6. Decreased expression of miR-125a is caused by hypomethylation and can be reversed by HMA treatment. (A) Bisulfite sequencing of U937 cells +/- 2,5µM Aza for 24h

revealing high levels of methylation in the upstream/promoter region of untreated cells and Aza-induced hypomethylation. The graph on the right site shows the percentage of methylated sequencing reds of 8 CpGs contained in the sequencing locus. The graph on the right depicts the percentage of methylated sequencing reads of all CpGs combined +/- SD. Statistical differences between groups were assessed using a paired t-test **(B-C)** qPCR analysis of miR-125a expression in myeloid cell lines +/- 5µM Dec for 48h or 2,5µM Aza for 24h. The x-fold increase of miR-125a expression in the HMA treated condition was calibrated to the vehicle treated control, which was set to a value of 1. Graphs represent the mean of at least three independent experiments +/- SD. Statistical differences between groups were assessed using a one-sample t-test against a reference value of 1. **(D)** Methylation data of the upstream/promoter region of miR-125a in primary AML specimen (n=8) treated with Dec or cytarabine (AraC) obtained from the GEO (https://www.ncbi.nlm.nih.gov/geo/; GSE40870; (179)). Box plots depict methylation β-values with 1 representing full methylation and 0 indicating no methylation present. The change in methylation levels is plotted on the y-axis and depicts the change in methylation β-values of Dec/AraC treated cells compared to the controls, which is represented by the dashed line. Statistical differences between the control and treatment group were assessed using a one-sample t-test against a reference value of 0. Aza, azacitidine; Dec, decitabine; AraC, cytarabine. This figure has been adapted from (163) with permission from Clinical Epigenetics.

HMAs, such as Dec and Aza are frequently used in CMML therapy, thus hypomethylating therapy could also potentially increase miR-125a levels in patients. To elaborate on this assumption, we analyzed seven serial patient samples before and after treatment with either Dec or Aza. Importantly, miR-125a expression was significantly higher in specimens obtained after HMA treatment compared to diagnostic samples (Fig. 7A). Moreover, we observed that five patients with a hematologic response to HMA therapy also showed a more pronounced increase in miR-125a expression in contrast to non-responding patients (Fig. 7B). The clinical benefits associated with HMA-induced upregulation ranged from complete remissions and partial response to clinical benefit or improved marrow response and were assessed according to response criteria for MDS/MPN in adults (179). It has to be taken into consideration that the

statistical testing of these clinical observations was not possible due the small cohort size. Taken together, we could show that miR-125a expression is downregulated by hypomethylation of its upstream/promoter region, which can be reversed by treatment with HMAs in myeloid cell lines. These *in-vitro* data could be corroborated in clinical CMML specimen, where response to HMA treatment seems to be correlated with therapy response.

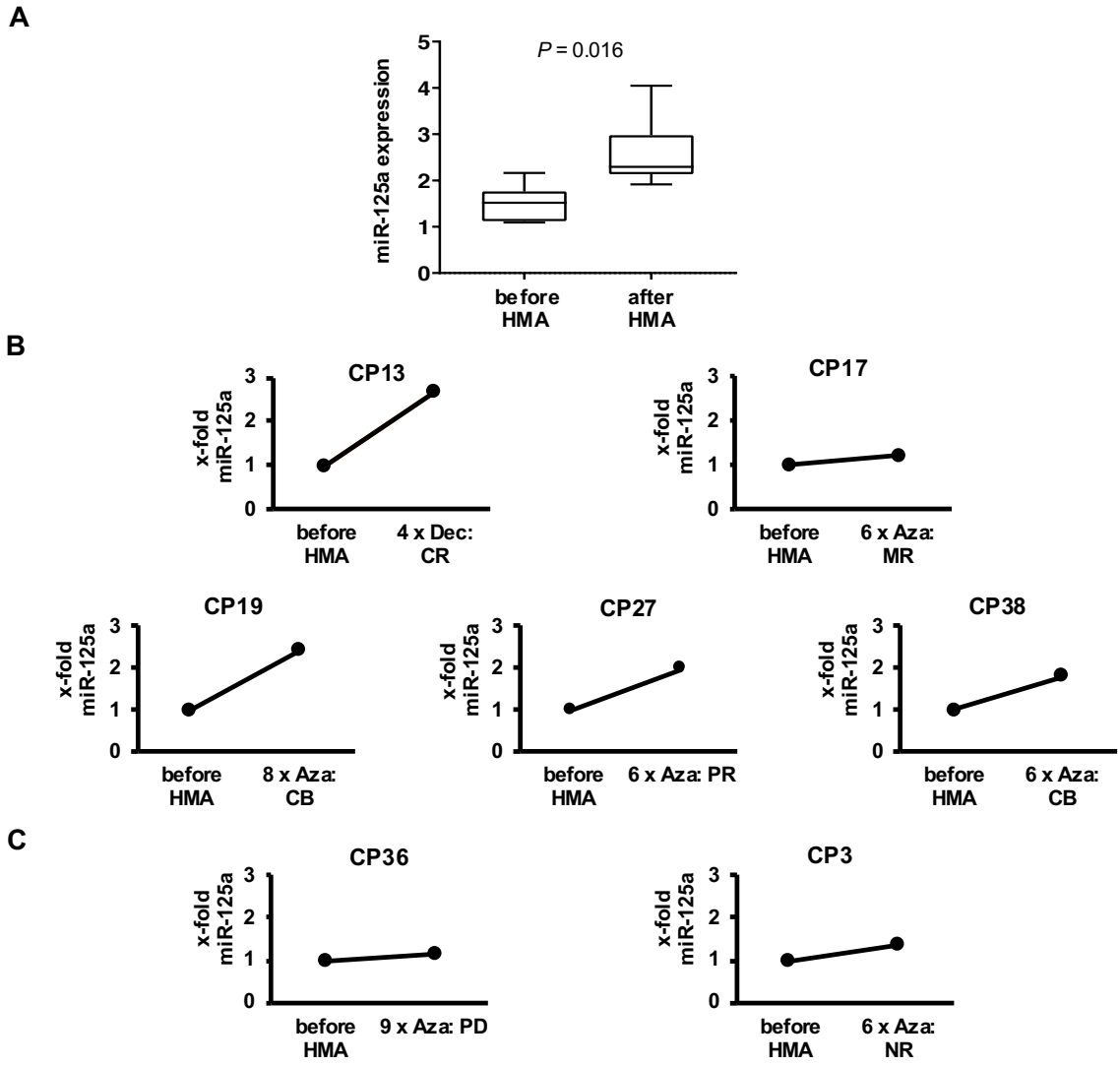

Figure 7. The expression of miR-125a increases in CMML patients after HMA treatment. **(A)** Box plots representing the miR-125a expression of seven paired CMML specimens obtained before and after HMA therapy (Dec or Aza). qPCR was employed for expression analysis, and results are shown as log-transformed x-fold expression of the calibrator U937.

Statistical differences between groups were assessed using a paired Wilcoxon signed-rank test. **(B-C)** Graphs depicting the x-fold increase of miR-125a expression levels of individual CMML patients after HMA therapy divided into responders (B) and non-responders (C). The clinical response was assessed according to recently published response criteria for MDS/MPN in adults (179). Relative miR-125a expression was calibrated to the control sample (before HMA) and set to a value of 1. HMA, hypomethylating agent; CP, CMML patient, Dec, decitabine; Aza, azacitidine, CR, complete response; MR, marrow response; CB, clinical benefit; PR, partial response; PD, progressive disease; NR, no response. This figure has been adapted from (163) with permission from Clinical Epigenetics.

4.1.4. The anti-leukemic effects of HMAs are partly mediated by increasing the expression of miR-125a

Next, we aimed to further delineate the connection between miR-125a increase and the clinical efficacy of HMAs that we observed in the serial specimen of our CMML patient cohort. Therefore, we focused on the HMA Aza, which is the most commonly used hypomethylating drug in CMML. At first, the myeloid leukemia cell lines THP1, U937 and NB4, all showing a miR-125a upregulation in response to HMAs, were treated with Aza to measure the cytotoxic effects in Annexin-V/7AAD apoptosis assays. In accordance with previously published literature, these cell underwent apoptosis after the exposure to Aza (Fig. 8, (180)).

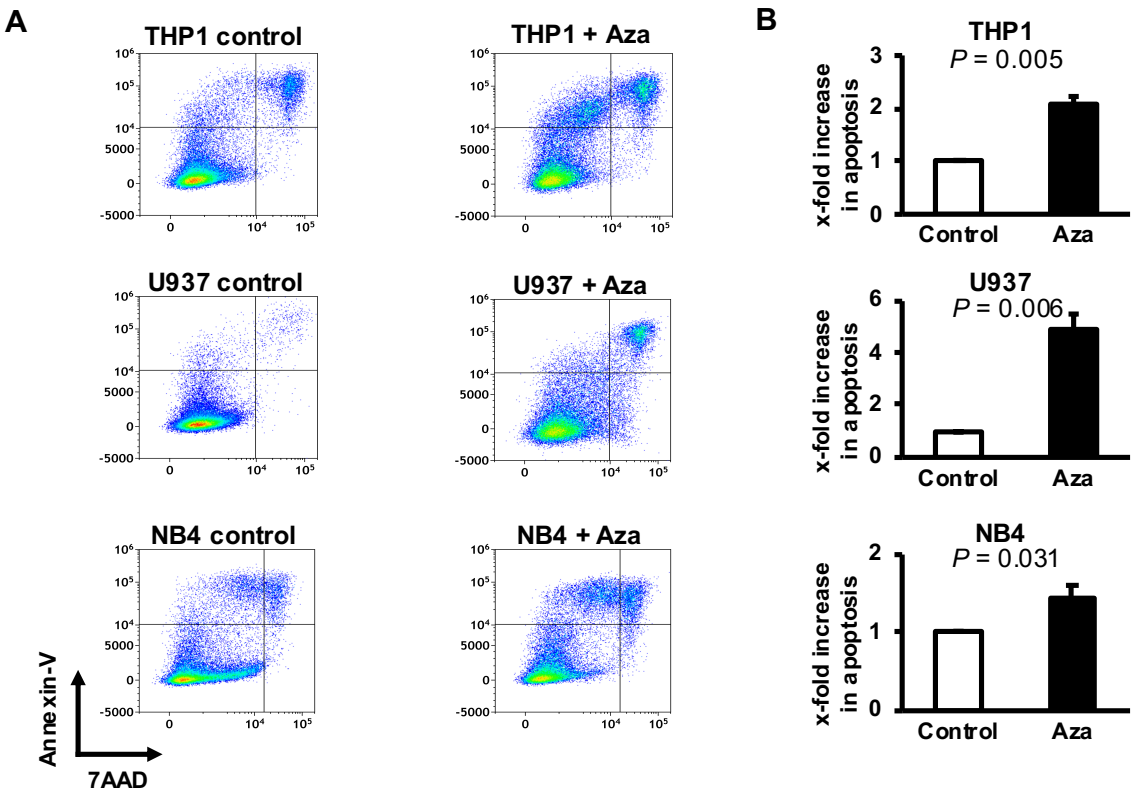

Figure 8. Aza treatment effectively induces apoptosis in myeloid cell lines. THP1, U937 and NB4 cells were incubated with 2.5µM Aza or vehicle for 24h and the induction apoptosis was measured in Annexin-V/7AAD assay. Cells were considered apoptotic when they stained positive for Annexin-V or Annexin-V/7AAD as shown in FACS plots on the left side. The graphs on the right side show the x-fold increase in apoptosis relative to the vehicle-treated control cells, which were set to a value of 1. Graphs represent the mean +/- SD of three independent experiments. Statistical differences between groups were assessed using a one-sample t-test against a reference value of 1. Aza, azacitidine. This figure has been adapted from (163) with permission from Clinical Epigenetics.

To see if these cytotoxic effects were actually linked to miR-125a upregulation, we performed transient miR-125a knockdown using a small hairpin inhibitor (shi-RNA) in THP1 cells before subsequent Aza treatment. Indeed, qPCR analysis confirmed that the miR-125a specific shi-RNA prevented miR-125a upregulation and lead to constant expression levels after the

application of Aza (Fig. 9A). Most interesting however, the blocking of miR-125a upregulation leads to a significant reduction of Aza efficacy in apoptosis assays, indicating that the increase of miR-125a is mediating some of the anti-leukemic effects of this drug (Fig. 9B). To further corroborate these findings, we additionally included the myeloid cell line U937. As shi-RNA-mediated knockdown could not be sufficiently calibrated in these cells, we employed CRISPR/Cas9 technology to knockout miR-125a completely. Sequencing of the miR-125a locus and qPCR expression analysis could confirm the homozygous deletion of miR-125a (Fig. 9C). In line with our previous experiments, miR-125a deletion alleviated the anti-leukemic effects of Aza when compared to parental control cells (Fig. 9D). These results further support the role of miR-125a as a mediator for Aza efficacy in myeloid cells.

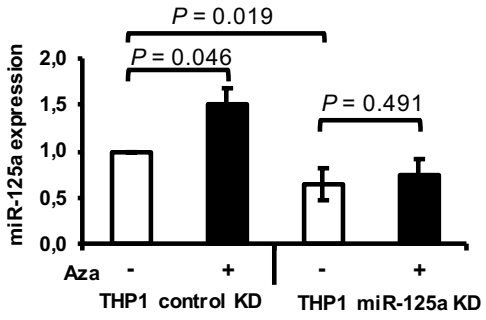
P = 0.019
P = 0.046
P = 0.491
miR-125a expression
2,0
1,5
1,0
0,5
0,0
Aza - + - +
THP1 control KD
THP1 miR-125a KD

B

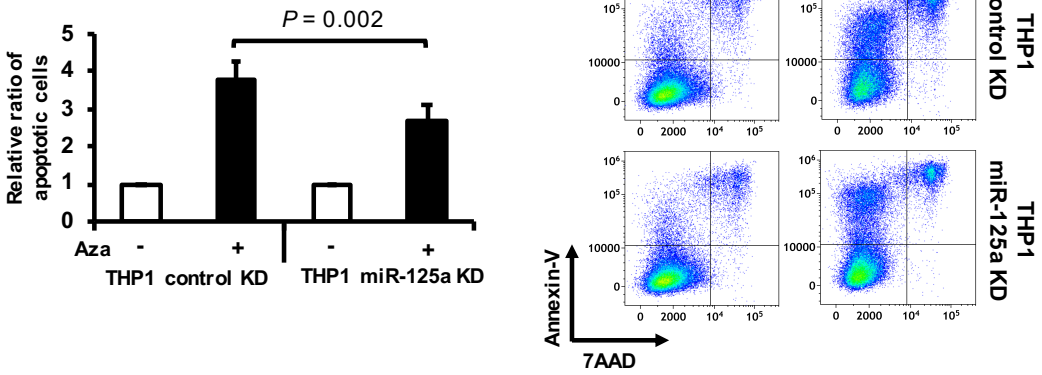
P = 0.002
Relative ratio of apoptotic cells
5
4
3
2
1
0
Aza - + - +
THP1 control KD
THP1 miR-125a KD
Control
Aza
THP1 control KD
THP1 miR-125a KD
Annexin-V
7AAD

C

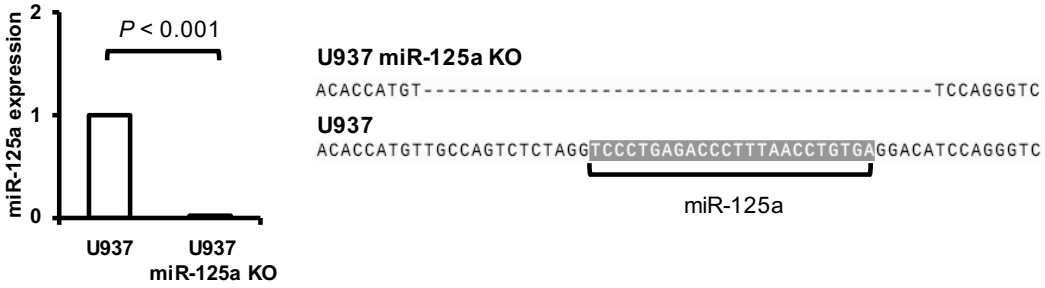
P < 0.001
miR-125a expression
2
1
0
U937
U937 miR-125a KO
U937 miR-125a KO
ACACCATGT----------TCCAGGGTC
U937
ACACCATGTTGCCAGTCTCTAGGTCCCTGAGACCCTTTAACCTGTGAGGACATCCAGGGTC
miR-125a

D

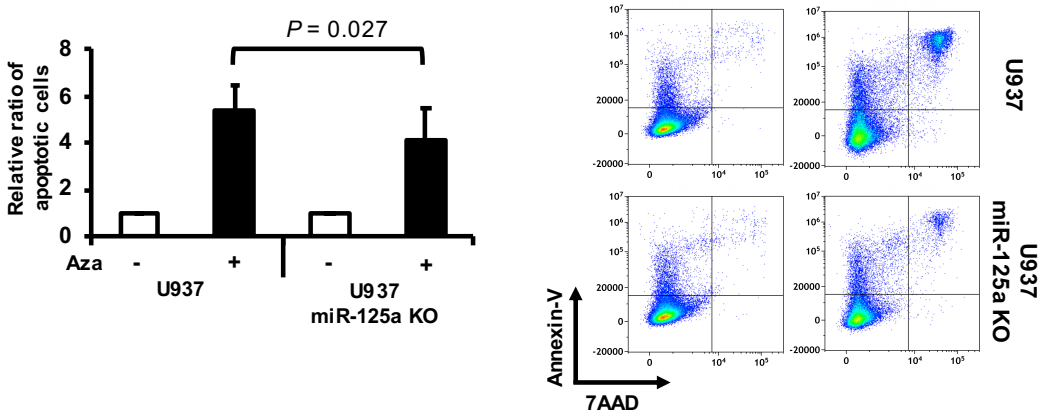
P = 0.027
Relative ratio of apoptotic cells
8
6
4
2
0
Aza - + - +
U937
U937 miR-125a KO
Control
Aza
U937
U937 miR-125a KO
Annexin-V
7AAD

Figure 9. miR-125a partly mediates the cytotoxic effects of Aza in myeloid cells. **(A)** THP1 cells were transfected with miR-125a shi-RNA or scrambled shi-RNA control (THP1 miR-125 KD and THP1 control KD) and treated for 24h with 2,5µM Aza. qPCR was employed to confirm the successful shi-RNA mediated knockdown and the blocking of Aza-induced miR-125a upregulation in THP1 miR-125a KD cells. Statistical differences between the untreated and treated THP1 control KD cells as well as the miR-125a KD cells were assessed by one-sample t-test. Differences between THP1 miR-125a with/without Aza were calculated using a paired t-test. **(B)** THP1 miR-125a KD cells show reduced apoptosis after Aza treatment compared to control KD cells in Annexin-V/7AAD apoptosis assays indicating that miR-125a upregulation aFffects the anti-leukemic effects of Aza. Cells were considered apoptotic when they stained positive for Annexin-V or Annexin-V/7AAD. The graphs denote the x-fold change in apoptosis relative to the vehicle-treated control, which was set to a value of 1. Graphs represent the mean of at least three independent experiments +/- SD and statistical differences between Aza treated cells were calculated using a paired t-test. **(C)** CRIPSPR/Cas9 genome editing was employed to delete miR-125a in U937 cells (U937 miR-125a KO). The knockout of miR-125a was verified with qPCR analysis shown on the left side and sequencing of the miR-125a locus on the right side using parental U937 as a reference control. **(D)** U937 miR-125a KO cells exhibited significantly lower levels of cell death after Aza treatment than parental control cells. Apoptosis was analyzed after the application of 5µM Aza for 24h in Annexin-V/7AAD assays. Graphs are represented and analyzed in the same way as described for the Annexin-V/7AAD assays above. Aza, azacitidine; 7AAD, 7-Aminoactinomycin. This figure has been adapted from (163) with permission from Clinical Epigenetics.

Lastly, we also treated THP1 miR-125a OE cells with Aza to see if high miR-125a levels would influence drug response. In qPCR miR-125a expression analysis we could show, that Aza treatment further increases miR-125a expression (Fig. 10A). Moreover, Aza caused an additional increase of apoptosis in comparison to control treated THP1 miR-125a OE cells, suggesting additive or synergistic anti-leukemic effects (Fig. 10B).

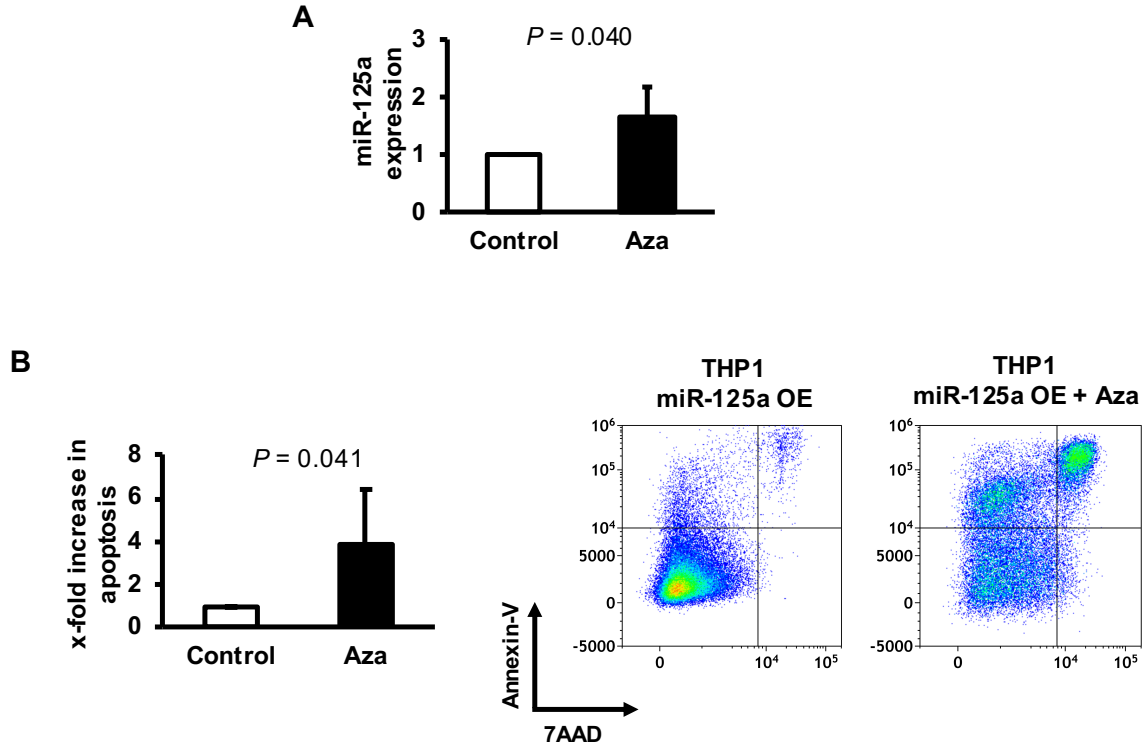

Figure 10. Combined Aza treatment and miR-125a overexpression exhibit a synergistic or additive effect in myeloid cells. (A) THP1 cells stably overexpressing miR-125a were incubated with 2.5µM Aza for 24h. qPCR analysis showed an additional increase of miR-125a levels after Aza treatment. **(B-C)** Annexin-V/7AAD apoptosis assays also demonstrate a further increase in cell death after Aza treatment of THP1 miR-125a OE cells suggesting a synergistic or additive effect. Graphs show the x-fold increase relative to the vehicle treated control, which was set to a value of 1 and represent the mean of at least three independent experiments +/- SD. Cells were considered apoptotic when they stained positive for Annexin-V or Annexin-V/7AAD. Statistical differences between groups were assessed using a one-sample t-test against a reference value of 1. Aza, azacitidine; 7AAD, 7-Aminoactinomycin. This figure has been adapted from (163) with permission from Clinical Epigenetics.

4.2. **Part 2**: The co-occurrence of *EZH2* inactivation and *RAS* pathway mutations hyperactivates MAPK/ERK-signaling and increases MEK inhibitor sensitivity in myeloid malignancies

4.2.1. *EZH2* inactivation is more frequent in myeloid leukemia patients with *RAS* pathway mutations

Initially, we re-analyzed NGS data from our CMML cohort, described above, and concentrated on molecular co-occurrences in *RAS*-mutated CMML. In this screening approach, we observed that *RAS* mutations were often co-existing with mutations in *EZH2*. (Fig. 4). To verify that *EZH2* mutations and *RAS* mutations indeed frequently co-exist in CMML we analyzed NGS data of 260 CMML patients from the Austrian Biodatabase for CMML (155). Thereby, we focused on mutations in *EZH2* and in genes modifying RAS. This includes *NRAS* and *KRAS* itself, as well as genes modifying *RAS (CBL, PTPN11* and *NF1)*. Mutations in these genes are hereafter referred to as RAS^{mut}. From these 260 patients 112 (43,1%) carried at least one RAS^{mut}, while mutations in *EZH2* were detected in 32 (19,2%) cases. Both mutations co-occurred in 23 of 260 (12,3%) patients. Of the 112 RAS^{mut} patients 28,6% (32/112) also had a *EZH2* mutations while 64% (32/50) of *EZH2* mutated patients were also carrying a RAS^{mut}, simultaneously. Remarkably, *EZH2* mutations were significantly enriched in patients carrying at least one RAS^{mut} (28.6% in RAS^{mut} vs. 12.2% in RAS^{wt}; Fig. 11A-B). To ensure that the detected mutations were relevant for myeloid pathogenesis we only included mutation variants that were either i) described in the literature to be clinically relevant for the treatment of MN (diagnostic, prognostic and/or treatment specific), ii) demonstrated to be pathogenic in *in-vitro* or *in-vivo* assays or iii) classified as pathogenic or likely pathogenic in the mutation database Varsome (https://varsome.com/) and/or COSMIC (Catalogue of Somatic Mutations in Cancer, https://cancer.sanger.ac.uk/cosmic, Table 5). According to these criteria, we excluded the mutations *NF1* p.M577I and *CBL* p.D460del, that were detected in one patient, each. These variants are listed, as the affected carriers were also detected with pathogenic *NRAS* p.G12D and *CBL* p.H398Y mutations, respectively. Additionally, we decided to include the *EZH2* p.D185H mutation into our analysis. This variant has been discussed to be either a pathogenic

mutation or a benign nucleotide polymorphism. Recent publications, however, demonstrate that the p.D185H aberration compromises EZH2 methyltransferase activity, is associated with decreased EZH2 protein levels in MN cells and represents a risk factor for carcinogenesis (181–184).

Additionally, we aimed to delineate if the co-occurrence of *EZH2* mutations and *RAS*^{mut} also negatively affects the clinical outcome for CMML patients. Indeed, the analysis of clinical parameters from CMML patients with both aberrations show a significantly shortened overall survival (median 14 vs 29 months; Fig. 11C).

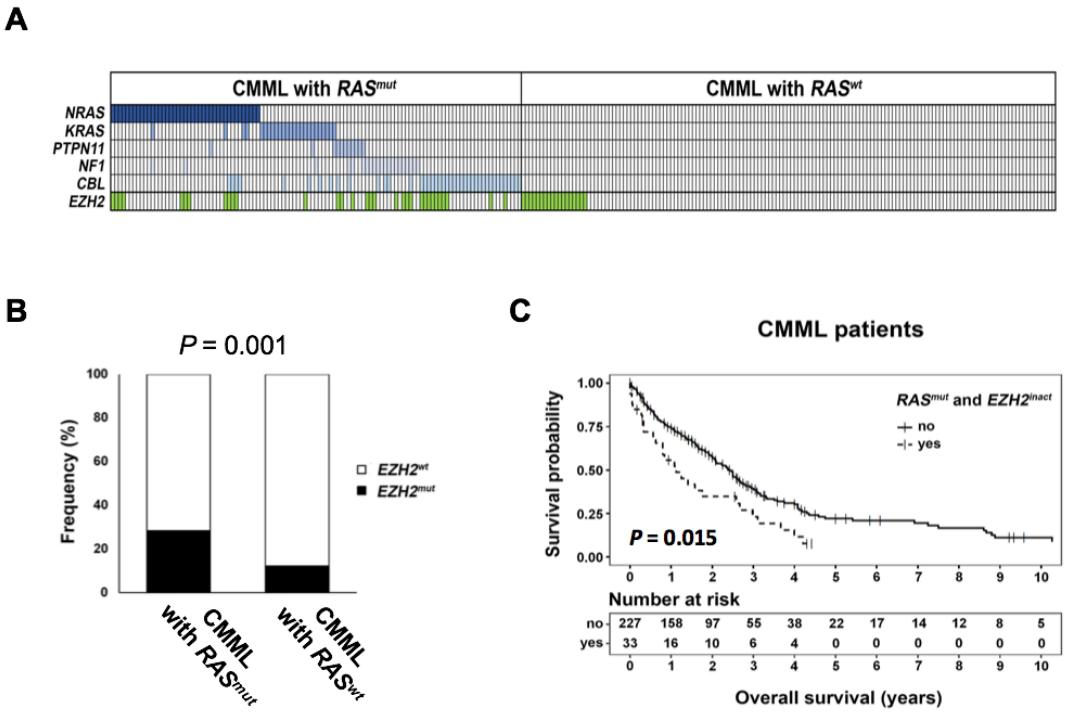

Figure 11. Co-existence of *RAS*^{mut} and *EZH2*^{inact} in CMML. (A-B) *EZH2* mutations show a significant enrichment in CMML patients also harboring *RAS*^{mut} in NGS data obtained from the ABCMML (155). The upper graph depicts mutations in *EZH2* (green) and *RAS* modifiers (*RAS*^{mut}, defined as mutations in *KRAS* and *NRAS*, *NF1*, *PTPN11* and *CBL; blue*) found in a cohort of 260 CMML patients. **(C)** Kaplan-Maier plots showing the inferior survival of CMML patients with combined *RAS*^{mut} and *EZH2*^{inact} compared to patients without the genetic

aberrations (median survival 14 vs 29 months). Vertical dashes indicate censored events. Statistical significance for the NGS mutation analysis was calculated using Fisher's exact test. For Kaplan-Maier plots, group differences were calculated using a log-rank test. CMML, chronic myelomonocytic leukemia. This figure has been adapted from (174) with permission from Leukemia.

Table 5

NRAS	A59D (1)	G12R (3)	G13V (5)	Y64N (1)
	G12A (1)	G12V (5)	Q61K (2)	
	G12D (16)	G13D (4)	Y64D (3)	
KRAS	A146T (2)	G12D (3)	G13C (1)	Q22K (1)
	A18D (3)	G12R (3)	G13D (1)	Q61R (1)
	D33E (1)	G12S (2)	G60V (1)	G60_Q61insRL(1)
	G12C (1)	G12V (1)	L19F (1)	T58I (2)
PTPN11	A72T (1)	G503R (1)	M504V (2)	V203M (1)
	D286Y (1)	G93E (1)	P144L (1)	
	D61G (1)	I96F (1)	Q510H (1)	
NF1	A2389V (1)	I1641T (1)	R1477T (1)	V533F (1)
	D176E (3)	I2015N (1)	R2258* (1)	Y2264* (1)
	E977* (1)	I558T (1)	R2452C (1)	Y794C (1)
	F1536S (1)	L1015P (1)	T1184fs (1)	Y1930fs (1)
	G751V (1)	M577I (1)	V1707D (1)	
CBL	C381R (1)	C416S (3)	F418S (2)	R420L (2)
	C381S (1)	C416W (1)	G413D (1)	R420Q (1)
	C381W (1)	C416Y (1)	H398Y (1)	S376P (1)
	C381Y (1)	C419S (1)	K382E (1)	Y371C (1)
	C384Y (1)	C419Y (1)	L380P (3)	Y371H (3)
	C404R (1)	D390H (1)	P417R (1)	E366fs (1)
	C404Y (3)	D390V (1)	P417S (2)	D460del (1)
			R420G (1)	
EZH2	D185H (28)	C536F (1)	K740Sfs (1)	R298H (1)
	D677G (1)	C571Y (1)	M121K (1)	R690H (2)
	Q553del (1)	C695W (1)	N130D (1)	S651L (1)
	S371R (1)	D659G (1)	N668Y (1)	T683I (1)
	D730*fs*1 (1)	G660E (1)	P587fs (1)	
	V675M (1)	H501Q (1)	R288Q (1)	

Table 5. Detected mutations in the ABCMML cohort. NGS sequencing results showed pathogenic mutations that were classified as either *RAS*^{mut} or *EZH2* mutated according to the following criteria: mutations were i) described in the literature to be clinically relevant for the treatment of MN (diagnostic, prognostic and/or treatment specific), ii) demonstrated to be pathogenic in *in-vitro* or *in-vivo* assays or iii) classified as pathogenic or likely pathogenic in the mutation database Varsome (https://varsome.com/) and/or COSMIC (Catalogue of Somatic Mutations in Cancer, https://cancer.sanger.ac.uk/cosmic). Non-pathogenic variants of patients carrying additional pathogenic or likely pathogenic mutations are marked in green. This table has been adapted from (174) with permission from Leukemia.

In a next step, we asked if our findings from CMML are also relevant for other related MNs, such as AML. Therefore, we analyzed a publicly available dataset from The Cancer Genome Atlas , including NGS, cytogenetic and gene expression data of 187 AML patients (171,185). Here we included patients with *EZH2*^{inact} caused by mutations and/or chromosomal deletion. From 187 AML patients 33 (17,6%) were detected with one or more *RAS*^{mut}, while 25 (13,4%) carried *EZH2*^{inact} and 9 (5%) patients exhibited both genetic lesions. Of the 33 *RAS*^{mut} patients 9 (27%) also had *EZH2*^{inact}, whereas 9 (36%) out of 25 *EZH2*^{inact} positive patients were also carrier of at least one *RAS*^{mut}. In agreement with our findings in CMML, *EZH2*^{inact} were significantly more frequent in *RAS*^{mut} AML patients (27,3% in in *RAS*^{mut} vs. 10.4% in *RAS*^{wt}; Fig. 12A-B, Tab. 6). The pathogenicity was evaluated as described above for the ABCMML cohort. In line with these criteria we excluded the in-frame *NF1*(+)LRRC37B(+) fusion gene, due to uncertain significance. Nevertheless, the patient with this variant was still included into the *RAS*^{mut} group, as our analysis revealed an additional activating *NRAS* p.G12D mutation.

Moreover, the co-occurrence of *EZH2* and *RAS* aberrations correlated with dismal prognosis and caused shorter overall survival (median survival 7 vs 19 months) underlining the clinical relevance of this molecular pathology (Fig. 12C).

In addition to missense mutations and chromosomal deletion, the reduction in gene expression has been described as a mechanism of *EZH2* inactivation in MN (150). Therefore, we analyzed

162 AML cases with available expression data and compared the *EZH2* mRNA levels of patients with (n=28) and without (n=134) *RAS*^{mut}. This revealed significantly diminished *EZH2* expression in patients with *RAS*^{mut} indicating that *EZH2* downregulation in addition to mutations and genomic copy number alterations are consistently associated with mutations modulating the RAS pathway in MN (Fig. 12D).

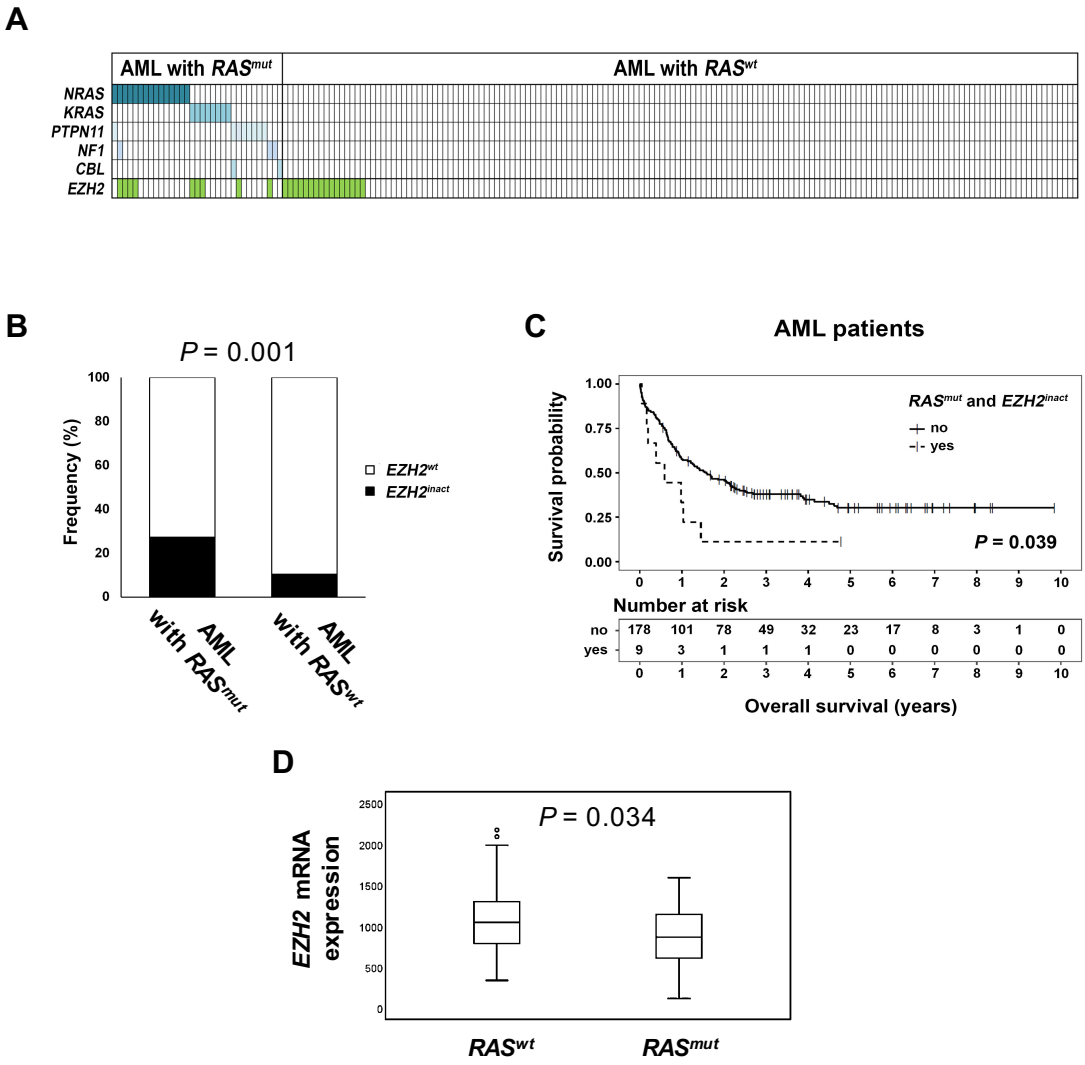

Figure 12. Co-existence of *RAS*^{mut} and *EZH2*^{inact} in AML. (A-B) NGS analysis of 187 AML cases show that patients with *RAS*^{mut} are more likely to carry additional *EZH2*^{inact} compared to patients without *RAS*^{mut}. *EZH2*^{inact} are defined as *EZH2* mutations and/or copy number losses. *RAS*^{mut} are defined as mutations in *KRAS* and *NRAS*, *NF1*, *PTPN11* and *CBL*. Cytogenetic and NGS data was obtained from The Cancer Genome Atlas (104). Colored fields indicate the

presence of at least one mutation (for *RAS*^{mut}) or *EZH2* inactivation (*EZH2*^{inact}), respectively. **(C)** Survival analysis of AML patients with combined *RAS*^{mut} and *EZH2*^{inact} displaying a significantly shortened overall survival (7 vs 19 months). Vertical dashes indicate censored events. **(D)** *EZH2* expression analysis of 162 AML patients from the TCGA cohort showing significantly lower *EZH2* mRNA levels in patients with *RAS*^{mut}. *RAS*^{mut} was present in 28 cases while 134 patients were classified as *RAS*^{wt}. *EZH2* expression is displayed as V2-RNA-seq by Expectation-Maximization (V2 RSEM). Statistical significance for the NGS mutation analysis was calculated using Fisher's exact test. For Kaplan-Maier plots group differences were calculated using a log-rank test and differences in *EZH2* mRNA expression were assessed employing Mann-Whitney U-test. AML, acute myeloid leukemia. This figure has been adapted from (174) with permission from Leukemia.

Table 6

NRAS	G12C(1) G12D(3)	G13D(5) Q61H(2)	Q61K(2) Q61P(1)	Q61R(1)
KRAS	G12D(2) G12V(1)	G13D(1) I36M(1)	A59E(1) Q61H(1)	A146T(1)
PTPN11	G60V(1) F71L(1)	A72V(1) P491L(1)	S502P(1) Q510H(1)	Q510L(1) I545L(1)
NF1	R1276Q(1) R1306*(1)	NF1(+)LRRC37B(+) fusion (In-frame)(1)		
CBL	Q367R(1)	X366_splice(1)		
EZH2	E740Afs*24 I739Mfs*25(1)		R685H(1)	X727_splice(1)

Table 6. Detected mutations in the TCGA cohort. NGS sequencing results showed pathogenic mutations that were classified as either *RAS*^{mut} or *EZH2*^{inact} according to the following criteria: mutations/chromosomal aberrations were i) described in the literature to be clinically relevant for the treatment of MN (diagnostic, prognostic and/or treatment specific), ii) demonstrated to be pathogenic in *in-vitro* or *in-vivo* assays or iii) classified as pathogenic or likely pathogenic in the mutation database Varsome (https://varsome.com/) and/or COSMIC (Catalogue of Somatic Mutations in Cancer, https://cancer.sanger.ac.uk/cosmic). Non-

pathogenic variants of patients carrying additional pathogenic or likely pathogenic mutations are marked in green. This table has been adapted from (174) with permission from Leukemia.

4.2.2. Inactivation of *EZH2* activity amplifies RAS^{mut} signaling in myeloid cells

Following our findings that RAS^{mut} and $EZH2^{inact}$ worsen patient survival we aimed to investigate the underlying cellular mechanism to this phenomenon. We hypothesized, that the loss of EZH2 activity affects oncogenic activation of mutant RAS signaling and its downstream effectors in the MAPK/ERK pathway. Similar observations have been made for NRAS mutations in combination with TET2 deficiency, which caused RAS hyperactivation and led to the development of a highly aggressive CMML-like disease in mice (104). To investigate this phenomenon in relation to EZH2, we chose the myeloid leukemia cells THP1 and HL60, which both carry hotspot mutation in *NRAS* (p.G12D and p.Q61L) and exhibit a normal EZH2 status. To verify that EZH2 levels were not downregulated in comparison to other cell lines, we analyzed the mRNA expression data from the Cancer Cell Line Encyclopedia, which showed no apparent $EZH2^{inact}$ (Fig. 13, (172)). This figure has been adapted from (174) with permission from Leukemia.

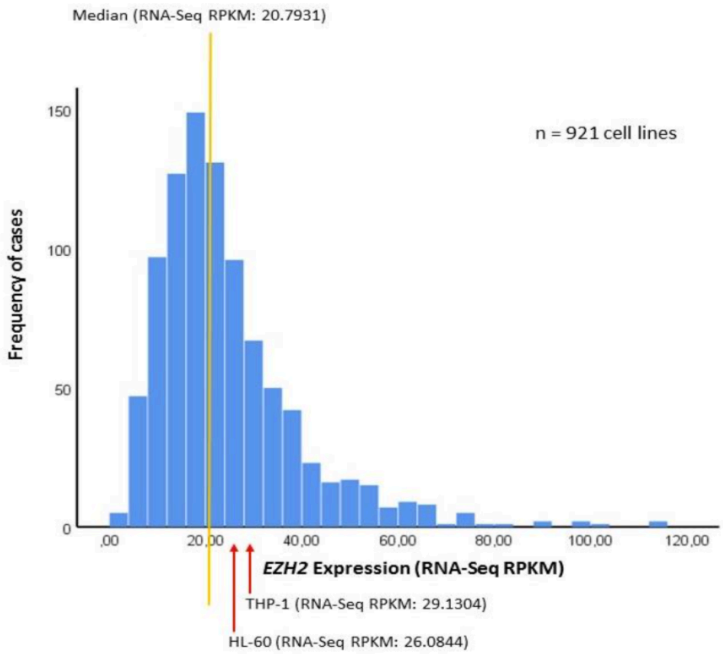

Figure 13. THP1 and HL60 cells exhibit normal EZH2 expression levels. EZH2 mRNA expression levels of 921 cell lines were analyzed via the Cancer Cell Line Encyclopedia showing no *EZH2* downregulation in THP1 or HL60 cells (172). The dataset was retrieved using the cBioPortal (173). The histogram depicts RNA sequencing reads per kilobase million (RPKM) values with the median expression being indicated by the orange line. This figure has been adapted from (174) with permission from Leukemia.

To mimic $EZH2^{inact}$ in these cell lines we utilized the pharmacological EZH2 inhibitors GSK-126 and DZNep. While GSK-126 inhibits the catalytic activity of EZH2, DZNep also causes EZH2 protein degradation. Administration of both compounds effectively blocked EZH2-mediated H3K27me3 in THP1 and HL60 cells. Most importantly, EZH2 inhibition also hyperactivated the RAS-MAPK/ERK pathway in both cell lines compared to vehicle treated controls. This was evident in immunoblots showing increased ERK phosphorylation (pERK), suggesting that averting EZH2 activity augments RAS^{mut} signaling in myeloid cells (Fig. 14A-B).

To dismiss the possibility that the hyperactivation of the RAS pathway caused by EZH2 inactivation was influenced by off-target effects of these drugs, we additionally created stable *EZH2* knockdown cell lines. Therefore, we employed lentiviral transduction of an *EZH2*-specific small hairpin RNA (shRNA) or empty vector constructs in THP1 and HL60 cells (*EZH2* KD and control KD). This caused a distinct reduction in EZH2 levels in these cell lines. Additionally, *EZH2* KD attenuated H3K27 trimethylation and lead to the significant augmentation of pERK levels, supporting the specific effects of EZH2 inhibition from our previous experiments (Fig. 15A-B).

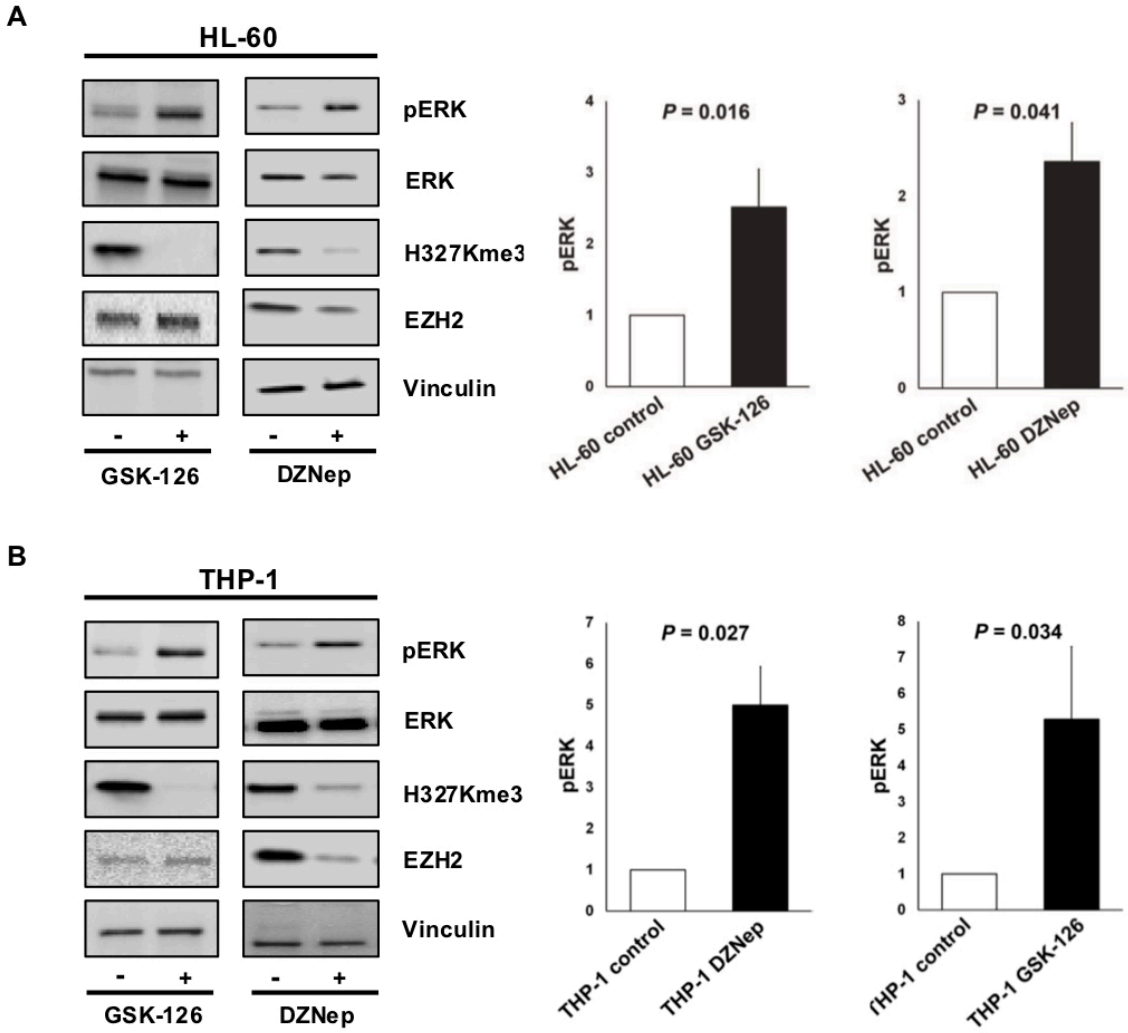

Figure 14. Pharmacologic inhibition of *EZH2* amplifies mutant RAS-signaling in myeloid leukemia cells. (A-B) The hyperactivation of MAPK/ERK activation in *RAS*^{mut} THP1 and HL60 cells was evaluated with immunoblots after pharmacologic inhibition of EZH2. Both cell lines were treated with 3µM GSK-126 for 7 days or 2µM DZNep for 24h, respectively. Immunoblots were labeled with anti-H3K27me3 antibodies to assess EZH2 inhibition and anti-pERK antibodies for MAPK/ERK hyperactivation. Graphs show the x-fold increase of pERK relative to the vehicle treated control, which was set to a value of 1 and represent the mean of at least three independent experiments +/- SD. Statistical differences between the treatment and control group were assessed using a one-sample t-test with a reference value of 1. This figure has been adapted from (174) with permission from Leukemia.

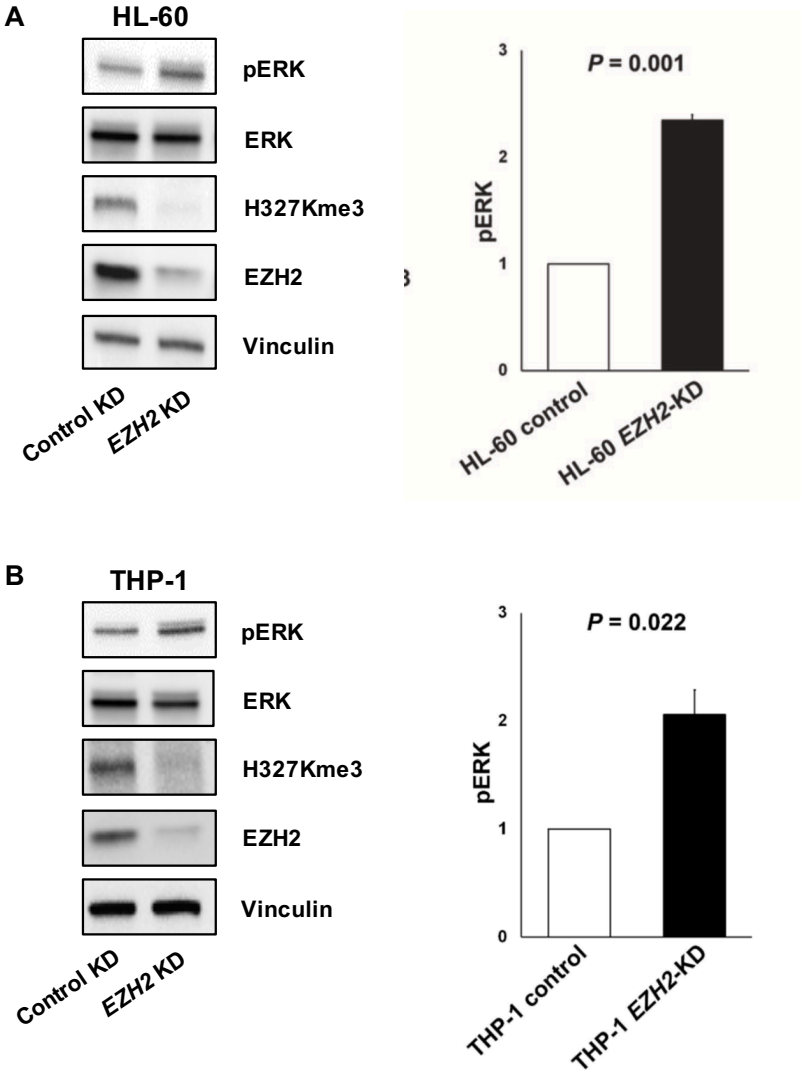

Figure 15. *EZH2* knockdown in myeloid leukemia cells causes the hyperactivation of mutant RAS signaling. (A-B) The *RAS*^{mut} myeloid cell lines HL60 (A) and THP1 (B) were transduced with *EZH2*-specific shRNA (*EZH2* KD) or with an empty vector control (control KD) to induce the knockdown of EZH2. The activation of pERK was assessed using immunoblots. In line with the EZH2 inhibitor experiments (Fig. 14), *RAS*^{mut} cells with shRNA-mediated *EZH2*^{inact} show decreased H327Kme3 and significantly higher pERK levels. Graphs denote the x-fold increase of pERK relative to the vehicle treated control, which was set to a value of 1 and represent the mean of at least three independent experiments +/- SD. Statistical differences between the knockdown and control cells were assessed using a one-sample t-test with a reference value of 1. This figure has been adapted from (174) with permission from Leukemia.

4.2.3. The co-occurrence of *EZH2*^{inact} and *RAS*^{mut} sensitize myeloid cells to MEK inhibition

It has been proposed that cancer cells with distinct driver mutations or genetic aberrations can solely rely on the excessive activation of a dominant growth pathway (186). Therefore, we hypothesized that the hyperactivation of MAPK/ERK signaling, triggered by the combination of *EZH2*^{inact} and *RAS*^{mut}, would increase the oncogenic dependency of myeloid cells. In this case, the cells would become vulnerable to targeted inhibition of the dominant oncogene pathway. To investigate this assumption, we blocked *RAS*^{mut} signaling in THP1 and HL60 *EZH2* KD cells by using 5µM of the pharmacologic MEK inhibitor U0126 and measured cell survival in AnnexinV/ 7-AAD assays. As expected, the application of U0126 successfully mitigated ERK activation and induced cell death after 24h (Fig. 16A-B). More importantly however, myeloid cells with *EZH2* KD showed significantly higher levels of apoptosis after inhibitor treatment compared to control KD cells. These observations could be supported with BrdU proliferation assays, which also showed reduced cell cycle progression in *EZH2* KD cells treated with U0126 compared to control KD cells (Fig. 16C). These results give a strong indication that *RAS*^{mut} myeloid leukemia cells become more dependent on *EZH2*^{inact}-induced ERK hyperactivation, evidenced by increased MEK inhibitor sensitivity.

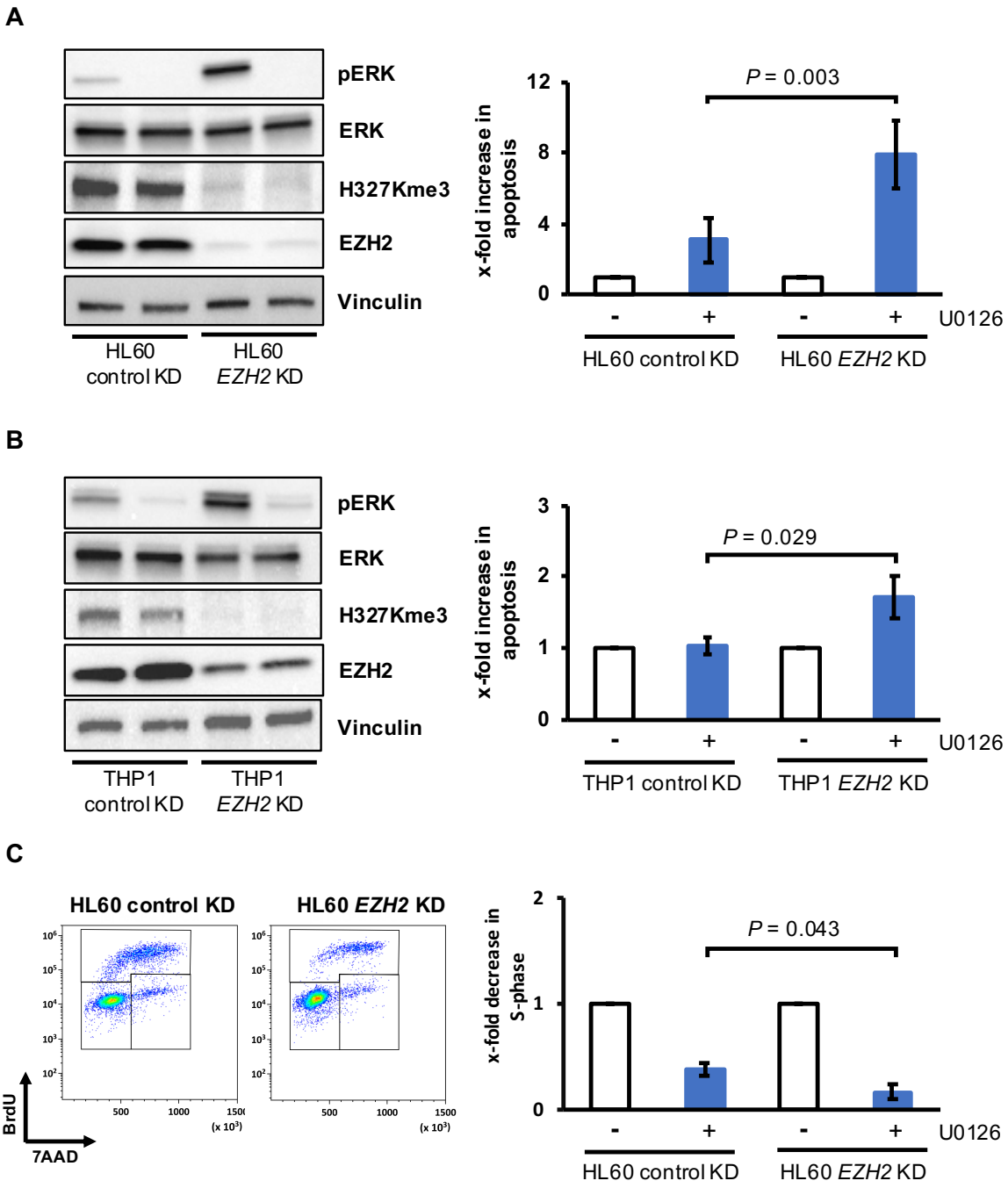

Figure 16. Myeloid leukemia cells with combined *RAS*^{mut} and *EZH2* knockdown show increased sensitivity to the MEK inhibitor U0126. (A-B) HL60 (A) and THP1 (B) cells with lentiviral knockdown of *EZH2* (*EZH2* KD) or empty control vector (control KD) were treated with 5µM of the MEK inhibitor U0126 for 24h. Successful MAPK/ERK pathway inhibition

was evaluated in immunoblots labeled with anti-pERK antibodies. MEK inhibitor sensitivity was assessed using Annexin-V/7AAD apoptosis assays shown in the graphs on the right side. The graphs denote the x-fold increase in apoptosis in U0126-treated cells compared to the respective vehicle-treated controls. **(C)** These findings could be supported with BrdU/7AAD cell cycle/proliferation assays performed in HL60 cells with *EZH2* KD and respective controls. U0126 treatment caused a reduction in proliferating cells progressing to the S-phase in *EZH2* KD cells compared to control KD cells. FACS blots on the left side show cells in S-phase (top gate), G0/G1-phase (left bottom gate), and G2/M-Phase (right bottom gate) after 30min of BrdU incubation. Graphs show the x-fold decrease in cells progressing to the S-phase in U0126-treated cells relative to vehicle-treated controls, which were set to a value of 1. All graphs represent the mean of at least 3 independent experiments +/- SD. Statistical differences were calculated using a paired t-test. This figure has been adapted from (174) with permission from Leukemia.

4.2.4. Gene expression analysis of myeloid cells with *EZH2*^{inact} upregulates RAS-signaling signatures

Finally, we wanted to identify EZH2 specific target genes that lead to the hyperactivation of MAPK/ERK signaling in myeloid leukemia cells carrying *RAS*^{mut} and *EZH2*^{inact}. As described above, *EZH2* KD leads to the loss of H3K27me3 causing the transcriptional de-repression of specific gene patterns. To investigate this phenomenon, we conducted RNA-seq followed by gene set enrichment analysis (GSEA) in HL60 *EZH2* KD cells and respective controls. This revealed a multitude of upregulated genes in cells with *EZH2* KD (Fig. 17A). GSEA showed that many of the activated genes belong to cancer relevant pathways (Tab. 7). Interestingly, two of the most significantly upregulated gene sets included RAS and RAF pathway genes, know to activate MAPK/ERK signaling (Fig. 17B).

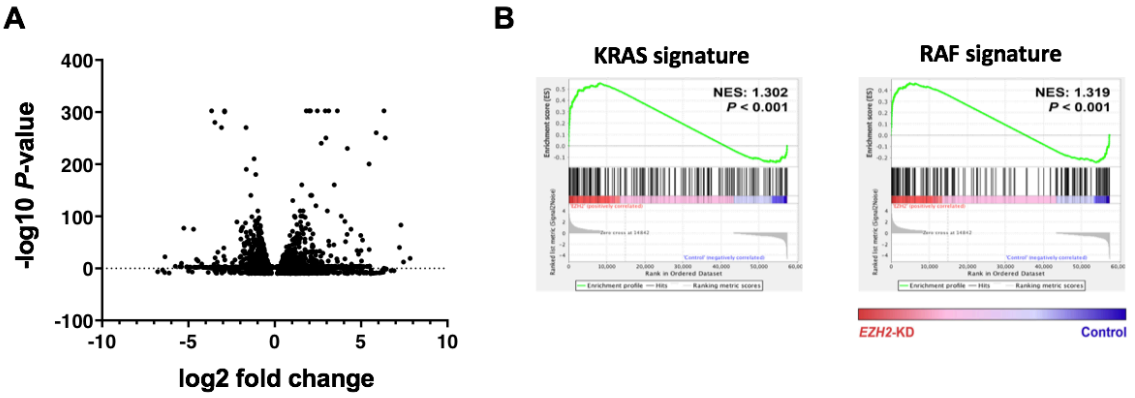

Figure 17. Knockdown of *EZH2* in HL60 cells induces RAS-signaling gene expression signatures. (A) Volcano plot representing RNA-seq expression results of HL-60 cells with and without shRNA-mediated knockdown of *EZH2* (HL60 *EZH2* KD vs HL60 control KD). The x-axis depicts the Log2-fold change gene expression. Genes with an increased expression in *EZH2* KD cells are displayed on the right side of the x-axis, while genes with decreased expression levels are depicted on the left. Statistical significance is presented as negative log10 transformed values on the y-axis. **(B)** Gene set enrichment analysis (GSEA) of RNA-seq data showing that differentially expressed genes belonging to RAS- and RAF-signaling are enriched in HL60 cells with *EZH2* KD. Enrichment plots showing the presence of KRAS and RAF associated genes in *EZH2* KD cells compared to control KD cells, which exhibit a false discovery rate lower than 25%. NES, normalized enrichment score. This figure has been adapted from (174) with permission from Leukemia.

Table 7

Category	Upregulated Genes
PI3K-Akt Signaling Pathway (WP4172)	*CDKN1A;TGFA;PIK3CB;THBS3;RPTOR;FGF5;PPP2CB;CCND2;PPP2R3C;MYC; AKT2;MYB;AKT1;THEM4;HSP90AA1;MAP2K2;ANGPT1;HGF;RPS6;OSM;RBL2; G6PC3;CCNE1;RHEB;CDC37;PPP2R2D;BCL2;SGK1;TLR4*
Ras Signaling (WP4223)	*RALA;MAP2K2;RAB5C;RASA4B;RALB;PLA2G2C;PIK3CB;RASGRP2;PLD1;ETS2; RASA3;RASA4;AKT2;AKT1;ABL2;RAC3;CALM3;CALM1;PRKACB;RALGDS;PAK4*
EGF/EGFR Signaling Pathway (WP437)	*VAV3;STAT5B;RALA;MAP2K2;RALB;SH3KBP1;STAT3;PEBP1;FOS;PLD1;PIK3C2B; DOK2;RPS6KA5;HGS;RPS6KA2;GRB10;AKT1;FOSB;SPRY2;ARHGEF1;RALGDS; CRK*
MAPK Signaling Pathway (WP382)	*ARRB1;ECSIT;RASGRP2;FGF5;RPS6KA5;PPP3CC;DUSP10;MYC;AKT2;CASP3; MKNK2;AKT1;RAC3;FLNB;PRKACB;MAP3K7;MAP2K3;MAP2K4;DAXX;DUSP2; MAP2K2;GADD45A;CACNA2D1;CACNA2D4;FOS;MAPK8IP2;MAPK12;CDC25B; MAPK13;NR4A1;PPP5C;CACNB3;FAS;TAB1;MAP3K14;CRK*
ErbB Signaling Pathway (WP673)	*MAP2K4;STAT5B;CDKN1A;MAP2K2;TGFA;PIK3CB;MYC;AKT2;AKT1;ABL2;CRK; HBEGF;PAK4*
PDGF Pathway (WP2526)	*NFKBIA;MAP2K4;STAT3;ARFIP2;WASL;FOS*
p38 MAPK Signaling Pathway (WP400)	*MAP2K4;DAXX;RPS6KA5;TRADD;MYC;MAP3K7*
VEGFA-VEGFR2 Signaling Pathway (WP3888)	*YWHAE;CXCL8;MAPKAP1;TXN;SHB;NDRG1;ICAM1;CAMKK2;HDAC7;RPS6KA5; ADAMTS1;RACK1;GRB10;AKT1;FLNB;WASF1;MAP2K3;EGR1;MAP2K4;HSP90AA1; JAG1;MAP2K2;STAT3;RPS6;LIMK1;PLAUR;NFATC2;F3;MAPK12;NFKBIA;NR4A1; HGS;AKT1S1;BCL2;CTNNB1;FAS;PRKD2;CRK;HBEGF*
TGF-beta Signaling Pathway (WP366)	*CDKN1A;CUL1;TERT;MYC;AKT1;E2F5;MAP3K7;JUNB;MAP2K3;TGIF1;MAP2K4; TRAP1;MAP2K2;SMURF2;WWP1;FOS;PJA1;RBL2;DAB2;ZEB2;ZFYVE16;TFDP1; HGS;STRAP;FOSB;SIK1;TAB1*
IL-2 Signaling Pathway (WP49)	*STAT5B;CCND2;MAP2K2;CISH;MYC;STAT3;RPS6;BCL2;AKT1;FOS*
AMP-activated Protein Kinase (AMPK) Signaling (WP1403)	*CDKN1A;CPT1A;PFKFB3;PRKAG1;PRKAG2;PIK3CB;EEF2;ADIPOR2;CAMKK1; CAMKK2;RPTOR;AKT2;FASN;LEPR;AKT1;PRKACB*
Wnt Signaling Pathway (WP363)	*GSK3A;CTBP1;LEF1;LRP5;NFATC2;CSNK1D;CSNK1E;MYC;DVL1;AKT1;CTNNB1; PIP5K1B;TCF3;MAP3K7*
Hedgehog Signaling Pathway (WP4249)	*SMURF2;PTCH1;PTCH2;ARRB1;CSNK1D;CSNK1E;GRK3;CCND2;SUFU;GPR161; BCL2;PRKACB;CSNK1G2*
TNF alpha Signaling Pathway (WP231)	*TRADD;CUL1;PYGL;TXN;CASP3;PSMD2;AKT1;RFFL;BID;MAP3K7;GLUL;MAP2K3; MAP2K4;TRAP1;HSP90AA1;CSNK2A1;CYBA;TRAF1;NFKBIA;CDC37;BAX;TAB1; MAP3K14;NSMAF;NFKBIB*

Table 7. Upregulated genes in HL60 with *EZH2* knockdown. RNA-seq data analysis showing genes with increased expression in HL60 cells with shRNA-mediated *EZH2* KD associated with RAS/MAPK signaling. Genes were classified using gene set enrichment analysis (WikiPathways_2019_Human; Enrichr; https://amp.pharm.mssm.edu/Enrichr/). This table has been adapted from (174) with permission from Leukemia.

To ensure that the identified target genes are truly regulated by EZH2-mediated histone modification we analyzed a publicly available dataset of chromatin immuno-precipitation coupled with high-throughput DNA sequencing (ChIP-seq) data obtained from the NCBI Gene Expression Omnibus (GSE61785, (187)). In this study Göllner and colleagues identified H3K27me3-associated genomic regions in AML cells after the loss of EZH2 activity. In our analysis we focused on known activators of the RAS-signaling pathway that were also significantly upregulated in our RNA-seq experiment and included YWHAE, HSP90AA1, STAT3, PSMD2 and CUL1 (Fig. 18m (188–193)). Indeed, sequencing after H3K27me3 ChIP revealed less reads for relevant promoter and intergenic loci in cells with loss of EZH2 activity, indicating that transcriptional upregulation in *EZH2*^{inact} myeloid cells is caused by loss of H3K27me3.

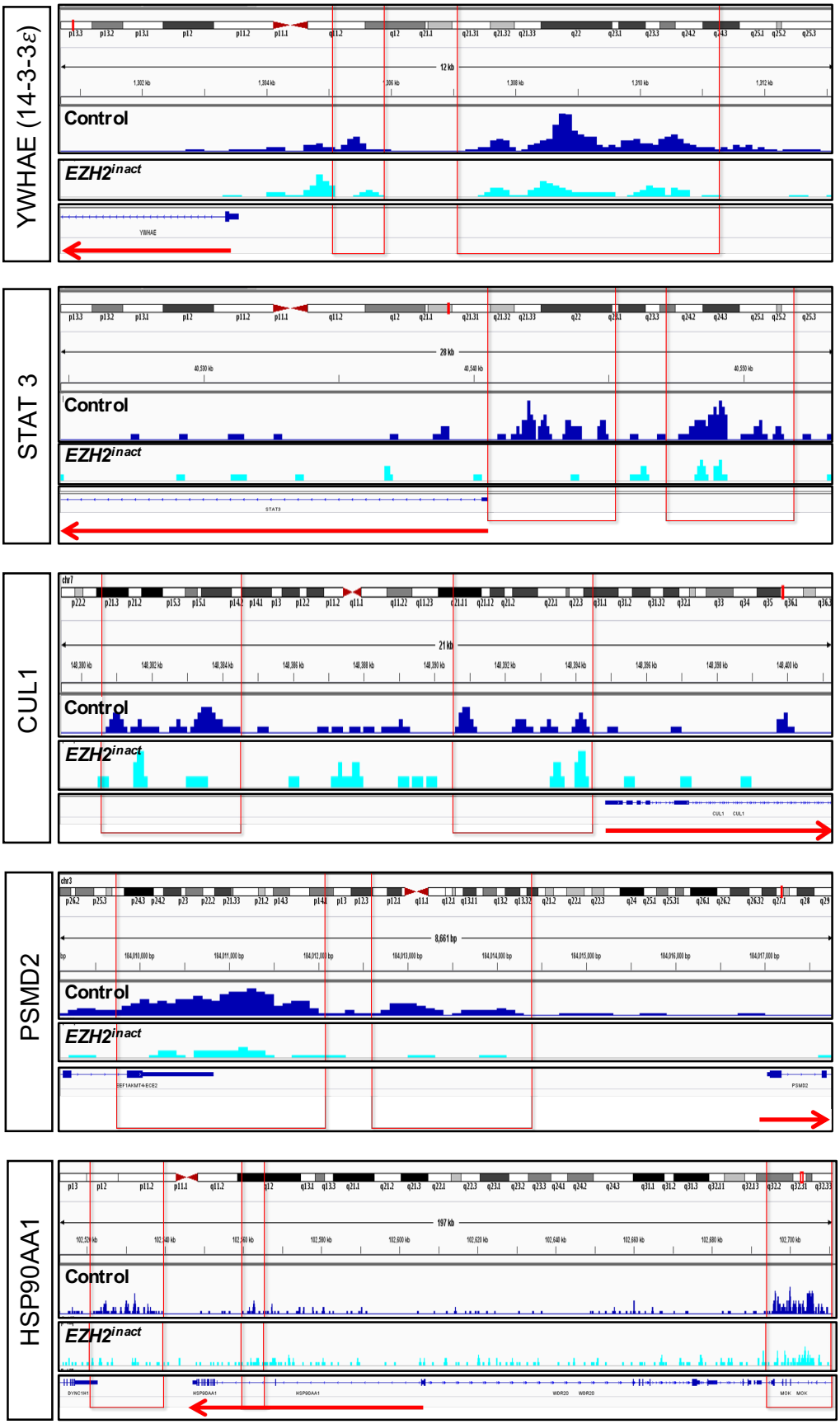
YWHAE (14-3-3ε)
Control
EZH2inact
STAT 3
Control
EZH2inact
CUL1
Control
EZH2inact
PSMD2
Control
EZH2inact
HSP90AA1
Control
EZH2inact

Figure 18. Genes that activate RAS-signaling show reduced H3K27me3 association in cells with loss of EZH2 activity. ChIP-seq analysis of selected RAS-signaling activators shows reduced H3K27me3 occupancy within gene promotors and/or intergenic regions in AML cells with and without loss of EZH2 activity (*EZH2*^{inact} and control). The dataset was retrieved from the NCBI's GEO (GSE61785, (187)). Mapped sequencing reads of genomic DNA that was immune-precipitated with anti-H3K27me3 antibodies are shown in blue (control) and turquoise (*EZH2*^{inact}) and indicate H3K27me3 association. Genomic regions with differences in H3K27me3 occupancy are marked in red. Gene location and orientation are indicated by red arrows. Isotype controls have been taken into consideration to detect unspecific antibody binding. ChIP-seq tracks have been uniformly scaled for the analysis of each gene locus. This figure has been adapted from (174) with permission from Leukemia.

5. Discussion

5.1. **Part 1**: The role of micro-RNAs in the development of chronic myelomonocytic leukemia

In this thesis, we aimed to identify and study miRNAs relevant for the development and leukemic growth of CMML cells. In prior work from our group, we characterized the miRNA expression profile of HSPCs isolated from *Kras*^{G12D}-mutated CMML mice and observed extensive miRNA dysregulation. As most aberrant miRNAs showed diminished expression, we further focused on the most downregulated candidates.

In the current study, we further validated the significant decrease of a highly repressed miRNA – miR-125a – in a more immature LSK cell population of early hematologic progenitor cells, regarded as the compartment where hematopoietic and leukemic stem cells reside (194). These findings could additionally be confirmed in 36 CMML patients, where we observed significantly reduced expression of miR-125a. This highlights the comparability of our *Kras*^{G12D}-mutated mouse model and clinical CMML specimens and is also in line with miRNA expression screens in other MN, such as cytogenetically normal AML patients, where miR-125a was one of the most prominently downregulated miRNAs (195). It has to be noted that we did not find any association between the RAS mutation status and miR-125a levels in our CMML cohort, suggesting different underlying mechanisms that govern miR-125a expression in this MN. However, as decreased expression of miR-125a seems to be a regularly occurring event in CMML, irrespective of the mutational profile, one might speculate that this miRNA is important for the manifestation of myeloid malignancies. Indeed, miR-125a has been reported as a tumor-suppressor in a miR-125a-specific knockout mouse model, were heterozygous as well as homozygous loss of miR-125a leads to the development of a MPD with enlarged spleen size and an increased HSC pool (196). Interestingly, the severances and frequency of the MPD was higher in mice with a heterozygous genotype and low residual miR-125a expression in result of compensatory mechanisms that became activated in the homozygous state. Similar median expression levels could be observed in our CMML cohort, whereas a complete loss of miR-125a expression did not occur. Moreover, the tumor-suppressive role of miR-125a is in line with our *in-vitro* experiments, where stable overexpression of miR-125a inhibited leukemic

proliferation and increased apoptosis in myeloid THP1 cells. These cells exhibit reduced endogenous miR-125a levels.
However, conflicting data about the role of miR-125a in myeloid malignancies have also been reported. Gerrits and colleges characterized the effects of ectopic miR-125a overexpression in murine HSCs that were transplanted into sublethaly irradiated recipient mice (175). In their study they could show, that increased miR-125a levels convey a growth advantage for HSCs and skews their differentiation towards the myeloid lineage, ultimately resulting in the development of a MPN in transplanted animals. These findings were supported in another study by Guo et al., who developed a doxycycline-inducible mouse model for miR-125a overexpression (197). Mice transplanted with miR-125a overexpressing BM cells manifested an atypical MPN that exhibited high levels of miR-125a oncogene dependence and resolved upon withdrawal of doxycycline. Considering these published findings and data from the current study, it is likely that miR-125a expression needs to be within a relatively narrow physiological range to maintain HSC homeostasis, while aberrations in expression levels can lead to myeloid leukemogenesis. Similar phenomena have been described for other miRNAs, such as miR-126. In functional *in-vivo* experiments, it was demonstrated that the overexpression as well as the knockout of miR-126 accelerated *AML1-ETO/RUNX1-RUNX1T1*-mutated leukemia development in mice by regulating different oncogenic signaling pathways (198).

Due to the complex consequences of miR-125a dysregulation in myeloid malignancies, it is important to consider data from primary patients to elucidate the role of miR-125a in CMML. Here, our investigation could show that miR-125a is significantly downregulated in the majority of our 36 diagnostic samples compared to CD34+ HPSCs and healthy BM aspirates. This indicates that miR-125a is primarily decreased in CMML and functions most likely as a tumor-suppressor in the development of this malignancy.

To further delineate the underlying mechanisms of miR-125a downregulation in CMML, we performed bisulfite sequencing in myeloid cell lines showing a hypermethylation of the upstream/promoter region of miR-125a. These results are consistent with studies in AML and solid cancers showing that miR-125a is often epigenetically silenced in these malignancies (199–202). Interestingly, the epigenetic repression of the miR-125a could be reversed in

myeloid cell lines with low endogenous miR-125a levels using the HMAs Dec and Aza - two drugs that are approved for the treatment of CMML patients. As methylation profiling in CMML patient specimen failed due to technical reasons, we reanalyzed previously published data of primary AML cells treated with Dec in an *ex-vivo* setting. In agreement with our bisulfite sequencing results, the data analysis revealed excessive methylation, which could be reduced in response to HMA treatment (178).

To investigate if HMA treatment could also increase miR-125a expression in a clinical setting, we analyzed primary CMML patients before and after/during HMA therapy. The qPCR measurements of miR-125a expression in these paired specimens revealed a significant increase in CMML patients after or during their treatment with HMAs. Furthermore, the level of miR-125a upregulation also corresponded with the clinical response to the treatment regime. We could observe that the miR-125a upregulation was more prominent in patients showing a response to HMAs as compared to non-responders. However, due to the small number of patients that where included in this cohort, we were not able to perform statistical testing for these conclusions. Furthermore, out of this cohort, five of seven patients exhibited a clinical response to HMAs. This overall response rate of more than 70% is higher compared to reported response rates of 40-50% in the current literature (34). This indicates that data from this patient cohort might be affected by a selection bias. To overcome this limitation, bigger clinical trials and prospective studies will be needed to elucidate the link of HMA-induced miR-125a increase and clinical response to HMA treatment. Interestingly, a previously published study in high-risk MDS patients investigated miR-125a levels after Aza treatment (203). The authors could show that miR-125a levels increased in serial specimen of Aza responders while no increase could be found in patients with therapy resistance. Additionally, they identified decreased levels of miR-125a to be associated with shorter OS and progression-free survival in multivariate analysis highlighting miR-125a as a potential biomarker for risk stratification in myeloid disorders.

Taken together, this evidence suggest that Aza treatment leads to an increase of miR-125a and could be needed to mediate HMA efficacy in CMML. To investigate this hypothesis, we first assessed the cytotoxic effects of Aza in myeloid cell lines using *in-vitro* apoptosis assays.

Subsequently, miR-125a-specific shRNA or CRISPR/Cas9 technology was used to either transiently knockdown or completely inactivate miR-125a in these cells. This could effectively inhibit the miR-125a upregulation after Aza treatment. Most noteworthy, the blocking of the Aza-induced miR-125a upregulation also significantly reduced the ability of Aza to induce apoptosis in these cells. This indicates that the anti-leukemic efficacy of HMAs is partly mediated by the upregulation of miR-125a. MicroRNAs have emerged as important players in mediating therapeutic effects of anti-cancer drugs (204–206). Recent work in AML patients has described HMA-induced miR-34a upregulation as an important mechanism of HMA efficacy in combination with all-trans retinoic acid treatment (207). In the current study, we identify miR-125a as an important target and effector molecule of Aza in myeloid leukemia cells, adding more insight into the mode of action of these drugs.

Lastly, we treated miR-125a overexpressing cells with Aza to explore potential combined effects. Indeed, we could show that Aza further upregulates miR-125a expression and leads to a higher rate of apoptosis in these cells, suggesting a synergistic or additive effect. This observation could be a starting point for future therapy combinations where artificial miRNA mimics are delivered into patient cells to increase Aza efficacy or overcome drug resistance of leukemic cells. Such new treatment strategies with miRNA-based therapeutics, aiming to replenish or overexpress tumor-suppressive miRNAs, are currently evaluated in preclinical and clinical trials (139,140,142,208–210). Although this might be an exciting perspective, more studies are necessary to make miRNA-based therapies applicable, safe and effective.

5.2. **Part 2**: The co-occurrence of *EZH2* inactivation and *RAS* pathway mutations hyperactivates MAPK/ERK-signaling and increases MEK inhibitor sensitivity in myeloid malignancies

The second part of this thesis is based on preliminary findings in our initial miRNA part, where we analyzed NGS data from our CMML patient cohort and observed a potential correlation of mutations modifying RAS (*KRAS, NRAS, CBL, NF1 and PTPN11*) and the epigenetic modifier *EZH2*. The RAS-MAPK/ERK pathway is frequently hyperactivated in CMML and related myeloid neoplasms where it results in more aggressive and myeloproliferative phenotypes (15,211). Therefore, targeted treatment strategies that block RAS effector pathways, such as MEK inhibitors preventing MAPK/ERK signaling, have been investigated as promising therapy options. Despite the fact, that these inhibitors effectively mitigate leukemogenesis in RAS^{mut} mouse models, clinical trials in humans showed only little efficacy (212–214). A contributing factor for the ineffectiveness of MEK inhibitors in RAS^{mut} malignancies might be the heterogenic mutational landscape of these leukemias, where often various additional genetic aberrations occur simultaneously. Additionally, some mutations in epigenetic regulatory proteins have been suggested to accelerate and cooperate with RAS^{mut} signaling, which potentially increases the sensitivity to targeted inhibition of this pathway (104,215). Based on the preliminary findings from part 1 of this thesis, we decided to study the RAS^{mut}/$EZH2^{inact}$ co-occurrence in more detail. Recently, a transgenic mouse model characterized the consequences of *Nras* mutations and the loss of *Ezh2*, causing the rapid development of aggressive MPD (153). However, the knowledge about the clinical consequences and underlying molecular mechanisms of RAS^{mut} and $EZH2^{inact}$ is scarce in myeloid neoplasm.

Here we investigated the co-existence of RAS^{mut} and $EZH2^{inact}$ in CMML and other myeloid neoplasms and their effect on RAS signaling and MEK inhibitor sensitivity. Initially, we analyzed NGS data from 260 primary CMML specimens to gather information about the prevalence of these mutations. Indeed, we could show that mutations in *RAS* modulators and *EZH2* frequently co-exist in this MN. Further, missense mutations in *EZH2* were significantly enriched in patients with RAS^{mut} verifying an increased co-occurrence of both mutations in CMML. It has to be noted, that the incidence of *EZH2* mutations (19,2%) in our cohort is

considerably higher compared to previously published literature (15,216). This was caused by the inclusion of the *EZH2* p.D185H mutation into our analysis. This variant was categorized as a non-pathogenic nucleotide polymorphism in mutation databases such as VarSome or COSMIC (217,218). However, functional *in-vitro* assays were able to demonstrate, that this mutation causes an impaired methyltransferase activity, indicating a pathogenic loss of function (182). Furthermore, the p.D185H mutation was identified as a risk factor for carcinogenesis in healthy individuals and correlated with lower EZH2 protein levels as well as poor outcome in clinical studies investigating MDS/MPN overlap syndromes and other MN (184). Our patient data analysis also demonstrates that the co-occurrence of *EZH2* and *RAS* pathway mutations is associated with a significantly shorter overall survival compared to patients where both aberrations are not present together. These findings are in line with data from preclinical mouse models, which shows that transgenic $Nras^{G12D}/Ezh2^{-/-}$ double-mutant mice succumb to a rapidly developing form of aggressive MPN (153). EZH2 mutations have been identified as independent prognostic marker in MDS and are associated with inferior outcome in CMML (15,219). Our data adds important evidence for a new high-risk group of CMML patients.

Next, we wanted to investigate, if these results are also valid in other MN, such as AML. Database analysis of 187 AML patients included information about mutations, as well as chromosomal copy number alterations and mRNA expression. In line with our data from CMML patients, $EZH2^{inact}$ by mutations and/or chromosomal deletion occurred more frequently together with RAS^{mut} and significantly worsened outcome for affected patients. Additionally, we analyzed gene expression data in our AML cohort showing reduced *EZH2* levels in patients with RAS^{mut}. Interestingly, $EZH2^{inact}$ in AML seems to play an ambivalent role in the context of different driver-mutations. Tanaka and colleges describe that *EZH2* knockout in murine progenitor cells, also carrying the MLL-AF9 oncogene, attenuates AML development and produces a more CMML-like disease phenotype (220). Moreover, *EZH2* loss might exhibit different leukemogenic potential in MLL-AF9 and AML1-ETO9a mutated mouse HSPCs, dependent on whether it occurs in an early or late stage of leukemia development (221). In conjunction with our findings, one could speculate, that $EZH2^{inact}$ might specifically cause an increased leukemogenic potential in the presence of RAS^{mut}. A potential reason for this has been suggested in recent studies, which demonstrated that mutations in epigenetic signaling

molecules can aggravate *RAS*^{mut}-driven leukemia by further activating downstream signaling (104,215). Interestingly, deletions of the epigenetic regulator *Tet2* in *Nras*^{G12D} mice caused a remarkable hyperactivation of the MAPK/ERK pathway. In consequence, these transgenic animals were also more sensitive to MEK inhibition due to an increased dependence on oncogenic RAS signaling. To investigate if this phenomenon can also be observed after *EZH2*^{inact} we used the *RAS*^{mut} / *EZH2*^{wt} myeloid cell lines THP1 and HL60. Importantly, pharmacologic inhibition of EZH2, using the inhibitors GSK-126 and DZNep, could not only successfully block EZH2 activity but also lead to a hyperactivation of MAPK/ERK pathway. Although, the EZH2 inhibitors used here, especially GSK-126 are highly selective, potential off-target effects cannot be excluded. Consequently, we sought other ways to mimic *EZH2* loss in our cell line models employing lentivirally delivered shRNA to knockdown *EZH2* expression. In support of our EZH2 inhibitor experiments knockdown of *EZH2* showed similar effects on ERK hyperactivation in THP1 and HL60. This excessive activation of the MAPK/ERK pathway has also been observed in a study focusing on KRAS-driven lung cancer, where additional *EZH2*^{inact} significantly increased pERK levels (222).

The hyperactivation of the MAPK/ERK pathway has been previously linked to increased sensitivity for MEK inhibitors. Consequently, we wanted to test if the *EZH2*^{inact}-induced hyperactivation of mutant RAS-signaling also increases the sensitivity to targeted pharmacologic inhibition. Therefore, we treated our *RAS*^{mut} and *EZH2* knockdown cell lines with the selective MEK inhibitor U0126. Most importantly, apoptosis and cell cycle arrest were more pronounced in cells with *EZH2*^{inact}. It is interesting, that MEK inhibitors failed to induce apoptosis in THP1 cells without *EZH2*^{inact}, however additional *EZH2* knockdown was able to overcome drug resistance and sensitized these cells to MEK inhibition, supporting our claim that *EZH2*^{inact} increases oncogene dependence. These findings could be of great relevance for the clinical management of MN cases with *RAS*^{mut} and *EZH2*^{inact}, especially because *EZH2* mutations are usually associated with resistance against other chemotherapeutic drugs (187).
To identify the underlying molecular mechanisms behind *EZH2*^{inact}-mediated MAPK/ERK hyperactivation we performed RNA-seq of HL60 cells with *EZH2* knockdown followed by GSEA. These analyses revealed the upregulation of different oncogenic gene signatures, including enrichment for *KRAS* and *RAF* related genes. We confirmed that the loss of EZH2-

specific H3K27 trimethylation is associated with the upregulation of selected target genes using previously published Chip-seq data (187).

Taken together, we demonstrate the frequent co-existence and negative prognostic impact of *EZH2*^{inact} in *RAS*^{mut} MNs. Additionally, we show that the *EZH2*^{inact} cooperates with *RAS*^{mut} to induce ERK hyperactivation, ultimately leading to high susceptibility for MEK inhibitor treatment. In this thesis, we present new evidence that could lay the foundations for targeted therapy approaches for a hard-to-treat patients collective.

6. Bibliography

1. Tefferi A, Vardiman JW. Classification and diagnosis of myeloproliferative neoplasms: The 2008 World Health Organization criteria and point-of-care diagnostic algorithms. Leukemia. 2008;22 (September 2007):14–22.
2. Patnaik MM, Parikh SA, Hanson CA, Tefferi A. Chronic myelomonocytic leukaemia : a concise clinical and pathophysiological review. British Journal of heamtology. 2014;165:273–86.
3. Fianchi L, Leone G, Posteraro B, Sanguinetti M, Guidi F, Valentini CG, et al. Impaired bactericidal and fungicidal activities of neutrophils in patients with myelodysplastic syndrome. Leukemia Research. 2012;36(3):331–3.
4. Prodan M, Tulissi P, Perticarari S, Presani G, Franzin F, Pussini E, et al. Flow cytometric assay for the evaluation of phagocytosis and oxidative burst of polymorphonuclear leukocytes and monocytes in myelodysplastic disorders. Haematologica. 1995;80(3):212–8.
5. Mathew RA, Bennett JM, Liu JJ, Komrokji RS, Lancet JE, Naghashpour M, et al. Cutaneous manifestations in CMML: Indication of disease acceleration or transformation to AML and review of the literature. Leukemia Research. 2012;36(1):72–80.
6. Arber DA, Orazi A. Update on the pathologic diagnosis of chronic myelomonocytic leukemia. Modern Pathology. 2019;32(6):732–40. Available from: http://dx.doi.org/10.1038/s41379-019-0215-y
7. Patnaik MM, Tefferi A. Chronic myelomonocytic leukemia: 2016 update on diagnosis, risk stratification, and management. American Journal of Hematology. 2016;91(6):631–42.
8. Patnaik MM, Lasho TL, Finke CM. Targeted next generation sequencing of PDGFRB rearranged myeloid neoplasms with monocytosis. American Journal of Hematology. 2016;91(3):E12–4.
9. Patterer V, Schnittger S, Kern W, Haferlach T, Haferlach C. Hematologic malignancies with PCM1-JAK2 gene fusion share characteristics with myeloid and lymphoid neoplasms with eosinophilia and abnormalities of PDGFRA, PDGFRB, and FGFR1. Annals of Hematology. 2013;92(6):759–69.
10. Jabbour EJ, Kanterjian H. CME Information: Chronic myeloid leukemia: 2014 update on diagnosis, monitoring, and management. American Journal of Hematology,. 2016;91(5):252–65.
11. Itzykson R, Duchmann M, Lucas N, Solary E. CMML: Clinical and molecular aspects. International Journal of Hematology. 2017;105(6):711–9.
12. Germing U, Strupp C, Knipp S, Kuendgen A, Giagounidis A, Hildebrandt B, et al. Chronic myelomonocytic leukemia in the light of the WHO proposals. 2007;92(07):974–7.
13. Courville EL, Wu Y, Kourda J, Roth CG, Brockmann J, Muzikansky A, et al. Clinicopathologic analysis of acute myeloid leukemia arising from chronic myelomonocytic leukemia. Modern Pathology. 2013;26(6):751–61.

14. Such E, Cervera J, Costa D, Solé F, Vallespí T, Luño E, et al. Cytogenetic risk stratification in chronic myelomonocytic leukemia. Haematologica. 2011;96(3):375–83.
15. Patnaik MM, Tefferi A. Cytogenetic and molecular abnormalities in chronic myelomonocytic leukemia. Blood Cancer Journal. 2016;6(November 2015):1–8. Available from: http://dx.doi.org/10.1038/bcj.2016.5
16. Tang G, Zhang L, Fu B, Hu J, Lu X, Hu S, et al. Cytogenetic risk stratification of 417 patients with chronic myelomonocytic leukemia from a single institution. American Journal of Hematology. 2014;89(8):813–8.
17. Such E, Germing U, Malcovati L, Kuendgen A, Porta MG della, Xicoy B, et al. Development and validation of a prognostic scoring system for patients with chronic myelomonocytic leukemia. Blood. 2017;121(15):3005–16.
18. Welch JS, Ley TJ, Link DC, Miller CA, Larson DE, Koboldt DC, et al. The Origin and Evolution of Mutations in Acute Myeloid Leukemia. 2011;
19. Steensma DP, Bejar R, Jaiswal S, Lindsley RC, Sekeres MA, Hasserjian RP, et al. Clonal hematopoiesis of indeterminate potential and its distinction from myelodysplastic syndromes. Blood. 2015;126(1):9–16.
20. Itzykson R, Solary E. An evolutionary perspective on chronic myelomonocytic leukemia. 2013;27(7):1441–50. Available from: http://dx.doi.org/10.1038/leu.2013.100
21. Gelsi-Boyer V, Trouplin V, Bonasea J, Lagarde A, Pebet T, Nezri M, et al. Mutations of polycomb-associated gene ASXL1 in myelodysplastic syndromes and chronic myelomonocytic leukaemia. British Journal of heamtology. 2009;145:788–800.
22. Kohlmann A, Grossmann V, Klein H, Schindela S, Weiss T, Kazak B, et al. Next-Generation Sequencing Technology Reveals a Characteristic Pattern of Molecular Mutations in 72 . 8 % of Chronic Myelomonocytic Leukemia by Detecting Frequent. JOURNAL OF CLINICAL ONCOLOGY. 2017;28(24).
23. Ricci C, Fermo E, Corti S, Molteni M, Faricciotti A, Cortelezzi A, et al. RAS Mutations Contribute to Evolution of Chronic Myelomonocytic Leukemia to the Proliferative Variant. Clinical Cancer Research. 2010;16(8):2246–57.
24. Padron E, Painter JS, Kunigal S, Mailloux AW, Mcgraw K, Mcdaniel JM, et al. GM-CSF – dependent pSTAT5 sensitivity is a feature with therapeutic potential in chronic myelomonocytic leukemia. 2016;121(25):5068–78.
25. Gelsi-boyer V, Trouplin V, Adélaïde J, Aceto N, Remy V, Pinson S, et al. Genome profiling of chronic myelomonocytic leukemia: frequent alterations of RAS and RUNX1 genes Véronique. BMC Cancer. 2008;14.
26. Ward AF, Braun BS, Shannon KM. Targeting oncogenic Ras signaling in hematologic malignancies. Blood. 2012;120(17):3397–406.
27. Patnaik MM, Parikh SA, Hanson CA, Tefferi A. Chronic myelomonocytic leukaemia : a concise clinical and pathophysiological review. 2014;(January):273–86.
28. Wang J, Li Z, He Y, Pan F, Chen S, Rhodes S, et al. Loss of Asxl1 leads to myelodysplastic syndrome-like disease in mice. Blood. 2014;123(4):541–53.

29. Li Z, Cai X, Cai CL, Wang J, Zhang W, Petersen BE, et al. Deletion of Tet2 in mice leads to dysregulated hematopoietic stem cells and subsequent development of myeloid malignancies. Vol. 118, Blood. 2011. 4509–4518.
30. Braun BS, Tuveson DA, Kong N, Le DT, Kogan SC, Rozmus J, et al. Somatic activation of oncogenic Kras in hematopoietic cells initiates a rapidly fatal myeloproliferative disorder. pnas. 2004;101(2):597–602.
31. Ward AF, Braun BS, Shannon KM. Review article Targeting oncogenic Ras signaling in hematologic malignancies. 2017;120(17):3397–407.
32. Patnaik MM, Itzykson R, Lasho TL, Kosmider O, Finke CM, Hanson CA, et al. ASXL1 and SETBP1 mutations and their prognostic contribution in chronic myelomonocytic leukemia: A two-center study of 466 patients. Leukemia. 2014;28(11):2206–12.
33. Such E, Germing U, Malcovati L, Hrodek O. Development and validation of a prognostic scoring system for patients with chronic myelomonocytic leukemia. Transfuze a Hematologie Dnes. 2013;19(3):191.
34. Patnaik MM, Tefferi A. Chronic Myelomonocytic leukemia: 2020 update on diagnosis, risk stratification and management. American Journal of Hematology. 2020;95(1):97–115.
35. Itzykson R, Kosmider O, Renneville A, Gelsi-Boyer V, Meggendorfer M, Morabito M, et al. Prognostic score including gene mutations in chronic Myelomonocytic Leukemia. Journal of Clinical Oncology. 2013;31(19):2428–36.
36. Onida F, Kantarjian HM, Smith TL, Ball G, Keating MJ, Estey EH, et al. Prognostic factors and scoring systems in chronic myelomonocytic leukemia : a retrospective analysis of 213 patients. Blood. 2002;99(3):840–50.
37. Grossmann V, Kohlmann A, Eder C, Haferlach C, Kern W, Cross NCP, et al. Molecular profiling of chronic myelomonocytic leukemia reveals diverse mutations in >80% of patients with TET2 and EZH2 being of high prognostic relevance Leukemia. Leukemia. 2011;25(5):877–9.
38. de Witte T, Bowen D, Robin M, Malcovati L, Niederwieser D, Yakoub-Agha I, et al. Allogeneic hematopoietic stem cell transplantation for MDS and CMML: Recommendations from an international expert panel. Blood. 2017;129(13):1753–62.
39. Costa R, Abdulhaq H, Haq B, Shadduck RK, Latsko J, Zenati M, et al. Activity of azacitidine in chronic myelomonocytic leukemia. Cancer. 2011;117(12):2690–6.
40. Yamazaki J, Jelinek J, Lu Y, Cesaroni M, Madzo J, Neumann F, et al. TET2 mutations affect Non-CpG island DNA methylation at enhancers and transcription factor-binding sites in chronic myelomonocytic Leukemia. Cancer Research. 2015;75(14):2833–43.
41. Meldi K, Qin T, Buchi F, Droin N, Sotzen J, Micol JB, et al. Specific molecular signatures predict decitabine response in chronic myelomonocytic leukemia. Journal of Clinical Investigation. 2015;125(5):1857–72.
42. Palomo L, Malinverni R, Cabezón M, Xicoy B, Arnan M, Coll R, et al. DNA methylation profile in chronic myelomonocytic leukemia associates with distinct clinical, biological and genetic features. Epigenetics. 2018;13(1):8–18. Available from: https://doi.org/10.1080/15592294.2017.1405199

43. Alfonso A, Montalban-Bravo G, Takahashi K, Jabbour EJ, Kadia T, Ravandi F, et al. Natural history of chronic myelomonocytic leukemia treated with hypomethylating agents. American Journal of Hematology. 2017;92(7):599–606.
44. Moyo TK, Savona MR. Therapy for Chronic Myelomonocytic Leukemia in a New Era. Current Hematologic Malignancy Reports. 2017;12(5):468–77.
45. Döhner H, Weisdorf DJ, Bloomfield CD. Acute myeloid leukemia. New England Journal of Medicine. 2015;373(12):1136–52.
46. Stölzel F, Lüer T, Löck S, Parmentier S, Kuithan F, Kramer M, et al. The prevalence of extramedullary acute myeloid leukemia detected by FDG-PET/CT: Final results from the prospective PETAML trial. Haematologica. 2020;105(6):1552–8.
47. Magdy M, Abdel Karim N, Eldessouki I, Gaber O, Rahouma M, Ghareeb M. Myeloid Sarcoma. Oncology Research and Treatment. 2019;42(4):219–24.
48. Byrd J, Mrózek K, Dodge R, Carroll A, Colin GE, Arthur CD, et al. Pretreatment cytogenetic abnormalities are predictive ofinduction success, cumulative incidence ofrelapse, and overall survival in adult patients with de novo acute myeloid leukemia: results from Cancer and Leukemia Group B (CALGB 8461). Blood 2002;100(13):4325–36.
49. Arber DA, Orazi A, Hasserjian R, Thiele J, Borowitz MJ. The 2016 revision to the World Health Organization (WHO) classification of myeloid neoplasms and acute leukemia. Blood; 2016. 1–46.
50. Bennett JM, Catovsky D, Daniel M -T, Flandrin G, Galton DAG, Gralnick HR, et al. Proposals for the Classification of the Acute Leukaemias French-American-British (FAB) Co-operative Group. British Journal of Haematology. 1976;33(4):451–8.
51. de Kouchkovsky I, Abdul-Hay M. 'Acute myeloid leukemia: A comprehensive review and 2016 update.' Blood Cancer Journal. 2016;6(7).
52. Deschler B, Lübbert M. Acute myeloid leukemia: Epidemiology and etiology. Cancer. 2006;107(9):2099–107.
53. Visser O, Trama A, Maynadié M, Stiller C, Marcos-Gragera R, de Angelis R, et al. Incidence, survival and prevalence of myeloid malignancies in Europe. European Journal of Cancer. 2012;48(17):3257–66.
54. de Rooij J, Zwaan C, van den Heuvel-Eibrink M. Pediatric AML: From Biology to Clinical Management. Journal of Clinical Medicine. 2015;4(1):127–49.
55. Sill H, Olipitz W, Zebisch A, Schulz E, Wölfler A. Therapy-related myeloid neoplasms: Pathobiology and clinical characteristics. British Journal of Pharmacology. 2011;162(4):792–805.
56. Ley TJ, Miller C, Ding L, Raphael BJ, Mungall AJ, Robertson G, et al. Genomic and epigenomic landscapes of adult de novo acute myeloid leukemia. New England Journal of Medicine. 2013;368(22):2059–74.
57. Hope KJ, Jin L, Dick JE. Acute myeloid leukemia originates from a hierarchy of leukemic stem cell classes that differ in self-renewal capacity. Nature Immunology. 2004;5(7):738–43.
58. Grove CS, Vassiliou GS. Acute myeloid leukaemia: A paradigm for the clonal evolution of cancer? DMM Disease Models and Mechanisms. 2014;7(8):941–51.

59. Grimwade D. The clinical significance of cytogenetic abnormalities in acute myeloid leukaemia. Best Practice and Research: Clinical Haematology. 2001;14(3):497–529.
60. Meyers J, Yu Y, Kaye JA, Davis KL. Medicare fee-for-service enrollees with primary acute myeloid leukemia: An analysis of treatment patterns, survival, and healthcare resource utilization and costs. Applied Health Economics and Health Policy. 2013;11(3):275–86.
61. Döhner H, Estey E, Grimwade D, Amadori S, Appelbaum FR, Ebert BL, et al. Diagnosis and management of AML in adults: 2017 ELN recommendations from an international expert panel. Blood. 2017;129(4):424–48.
62. Burnett AK, Goldstone A, Hills RK, Milligan D, Prentice A, Yin J, et al. Curability of patients with acute myeloid leukemia who did not undergo transplantation in first remission. Journal of Clinical Oncology. 2013;31(10):1293–301.
63. Burnett AK, Russell NH, Hills RK, Hunter AE, Kjeldsen L, Yin J, et al. Optimization of chemotherapy for younger patients with acute myeloid leukemia: Results of the medical research council AML15 trial. Journal of Clinical Oncology. 2013;31(27):3360–8.
64. Kaya AH, Tekgündüz E, Ilkkiliç K, Dal MS, Merdin A, Karakus A, et al. Efficacy of CLARA in recurrent/refractory acute myeloid leukaemia patients unresponsive to FLAG chemotherapy. Journal of Chemotherapy. 2018;30(1):44–8.
65. Zeijlemaker W, Gratama JW, Schuurhuis GJ. Tumor heterogeneity makes AML a “moving target” for detection of residual disease. Cytometry Part B - Clinical Cytometry. 2014;86(1):3–14.
66. Stone RM, Mandrekar SJ, Sanford BL, Laumann K, Geyer S, Bloomfield CD, et al. Midostaurin plus chemotherapy for acute myeloid leukemia with a FLT3 Mutation. New England Journal of Medicine. 2017;377(5):454–64.
67. Stone RM, Mandrekar SJ, Sanford BL, Laumann K, Geyer S, Bloomfield CD, et al. Midostaurin plus chemotherapy for acute myeloid leukemia with a FLT3 Mutation. New England Journal of Medicine. 2017;377(5):454–64.
68. Perl AE, Martinelli G, Cortes JE, Neubauer A, Berman E, Paolini S, et al. Gilteritinib or Chemotherapy for Relapsed or Refractory FLT3 -Mutated AML . New England Journal of Medicine. 2019;381(18):1728–40.
69. DiNardo CD, Pratz K, Pullarkat V, Jonas BA, Arellano M, Becker PS, et al. Venetoclax combined with decitabine or azacitidine in treatment-naive, elderly patients with acute myeloid leukemia. Blood. 2019;133(1):7–17.
70. Stein EM, DiNardo CD, Pollyea DA, Fathi AT, Roboz GJ, Altman JK, et al. Enasidenib in mutant IDH2 relapsed or refractory acute myeloid leukemia. Blood. 2017;130(6):722–31.
71. DiNardo CD, Stein EM, de Botton S, Roboz GJ, Altman JK, Mims AS, et al. Durable remissions with ivosidenib in IDH1-mutated relapsed or refractory AML. New England Journal of Medicine. 2018;378(25):2386–98.
72. Roboz GJ, DiNardo CD, Stein EM, de Botton S, Mims AS, Prince GT, et al. Ivosidenib induces deep durable remissions in patients with newly diagnosed IDH1-mutant acute myeloid leukemia. Blood. 2020;135(7):463–71.

73. Cortes JE, Heidel FH, Hellmann A, Fiedler W, Smith BD, Robak T, et al. Randomized comparison of low dose cytarabine with or without glasdegib in patients with newly diagnosed acute myeloid leukemia or high-risk myelodysplastic syndrome. Leukemia. 2019;33(2):379–89.
74. Malumbres M, Barbacid M. RAS oncogenes : the first 30 years. Nature Reviews Cancer. 2003;3(June):7–13.
75. Chung E, Kondo M. Role of Ras/Raf/MEK/ERK signaling in physiological hematopoiesis and leukemia development. Immunol Res. 2011;49:248–68.
76. Rajalingam K, Schreck R, Rapp UR, Albert Š. Ras oncogenes and their downstream targets. Biochimica et Biophysica Acta - Molecular Cell Research. 2007;1773(8):1177–95.
77. Jackson JH, Cochrane CG, Bourne JR, Solski PA, Buss JE, Der CJ. Farnesol modification of Kirsten-ras exon 4B protein is essential for transformation. Proceedings of the National Academy of Sciences of the United States of America. 1990;87(8):3042–6.
78. Steelman LS, Abrams SL, Whelan J, Bertrand FE, Ludwig DE, McCubery J. Contributions of the Raf / MEK / ERK , PI3K / PTEN / Akt / mTOR and Jak / STAT pathways to leukemia. Leukemia. 2008;22:686–707.
79. Yoon S, Seger R. The extracellular signal-regulated kinase : Multiple substrates regulate diverse cellular functions. 2006;24(March):21–44.
80. Saj A, Lai EC. Control of microRNA biogenesis and transcription by cell signaling pathways. Curr Opin Genet Dev. 2011;21(4):504–10.
81. MacLeod R, Rouleau J, Szyf M. Regulation of DNA Methylation by the RAS Signaling Pathway. The Journal of Biological Chemestry. 1995;270:11327–37.
82. Gazin C, Wajapeyee N, Gobeil S, Virbasius CM, Green MR. An elaborate pathway required for Ras-mediated epigenetic silencing. Nature. 2007;449(7165):1073–7.
83. Campbell SL, Khosravi-far R, Rossman KL, Clark GJ. Increasing complexity of RAS signaling Increasing complexity of Ras signaling. Oncogene. 1998;17:1395.
84. Steelman LS, Franklin RA, Abrams SL, Chappell W, Kempf CR, Bäsecke J, et al. Roles of the Ras / Raf / MEK / ERK pathway in leukemia therapy. Leukemia. 2011;1–15.
85. Castellano E, Santos E. Functional specificity of ras isoforms: so similar but so different. Genes & Cancer. 2011;2(3):216–31.
86. Prior IA, Lewis PD, Mattos C. A comprehensive survey of ras mutations in cancer. Cancer Research. 2012;72(10):2457–67.
87. Bos JL. Ras Oncogenes in Human Cancer: A Review. Cancer Research. 1989;49(17):4682–9.
88. Beaupre D, Kurzrock R. RAS and Leukemia : From Basic Mechanisms. Journal of Clinical Oncology. 1999;17(3):1071–9.
89. Liu X, Ye Q, Zhao XP, Zhang PB, Li S, Li RQ, et al. RAS mutations in acute myeloid leukaemia patients: A review and meta-analysis. Clinica Chimica Acta. 2019;489(August 2018):254–60.
90. Frese KK, Tuveson DA. Maximizing mouse cancer models. 2007;7.

91. Mangaonkar AA, Patnaik MM. Advances in chronic myelomonocytic leukemia and future prospects: Lessons learned from precision genomics. Vol. 2, Advances in Cell and Gene Therapy. 2019. p. e48.
92. Chung SS, Hu W, Park CY. The role of microRNAs in hematopoietic stem cell and leukemic stem cell function. 2011;
93. Rieske P, Pongubala JMR. AKT Induces Transcriptional Activity of PU.1 through Phosphorylation-mediated Modifications within its Transactivation Domain. Journal of Biological Chemistry. 2001;276(11):8460–8.
94. Bonni A, Brunet A, West AE, Datta SR, Takasu MA, Greenberg ME, et al. Cell Survival Promoted by the Ras-MAPK Signaling Pathway by Transcription-Dependent and -Independent Mechanisms. Science. 1999;286(5443):1358–62.
95. Boudry-Labis E, Roche-Lestienne C, Nibourel O, Boissel N, Terre C, Perot C, et al. Neurofibromatosis-1 gene deletions and mutations in de novo adult acute myeloid leukemia. American Journal of Hematology. 2013;88(4):306–11.
96. Sanada M, Suzuki T, Shih LY, Otsu M, Kato M, Yamazaki S, et al. Gain-of-function of mutated C-CBL tumour suppressor in myeloid neoplasms. Nature. 2009;460(7257):904–8.
97. Schubbert S, Lieuw K, Rowe SL, Lee CM, Li XX, Loh ML, et al. Functional analysis of leukemia-associated PTPN11 mutations in primary hematopoietic cells. Blood. 2005;106(1):311–7.
98. Milella M, Kornblau SM, Estrov Z, Carter BZ, Lapillonne H, Harris D, et al. Therapeutic targeting of the MEK/MAPK signal transduction module in acute myeloid leukemia. Journal of Clinical Investigation. 2001;108(6):851–9.
99. Zebisch A, Staber PB, Delavar A, Bodner C, Hiden K, Fischereder K, et al. Two transforming C-RAF germ-line mutations identified in patients with therapy-related acute myeloid leukemia. Cancer Research. 2006;66(7):3401–8.
100. Zebisch A, Czernilofsky A, Keri G, Smigelskaite J, Sill H, Troppmair J. Signaling Through RAS-RAF-MEK-ERK: from Basics to Bedside. Current Medicinal Chemistry. 2007;14(5):601–23.
101. Downward J. Targeting RAS signalling pathways in cancer therapy. Nature Reviews Cancer [Internet]. 2003;3(1):11–22. Available from: http://www.nature.com/doifinder/10.1038/nrc969
102. Smith CC, Shah NP. The Role of Kinase Inhibitors in the Treatment of Patients with Acute Myeloid Leukemia. American Society of Clinical Oncology Educational Book. 2013;33:313–8.
103. Navada SC, Garcia-Manero G, OdchimarReissig R, Pemmaraju N, Alvarado Y, Ohanian MN, et al. Rigosertib in combination with azacitidine in patients with myelodysplastic syndromes or acute myeloid leukemia: Results of a phase 1 study. Leukemia Research. 2020;94(May):106369.
104. Kunimoto H, Meydan C, Nazir A, Whitfield J, Levine RL, Shih AH. Cooperative Epigenetic Remodeling by TET2 Loss and NRAS Mutation Drives Myeloid Transformation and MEK Inhibitor Sensitivity. Cancer Cell. 2018;176(12):139–48.
105. Athuluri-Divakar SK, Vasquez-Del Carpio R, Dutta K, Baker SJ, Cosenza SC, Basu I, et al. A Small Molecule RAS-Mimetic Disrupts RAS Association with Effector Proteins to Block Signaling. Cell. 2016;165(3):643–55.

106. Navada SC, Fruchtman SM, Odchimar-Reissig R, Demakos EP, Petrone ME, Zbyszewski PS, et al. A phase 1/2 study of rigosertib in patients with myelodysplastic syndromes (MDS) and MDS progressed to acute myeloid leukemia. Leukemia Research. 2018;64 (November 2017):10–6.
107. Wiemer EAC. The role of microRNAs in cancer: No small matter. European Journal of Cancer. 2007;43(10):1529–44.
108. Yu J, Wang F, Yang G-H, Wang F-L, Ma Y-N, Du Z-W, et al. Human microRNA clusters: genomic organization and expression profile in leukemia cell lines. Biochemical and biophysical research communications. 2006;349(1):59–68.
109. Altuvia Y, Landgraf P, Lithwick G, Elefant N, Pfeffer S, Aravin A, et al. Clustering and conservation patterns of human microRNAs. Nucleic Acids Research. 2005;33(8):2697–706.
110. Hausser J, Zavolan M. Identification and consequences of miRNA-target interactions - beyond repression of gene expression. Nature reviews Genetics. 2014;15(9):599–612.
111. Bartel DP. MicroRNAs : Genomics , Biogenesis , Mechanism , and Function. 2004;116:281–97.
112. Zeng Y, Yi R, Cullen BR. Recognition and cleavage of primary microRNA precursors by the nuclear processing enzyme Drosha. EMBO Journal. 2005;24(1):138–48.
113. Nilsen TW. Mechanisms of microRNA-mediated gene regulation in animal cells. Trends Genet. 2007;23(5):243–9.
114. Helwak A, Kudla G, Dudnakova T, Tollervey D. Mapping the human miRNA interactome by CLASH reveals frequent noncanonical binding. Cell. 2013;153(3):654–65.
115. Filipowicz W, Bhattacharyya SN, Sonenberg N. Mechanisms of post-transcriptional regulation by microRNAs: Are the answers in sight? Nature Reviews Genetics. 2008;9(2):102–14.
116. Johnson SM, Grosshans H, Shingara J, Byrom M, Jarvis R, Cheng A, et al. RAS Is Regulated by the let-7 MicroRNA Family. 2005;120:635–47.
117. Garzon R, Volinia S, Liu C, Fernandez-cymering C, Palumbo T, Pichiorri F, et al. MicroRNA signatures associated with cytogenetics and prognosis in acute myeloid leukemia MicroRNA signatures associated with cytogenetics and prognosis in acute myeloid leukemia. 2008;111(6):3183–9.
118. Duan R, Pak CH, Jin P. Single nucleotide polymorphism associated with mature miR-125a alters the processing of pri-miRNA. Human Molecular Genetics. 2007;16(9):1124–31.
119. Chang TC, Yu D, Lee YS, Wentzel EA, Arking DE, West KM, et al. Widespread microRNA repression by Myc contributes to tumorigenesis. Nature Genetics. 2008;40(1):43–50.
120. Gao XN, Lin J, Li YH, Gao L, Wang XR, Wang W, et al. MicroRNA-193a represses c-kit expression and functions as a methylation-silenced tumor suppressor in acute myeloid leukemia. Oncogene. 2011;30(31):3416–28.
121. Baer C, Claus R, Plass C. Genome-wide epigenetic regulation of miRNAs in cancer. Cancer Research. 2013;73(2):473–7.

122. O'Connell RM, Rao DS, Chaudhuri AA, Boldin MP, Taganov KD, Nicoll J, et al. Sustained expression of microRNA-155 in hematopoietic stem cells causes a myeloproliferative disorder. Journal of Experimental Medicine. 2008;205(3):585–94.

123. Garzon R, Garofalo M, Martelli MP, Briesewitz R, Wang L, Fernandez-Cymering C, et al. Distinctive microRNA signature of acute myeloid leukemia bearing cytoplasmic mutated nucleophosmin. Proceedings of the National Academy of Sciences. 2008;105(10):3945–50.
124. Zhao JL, Rao DS, Boldin MP, Taganov KD, O'Connell RM, Baltimore D. NF-κB dysregulation in microRNA-146a-deficient mice drives the development of myeloid malignancies. Proceedings of the National Academy of Sciences of the United States of America. 2011;108(22):9184–9.
125. Starczynowski DT, Kuchenbauer F, Argiropoulos B, Sung S, Morin R, Muranyi A, et al. Identification of miR-145 and miR-146a as mediators of the 5q-syndrome phenotype. Nature Medicine. 2010;16(1):49–58.
126. Palanichamy JK, Rao DS. miRNA dysregulation in cancer: Towards a mechanistic understanding. Frontiers in Genetics. 2014;5(MAR):1–10.
127. Liao Q, Wang B, Li X, Jiang G. miRNAs in acute myeloid leukemia. Oncotarget. 2017;8(2):3666–82.
128. Mardani R, Jafari Najaf Abadi MH, Motieian M, Taghizadeh-Boroujeni S, Bayat A, Farsinezhad A, et al. MicroRNA in leukemia: Tumor suppressors and oncogenes with prognostic potential. Journal of Cellular Physiology. 2019;234(6):8465–86.
129. Weng H, Lal K, Yang FF, Chen J. The pathological role and prognostic impact of miR-181 in acute myeloid leukemia. Cancer Genetics. 2015;208(5):225–9.
130. Zebisch A, Hatzl S, Pichler M, Wölfler A, Sill H. Therapeutic resistance in acute myeloid leukemia: The role of non-coding RNAs. International Journal of Molecular Sciences. 2016;17(12):1–18.
131. Hatzl S, Perfler B, Wurm S, Uhl B, Quehenberger F, Ebner S, et al. Increased expression of micro-RNA-23a mediates chemoresistance to cytarabine in acute myeloid leukemia. Cancers. 2020;12(2):1–19.
132. Lu J, Getz G, Miska EA, Alvarez-Saavedra E, Lamb J, Peck D, et al. MicroRNA expression profiles classify human cancers. Nature. 2005;435(7043):834–8.
133. Mi S, Lu J, Sun M, Li Z, Zhang H, Neilly MB, et al. MicroRNA expression signatures accurately discriminate acute lymphoblastic leukemia from acute myeloid leukemia. Proceedings of the National Academy of Sciences of the United States of America. 2007;104(50):19971–6.
134. Schotte D, Pieters R, den Boer ML. MicroRNAs in acute leukemia: from biological players to clinical contributors. Leukemia. 2012;26(1):1–12.
135. Hussein K, Büsche G, Muth M, Göhring G, Kreipe H, Bock O. Expression of myelopoiesis-associated microRNA in bone marrow cells of atypical chronic myeloid leukaemia and chronic myelomonocytic leukaemia. Annals of Hematology. 2011;90(3):307–13.

136. Nassiri M, Olczyk J, Knapp S, Vance G, Tewari A, Kemp S, et al. MicroRNA Expression Profiles in Chronic Myelomonocytic Leukemia. Blood. 2008 Nov 16;112(11):2699.
137. Berg JL. Micro RNA expression profiling in a murine in vivo model of KRAS induced chronic myelomonocytic leukemia. 2017.
138. Popovic R, Riesbeck LE, Velu CS, Chaubey A, Zhang J, Achille NJ, et al. Regulation of mir-196b by MLL and its overexpression by MLL fusions contributes to immortalization. Blood. 2009;113(14):3314–22.
139. Velu CS, Chaubey A, Phelan JD, Horman SR, Wunderlich M, Guzman ML, et al. Therapeutic antagonists of microRNAs deplete leukemia-initiating cell activity. Journal of Clinical Investigation. 2014;124(1):222–36.
140. Hong DS, Kang YK, Borad M, Sachdev J, Ejadi S, Lim HY, et al. Phase 1 study of MRX34, a liposomal miR-34a mimic, in patients with advanced solid tumours. British Journal of Cancer. 2020;122(11):1630–7.
141. Abba ML, Patil N, Leupold JH, Moniuszko M, Utikal J, Niklinski J, et al. MicroRNAs as novel targets and tools in cancer therapy. Cancer Letters. 2017;387:84–94.
142. Huang X, Schwind S, Yu B, Santhanam R, Wang H, Hoellerbauer P, et al. Targeted delivery of microRNA-29b by transferrin-conjugated anionic lipopolyplex nanoparticles: A novel therapeutic strategy in acute myeloid leukemia. Clinical Cancer Research. 2013;19(9):2355–67.
143. Lotfabadi NN, Kouchesfehani HM, Sheikhha MH, Kalantar SM. Development of a novel cationic liposome: Evaluation of liposome mediated transfection and anti-proliferative effects of miR-101 in acute myeloid leukemia. Journal of Drug Delivery Science and Technology. 2018;45:196–202.
144. Memari F, Joneidi Z, Taheri B, Aval SF, Roointan A, Zarghami N. Epigenetics and Epi-miRNAs: Potential markers/therapeutics in leukemia. Biomedicine and Pharmacotherapy. 2018;106(July):1668–77.
145. Iorio M v., Croce CM. MicroRNA dysregulation in cancer: Diagnostics, monitoring and therapeutics. A comprehensive review. EMBO Molecular Medicine. 2012;4(3):143–59.
146. Krejcik Z, Belickova M, Hrustincova A, Votavova H, Jonasova A, Cermak J, et al. MicroRNA profiles as predictive markers of response to azacitidine therapy in myelodysplastic syndromes and acute myeloid leukemia. Cancer Biomarkers. 2018;22(1):101–10.
147. Margueron R, Reinberg D. The Polycomb complex PRC2 and its mark in life. Nature. 2011;469(7330):343–9.
148. Ernst T, Chase AJ, Score J, Hidalgo-Curtis CE, Bryant C, Jones A v., et al. Inactivating mutations of the histone methyltransferase gene EZH2 in myeloid disorders. Nature Genetics. 2010;42(8):722–6.
149. Cui K, Zang C, Roh TY, Schones DE, Childs RW, Peng W, et al. Chromatin Signatures in Multipotent Human Hematopoietic Stem Cells Indicate the Fate of Bivalent Genes during Differentiation. Cell Stem Cell. 2009;4(1):80–93.
150. Chase A, Score J, Lin F, Bryant C, Waghorn K, Yapp S, et al. Mutational mechanisms of EZH2 inactivation in myeloid neoplasms. Leukemia. 2020;

151. Kim KH, Roberts CWM. Targeting EZH2 in cancer. Physiology & behavior. 2017;176(12):139–48.
152. Wang X, Dai H, Wang Q, Wang Q, Xu Y, Wang Y, et al. EZH2 Mutations Are Related to Low Blast Percentage in Bone Marrow and -7/del(7q) in De Novo Acute Myeloid Leukemia. PLoS ONE. 2013;8(4).
153. Gu Z, Liu Y, Cai F, Patrick M, Zmajkovic J, Cao H, et al. Loss of EZH2 reprograms BCAA metabolism to drive leukemic transformation. Cancer Discovery. 2019;9(9):1228–47.
154. Wang Y, Hou N, Cheng X, Zhang J, Tan X, Zhang C, et al. Ezh2 acts as a tumor suppressor in kras-driven lung adenocarcinoma. International Journal of Biological Sciences. 2017;13(5):652–9.
155. Geissler K, Jäger E, Barna A, Gurbisz M, Marschon R, Graf T, et al. The Austrian biodatabase for chronic myelomonocytic leukemia (ABCMML): A representative and useful real-life data source for further biomedical research. Wiener Klinische Wochenschrift. 2019;131(17–18):410–8.
156. Kashofer K, Gornicec M, Lind K, Caraffini V, Schauer S, Beham-Schmid C, et al. Detection of prognostically relevant mutations and translocations in myeloid sarcoma by next generation sequencing. Leukemia and Lymphoma. 2018;59(2):501–4.
157. Auton A, Abecasis GR, Altshuler DM, Durbin RM, Bentley DR, Chakravarti A, et al. A global reference for human genetic variation. Nature. 2015;526(7571):68–74.
158. Wandler A, Shannon K. Mechanistic and preclinical insights from mouse models of hematologic cancer characterized by hyperactive ras. Cold Spring Harbor Perspectives in Medicine. 2018;8(4):1–18.
159. Sauer B, Henderson N. Site-specific DNA recombiation in mammalian cells by the Cre recombinase bacteriophage P1. Genetics. 1988;85(14):5166–70.
160. Kuhn R, Schwenk F, Aguet M, Rajewsky K. Inducible Gene Targeting in Mice 2016;269(5229):1427–9.
161. Velasco-Hernandez T, Säwén P, Bryder D, Cammenga JJ. Potential Pitfalls of the Mx1-Cre System: Implications for Experimental Modeling of Normal and Malignant Hematopoiesis. Stem Cell Reports. 2016;7(1):11–8.
162. Spangrude GJ, Heimfeld S, Weissman IL, Spangrude GJ, Heimfeld S, Weissman IL. Purification and Characterization of Mouse Hematopoietic Stem Cells. Science. 1988;241(4861):58–62.
163. Berg JL, Perfler B, Hatzl S, Mayer MC, Wurm S, Uhl B, et al. Micro-RNA-125a mediates the effects of hypomethylating agents in chronic myelomonocytic leukemia. Clinical Epigenetics. 2021;13(1):1–11.
164. Schmittgen TD, Livak KJ. Analyzing real-time PCR data by the comparative CT method. Nature Protocols. 2008;3(6):1101–8.
165. Galluzzi L. Guidelines for the use and interpretation of assays for monitoring cell death in higher eukaryotes. Cell death and differentiation. 2009;16(8):1093–107.
166. Schneider CA, Rasband WS, Eliceiri KW. NIH Image to ImageJ: 25 years of image analysis. Nature Methods. 2012;9(7):671–5.
167. Lutsik P, Feuerbach L, Arand J, Lengauer T, Walter J, Bock C. BiQ Analyzer HT: Locus-specific analysis of DNA methylation by high-throughput bisulfite sequencing. Nucleic Acids Research. 2011;39(SUPPL. 2):551–6.

168. Chang H, Yi B, Ma R, Zhang X, Zhao H, Xi Y. CRISPR/cas9, a novel genomic tool to knock down microRNA in vitro and in vivo. Scientific Reports. 2016;6(October 2015):1–12.
169. Villanueva RAM, Chen ZJ. ggplot2: Elegant Graphics for Data Analysis (2nd ed.). Measurement: Interdisciplinary Research and Perspectives. 2019;17(3):160–7.
170. Subramanian A, Tamayo P, Mootha VK, Mukherjee S, Ebert BL, Gillette MA, et al. Gene set enrichment analysis: A knowledge-based approach for interpreting genome-wide expression profiles. Proceedings of the National Academy of Sciences of the United States of America. 2005;102(43):15545–50.
171. Weinstein JN, Collisson EA, Mills GB, Shaw KRM, Ozenberger BA, Ellrott K, et al. The cancer genome atlas pan-cancer analysis project. Nature Genetics. 2013;45(10):1113–20.
172. Ghandi M, Huang FW, Jané-Valbuena J, Kryukov G v., Lo CC, McDonald ER, et al. Next-generation characterization of the Cancer Cell Line Encyclopedia. Nature. 2019;569:503–8.
173. Cerami E, Gao J, Dogrusoz U, Gross BE, Sumer SO, Aksoy BA, et al. The cBio Cancer Genomics Portal: An open platform for exploring multidimensional cancer genomics data. Cancer Discovery. 2012;2(5):401–4.
174. Berg JL, Perfler B, Hatzl S, Uhl B, Reinisch A, Pregartner G, et al. EZH2 inactivation in RAS-driven myeloid neoplasms hyperactivates RAS-signaling and increases MEK inhibitor sensitivity. Leukemia. 2021;ahead of print; Available from: https://doi.org/10.1038/s41375-021-01161-0
175. Gerrits A, Walasek MA, Olthof S, Weersing E, Ritsema M, Zwart E, et al. Genetic screen identifies microRNA cluster 99b / let-7e / 125a as a regulator of primitive hematopoietic cells. Blood. 2012;119(2):377–88.
176. Palomo L, Malinverni R, Cabezón M, Xicoy B, Arnan M, Coll R, et al. DNA methylation profile in chronic myelomonocytic leukemia associates with distinct clinical, biological and genetic features. Epigenetics. 2018;13(1):8–18.
177. Potenza N, Panella M, Castiello F, Mosca N, Amendola E, Russo A. Molecular mechanisms governing microRNA-125a expression in human hepatocellular carcinoma cells. Scientific Reports. 2017;7(1):1–9.
178. Klco JM, Spencer DH, Lamprecht TL, Sarkaria SM, Wylie T, Magrini V, et al. Genomic impact of transient low-dose decitabine treatment on primary AMLcells. Blood. 2013;121(9):1633–43.
179. Savona MR, Malcovati L, Komrokji R, Tiu R v., Mughal TI, Orazi A, et al. An international consortium proposal of uniform response criteria for myelodysplastic/myeloproliferative neoplasms (MDS/MPN) in adults. Blood. 2015;125(12):1857–65.
180. Flotho C, Claus R, Batz C, Schneider M, Sandrock I, Ihde S, et al. The DNA methyltransferase inhibitors azacitidine, decitabine and zebularine exert differential effects on cancer gene expression in acute myeloid leukemia cells. Leukemia. 2009;23(6):1019–28.
181. McGraw KL, Nguyen J, al Ali NH, Komrokji RS, Sallman D, Zhang X, et al. Association of EZH2 protein expression by immunohistochemistry in myelodysplasia related neoplasms with mutation status, cytogenetics and clinical outcomes. British Journal of Haematology. 2019;184(3):450–5.

182. Cohen ASA, Yap DB, Lewis MES, Chijiwa C, Ramos-Arroyo MA, Tkachenko N, et al. Weaver Syndrome-Associated EZH2 Protein Variants Show Impaired Histone Methyltransferase Function In Vitro. Human Mutation. 2016;37(3):301–7.
183. Burgos S, Montalban-Bravo G, Fuente L, Jabbour EJ, Kanagal-Shamanna R, Soltysiak KA, et al. Novel EZH2 mutation in a patient with secondary B-cell acute lymphocytic leukemia after deletion 5q myelodysplastic syndrome treated with lenalidomide: A case report. Medicine. 2019;98(1):e14011.
184. Li H, Chang C, Shang Y, Qiang L, Zhang B, Bu B, et al. A missense variant in EZH2 is associated with colorectal cancer risk in a Chinese population. Oncotarget. 2017;8(55):94738–42.
185. Ley TJ, Miller C, Ding L, Raphael BJ, Mungall AJ, Robertson G, et al. Genomic and Epigenomic Landscapes of Adult De Novo Acute Myeloid Leukemia. New England Journal of Medicine. 2013;368(22):2059–74.
186. Weinstein IB, Joe A. Oncogene addiction. Cancer Research. 2008;68(9):3077–80.
187. Göllner S, Oellerich T, Agrawal-Singh S, Schenk T, Klein HU, Rohde C, et al. Loss of the histone methyltransferase EZH2 induces resistance to multiple drugs in acute myeloid leukemia. Nature Medicine. 2017;23(1):69–78.
188. Banerji U. Heat shock protein 90 as a drug target: Some like it hot. Clinical Cancer Research. 2009;15(1):9–14.
189. Brachet-Botineau M, Polomski M, Neubauer HA, Juen L, Hédou D, Viaud-Massuard MC, et al. Pharmacological inhibition of oncogenic STAT3 and STAT5 signaling in hematopoietic cancers. Cancers. 2020;12(1):1–48.
190. Fischer A, Baljuls A, Reinders J, Nekhoroshkova E, Sibilski C, Metz R, et al. Regulation of RAF activity by 14-3-3 proteins: RAF kinases associate functionally with both homo- and heterodimeric forms of 14-3-3 proteins. Journal of Biological Chemistry. 2009;284(5):3183–94.
191. Kalkman HO. Potential opposite roles of the extracellular signal-regulated kinase (ERK) pathway in autism spectrum and bipolar disorders. Neuroscience and Biobehavioral Reviews. 2012;36(10):2206–13.
192. Ren ZQ, Yan WJ, Zhang XZ, Zhang PB, Zhang C, Chen SK. CUL1 Knockdown Attenuates the Adhesion, Invasion, and Migration of Triple-Negative Breast Cancer Cells via Inhibition of Epithelial-Mesenchymal Transition. Pathology and Oncology Research. 2020;26(2):1153–63.
193. Zhang Z, Li H, Zhao Y, Guo Q, Yu Y, Zhu S, et al. Asporin promotes cell proliferation via interacting with PSMD2 in gastric cancer. Frontiers in Bioscience - Landmark. 2019;24(6):1178–89.
194. Chen J, Ellison FM, Keyvanfar K, Omokaro SO, Desierto MJ, Eckhaus MA, et al. Enrichment of hematopoietic stem cells with SLAM and LSK markers for the detection of hematopoietic stem cell function in normal and Trp53 null mice. Experimental Hematology. 2008;36(10):1236–43.
195. Garzon R, Volinia S, Liu CG, Fernandez-cymering C, Palumbo T, Pichiorri F, et al. MicroRNA signatures associated with cytogenetics and prognosis in acute myeloid leukemia. Blood. 2008;111(6):3183–9.
196. Tatsumi N, Hojo N, Yamada O, Ogawa M, Katsura Y, Kawata S, et al. Deficiency in WT1-targeting microRNA-125a leads to myeloid malignancies and urogenital abnormalities. Oncogene. 2016;35(8):1003–14.

197. Guo S, Bai H, Megyola CM, Halene S, Krause DS, Scadden DT. Complex oncogene dependence in microRNA-125a – induced myeloproliferative neoplasms. 2012;
198. Li Z, Chen P, Su R, Li Y, Hu C, Wang Y, et al. Overexpression and knockout of miR-126 both promote leukemogenesis. Blood. 2015;126(17):2005–15.
199. Chen H, Xu Z. Hypermethylation-Associated Silencing of miR-125a and miR-125b: A Potential Marker in Colorectal Cancer. Disease Markers. 2015;2015.
200. Ufkin ML, Peterson S, Yang X, Driscoll H, Duarte C, Sathyanarayana P. MiR-125a regulates cell cycle, proliferation, and apoptosis by targeting the ErbB pathway in acute myeloid leukemia. Leukemia Research. 2014;38(3):402–10.
201. Cai M, Chen Q, Shen J, Lv C, Cai L. Epigenetic silenced miR-125a-5p could be self-activated through targeting Suv39h1 in gastric cancer. Journal of Cellular and Molecular Medicine. 2018;22(10):4721–31.
202. Sun L, Zhang B, Liu Y, Shi L, Li H, Lu S. MiR125a-5p acting as a novel Gab2 suppressor inhibits invasion of glioma. Molecular Carcinogenesis. 2016;55(1):40–51.
203. Solly F, Koering C, Mohamed AM, Maucort-Boulch D, Robert G, Auberger P, et al. An miRNA-DNMT1 axis is involved in azacitidine resistance and predicts survival in higher-risk myelodysplastic syndrome and low blast count acute myeloid leukemia. Clinical Cancer Research. 2017;23(12):3025–34.
204. Wang Y, Liu C, Luo M, Zhang Z, Gong J, Li J, et al. Chemotherapy-induced miRNA-29c/catenin-δ signaling suppresses metastasis in gastric cancer. Cancer Research. 2015;75(7):1332–44.
205. Saito Y, Friedman JM, Chihara Y, Egger G, Chuang JC, Liang G. Epigenetic therapy upregulates the tumor suppressor microRNA-126 and its host gene EGFL7 in human cancer cells. Biochemical and Biophysical Research Communications. 2009;379(3):726–31.
206. Memari F, Joneidi Z, Taheri B, Aval SF, Roointan A, Zarghami N. Epigenetics and Epi-miRNAs: Potential markers/therapeutics in leukemia. Biomedicine and Pharmacotherapy. 2018;106(July):1668–77.
207. Cao Y, Liu Y, Shang L, Wei W, Shen Y, Gu Q, et al. Decitabine and all-trans retinoic acid synergistically exhibit cytotoxicity against elderly AML patients via miR-34a/MYCN axis. Biomedicine and Pharmacotherapy. 2020;125(October 2019):109878. Available from: https://doi.org/10.1016/j.biopha.2020.109878
208. Christopher A, Kaur R, Kaur G, Kaur A, Gupta V, Bansal P. MicroRNA therapeutics: Discovering novel targets and developing specific therapy. Perspectives in Clinical Research. 2016;7(2):68.
209. Reid G, Kao SC, Pavlakis N, Brahmbhatt H, MacDiarmid J, Clarke S, et al. Clinical development of TargomiRs, a miRNA mimic-based treatment for patients with recurrent thoracic cancer. Epigenomics. 2016;8(8):1079–85.
210. Yoshikawa Y, Taniguchi K, Tsujino T, Heishima K, Inamoto T, Takai T, et al. Anti-cancer Effects of a Chemically Modified miR-143 on Bladder Cancer by Either Systemic or Intravesical Treatment. Molecular Therapy - Methods and Clinical Development. 2019;13(June):290–302.

211. Ricci C, Fermo E, Corti S, Molteni M, Faricciotti A, Cortelezzi A, et al. RAS Mutations Contribute to Evolution of Chronic Myelomonocytic Leukemia to the Proliferative Variant. Clinical Cancer Research. 2010;16(8):2246–56.
212. Lyubynska N, Gorman MF, Lauchle JO, Hong WX, Akutagawa JK, Shannon K, et al. A MEK inhibitor abrogates myeloproliferative disease in Kras mutant mice. Sci Transl Med. 2011;3(76):76ra27.

213. Borthakur G, Popplewell L, Boyiadzis M, Foran J, Platzbecker U, Vey N, et al. Activity of the oral mitogen-activated protein kinase kinase inhibitor trametinib in RAS-mutant relapsed or refractory myeloid malignancies. Cancer. 2016;122(12):1871–9.
214. Maiti A, Naqvi K, Kadia TM, Borthakur G, Takahashi K, Bose P, et al. Phase II Trial of MEK Inhibitor Binimetinib (MEK162) in RAS-mutant Acute Myeloid Leukemia. Clinical Lymphoma, Myeloma and Leukemia. 2019;19(3):142-148.e1.
215. Zhang P, He F, Bai J, Yamamoto S, Chen S, Zhang L, et al. Chromatin regulator Asxl1 loss and Nf1 haploinsufficiency cooperate to accelerate myeloid malignancy. Journal of Clinical Investigation. 2018;128(12):5383–98.
216. Shih AH, Abdel-Wahab O, Patel JP, Levine RL. The role of mutations in epigenetic regulators in myeloid malignancies. Nature Reviews Cancer. 2012;12(9):599–612.
217. Tate JG, Bamford S, Jubb HC, Sondka Z, Beare DM, Bindal N, et al. COSMIC: The Catalogue Of Somatic Mutations In Cancer. Nucleic Acids Research. 2019;47(D1):D941–7.
218. Kopanos C, Tsiolkas V, Kouris A, Chapple CE, Albarca Aguilera M, Meyer R, et al. VarSome: the human genomic variant search engine. Bioinformatics. 2019;35(11):1978–80.
219. Bejar R, Stevenson K, Abdel-Wahab O, Galili N, Nilsson B, Garcia-Manero G, et al. Clinical Effect of Point Mutations in Myelodysplastic Syndromes. New England Journal of Medicine. 2011;364(26):2496–506.
220. Tanaka S, Miyagi S, Sashida G, Chiba T, Yuan J, Mochizuki-Kashio M, et al. Ezh2 augments leukemogenicity by reinforcing differentiation blockage in acute myeloid leukemia. Blood. 2012;120(5):1107–17.
221. Basheer F, Giotopoulos G, Meduri E, Yun H, Mazan M, Sasca D, et al. Contrasting requirements during disease evolution identify EZH2 as a therapeutic target in AML. Journal of Experimental Medicine. 2019;216(4):966–81.
222. Wang Y, Hou N, Cheng X, Zhang J, Tan X, Zhang C, et al. Ezh2 acts as a tumor suppressor in kras-driven lung adenocarcinoma. International Journal of Biological Sciences. 2017;13(5):652–9.